REVIEW ARTICLE

Advanced wearable biosensors for the detection of body fluids and exhaled breath by graphene

Santoshi U. Singh[1,2] · Subhodeep Chatterjee[2,3] · Shahbaz Ahmad Lone[2] · Hsin-Hsuan Ho[2] · Kuldeep Kaswan[2] · Kiran Peringeth[2,3] · Arshad Khan[2] · Yun-Wei Chiang[1] · Sangmin Lee[5] · Zong-Hong Lin[2,3,4]

Abstract

Given the huge economic burden caused by chronic and acute diseases on human beings, it is an urgent requirement of a cost-effective diagnosis and monitoring process to treat and cure the disease in their preliminary stage to avoid severe complications. Wearable biosensors have been developed by using numerous materials for non-invasive, wireless, and consistent human health monitoring. Graphene, a 2D nanomaterial, has received considerable attention for the development of wearable biosensors due to its outstanding physical, chemical, and structural properties. Moreover, the extremely flexible, foldable, and biocompatible nature of graphene provide a wide scope for developing wearable biosensor devices. Therefore, graphene and its derivatives could be trending materials to fabricate wearable biosensor devices for remote human health management in the near future. Various biofluids and exhaled breath contain many relevant biomarkers which can be exploited by wearable biosensors non-invasively to identify diseases. In this article, we have discussed various methodologies and strategies for synthesizing and pattering graphene. Furthermore, general sensing mechanism of biosensors, and graphene-based biosensing devices for tear, sweat, interstitial fluid (ISF), saliva, and exhaled breath have also been explored and discussed thoroughly. Finally, current challenges and future prospective of graphene-based wearable biosensors have been evaluated with conclusion.

Keywords Wearable biosensors · Body fluids · Exhaled breath · Non-invasive detection · Graphene · Biomarkers

Introduction

Sensors in medicine and life science have been used to measure internal body parameters in disease diagnosis and health management techniques [1]. Many innovative

✉ Sangmin Lee
slee98@cau.ac.kr

✉ Zong-Hong Lin
linzh@mx.nthu.edu.tw

1   Department of Chemistry, National Tsing Hua University, Hsinchu 30013, Taiwan

2   Institute of Biomedical Engineering, National Tsing Hua University, Hsinchu 30013, Taiwan

3   Department of Power and Mechanical Engineering, National Tsing Hua University, Hsinchu 30013, Taiwan

4   Frontier Research Center On Fundamental and Applied Sciences of Matters, National Tsing Hua University, Hsinchu 30013, Taiwan

5   School of Mechanical Engineering, Chung-Ang University, Seoul 06974, South Korea

sensors have been developed in response to the demand for early detection and diagnosis of disease as well as minimally invasive technologies [2]. Biosensing has become a critical strategy because it provides highly desirable qualities such as portablity, high sensitivity, quick findings, and longer shelf life. A biosensor is an analytical instrument made up of two independent parts: biologicals (enzyme, antibody, nucleic acid, hormone, organelle, or complete cell) and physicals (transducer, amplifier). A typical approach is used to immobilize the biological material on the transducer. In this regard, as the immobilized biological material is in close proximity to the transducer, it can precisely interact with analytes (for example, glucose, urea, medication, pesticide) to generate detectable physical, chemical, electrical, or optical signals [3, 4]. Biosensor technologies provide direct connection to human skin, body movement compliance, fast response, enhanced application, point of care testing, and self-health management without causing harm to human organs [5–8]. In this regard, biofluids (sweat, tears, saliva, and interstitial fluid (ISF)) and exhaled breath play a very important

role in wearable device–based biosensing application as all of those can be readily sampled without disrupting the outermost protecting layers of the body's skin (the stratum corneum). Besides, exhaled breath has also received much attention in the past decade as it contains thousands of components which arise from the lungs, nasal cavities, and have systemic origins in blood [5, 9–11]. Moreover, implantable devices also attract considerable interest in the recent past. Wearable (non-invasive) and implantable (invasive) biosensor devices are available in the market. Both types of devices have a good sensitivity and specificity in measuring analyte signals [12]. However, implantable devices can readily injure surrounding tissues because of their sharp edges, stiffness, and design. On the other hand, some characteristics such as wireless power and data transmission capacity significantly increase the need for wearable biosensors for the need of remote monitoring and Internet of thing (IoT)-based sensing. Wristbands, headbands, eyeglasses, mouth guards, bandages, smart garments, wearable gloves, tattoos, and stickers are all examples of wearable biosensor platforms. Moreover, they have exceptional flexibility and stretchability as well as remarkable sensitivity to detect wide-range signals [13, 14]. Interestingly, a variety of nanoscale materials, including metal nanowires, nanoparticles, silicon nanoribbons, carbon black, carbon nanotubes, and graphene have been utilized as sensing materials in wearable devices when they are combined with an elastomer supporting substrate. Especially, graphene has attracted considerable interest after acquiring its single layer by mechanical exfoliation in 2004 [15]. Graphene exhibits excellent electrical, mechanical, thermal, and optical properties such as high thermal conductivity, electron mobility, a large specific surface area, high optical transmittance, exceptional mechanical flexibility, and biocompatible in nature. The atomic thickness of graphene layers allows entire carbon atoms to interact with analytes directly [16]. Interestingly, the recent trends also indicate that wearable biosensors

especially graphene-based wearable biosensors attract considerable interest in the recent past as concluded from Table 1.

Graphene has also demonstrated potential in prevention of contagious diseases such as COVID-19. In this regard, wearable e-textiles has played indispensable role in COVID-19 combat [22, 23]. Moreover, graphene and graphene-based materials also exhibit biocompatible property to some extent in terms of wearability. Skin is an ideal bio-integrating platform with graphene-based wearable biosensor and skin is the most usual exposure site for graphene-based materials [24]. Therefore, in order to assess the biocompatibility of graphene in terms of wearability, cutaneous toxicity mechanism of graphene nanomaterials exposed to human HaCaT skin keratinocytes have been studied by few groups. In this regard, mostly, it was observed that few layer graphene (FLG) and graphene oxide (GO) stimulates cytotoxicity as a consequence of persistent mitochondrial depolarization [25]. On the other hand, in vitro cytotoxicity of graphene towards skin keratinocytes and fibroblast has also been investigated in some studies [26]. It was well concluded by the previous works that cytotoxicity of graphene-based materials depends on their oxidative state. As an example, FLG has less toxic effect than that of GO. In addition, micro size graphene structure has high ability to interact with primary human keratinocytes [27]. However, there are too less studies to conclude the biocompatibility of graphene. In order to reduce the toxic effect of graphene-based materials (GBMs), graphene-biomacromolecule-based hybrid materials (graphene biopolymer nanohybrids, graphene polysaccharides) have been synthesized in biomedical and pharmaceutical [28, 29] field. Besides, toxicity can be reduced in a huge margin in case of graphene-based wearable biosensor by avoiding direct contact between GBMs, human body, and biofluids.

In the recent time, there are several literature reviews which mostly focus on either biosensing or wearable application of graphene. For an example, Huang et al.

Table 1 Recent literature trend based on number of citations for wearable biosensor and graphene-based wearable sensor

Paper/book title	Topic	Citation no	Ref
Graphene based biosensors accelerating medical diagnostics to new dimensions	Real time clinical diagnosis by nanoelectronics/microfluidics	68	[17]
Graphene-based biosensor: going sample	Electrical/optical biosensing integrated with paper/plastic-based substrate	126	[3]
Graphene for flexible and wearable device applications	Applications in optoelectronics/photovoltaics/physical sensors	138	[18]
Flexible graphene-based gas and chemical sensor	Detection of toxic gases, metal ions and VOCs	454	[19]
Graphene-based wearable sensors	Wearable sensing of Electrophysiological/fluid/gas signal	46	[20]
Wearable biosensors for healthcare monitoring	Fundamental principles, key challenges for wearable sensor for detection from non-invasive biofluids	1003	[9]
Wearable and flexible electronics for continuous molecular monitoring	Non-invasive detection of analyte from sweat, saliva, ISF as well as breath	454	[21]

[15] explored all the aspects of the biosensing application of graphene including invasive and non-invasive sampling strategy in the recent times but there is no thorough discussion regarding wearable application of graphene. Healthcare application of graphene in terms of biosensor has been thoroughly discussed by E. Narváez and N. Chauhan et al. [3, 17]. On the other hand, gas and other chemical sensing application of graphene-based flexible sensors have been explored well by Singh et al. [19] with wearable prospective of graphene-based sensors. Similarly, recent advancement and development of graphene-based wearable sensors including physical and chemical sensors have also been well explored by Qian et al. and Kim et al. in their respective literature review [9, 20]. However, all of those reviews failed to provide any detailed insights of wearable biosensing applications of graphene, including non-invasive and minimally invasive sampling strategy. Therefore, this proposed literature review addresses the recent development and advancement of graphene-based wearable sensor for the detection of biofluids such as ISF, sweat, saliva extracted by non-invasive or minimally invasive sampling strategy for the first time. Moreover, discussion regarding detection of analytes from exhaled breath has also been included in this literature review as

an extensive application of wearable graphene-based non-invasive biosensor.

In this review, firstly, we have discussed the characteristics and synthesis procedures of graphene, followed by several patterning methods utilized to investigate its application as wearable biosensor along with its sensing mechanism. Moreover, various graphene-based sensing devices based on detection of various analytes from non-invasively collected biofluids sample such as sweat, saliva, ISF, tear as well as exhaled breath have been explored and discussed. Finally, the review has been concluded with challenges and future perspectives for graphene-based wearable biosensors to detect various biofluids. Figure 1 summarizes the prime concept of this review regarding wearable graphene-based biosensors for the detection of biomarkers presence in several biofluids.

Properties and synthesis of graphene

Graphene is a thin-sheet 2D-nanomaterial having honeycomb-like structure with sp^2 hybridized carbon atoms. Several forms of the graphene have been discovered so far such as single/mono layer, few layers (2–10), multilayers

Fig. 1 Schematic overview of graphene-based wearable biosensors for the detection of differnt biomarkers
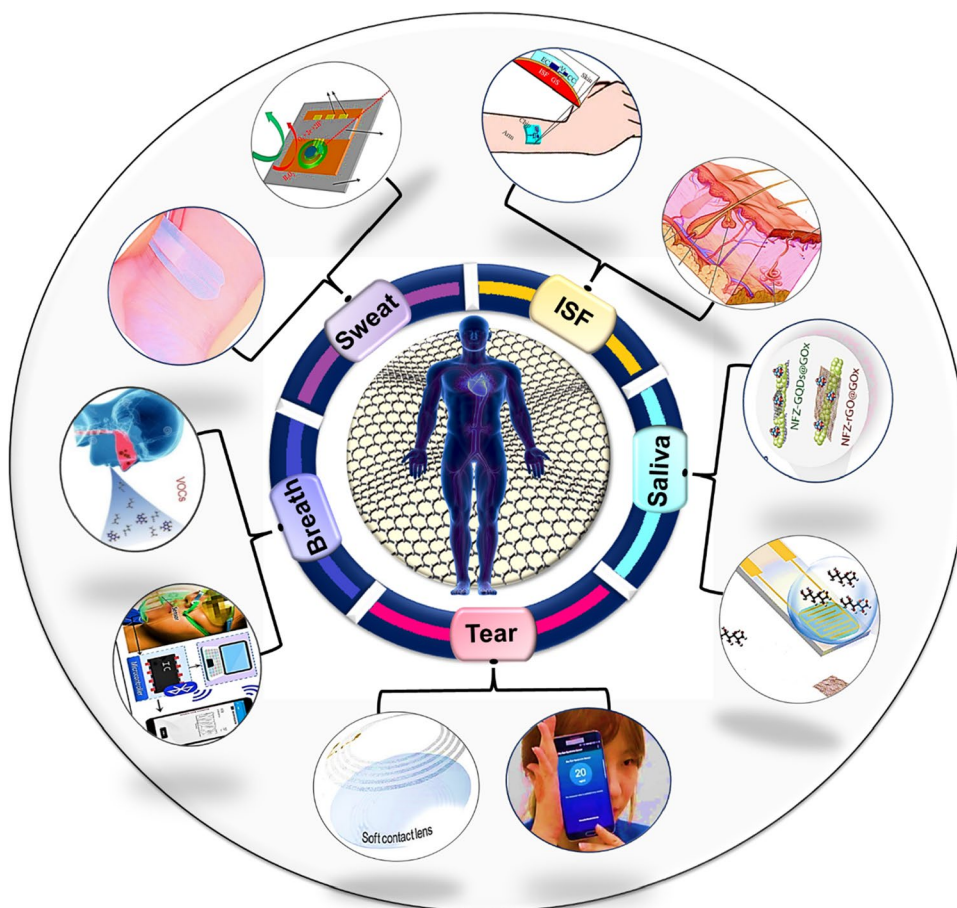
(> 10), and different derivatives of graphene (e.g., graphene oxide and reduced graphene oxide). Graphene oxide (GO) is a derivative of graphene having surface modified with different functional groups which contain oxygen such as -COOH, -CHO, -COON, OH, and C = O. GO is produced using oxidation of graphite in the presence of some acids [30–32]. After oxidation, by applying further steps like ultrasonication and purification, few layers of GO and even mono layer of GO can be obtained. GO has several advantages over pristine graphene such as high surface area, increased binding sites, easier and cheaper fabrication methodologies, easy blending ability with different other materials to produce high quality composites, etc. However, it has low thermal and electrical conductivity than pristine graphene. Therefore, GO is converted to another form of oxidized graphene called reduced graphene oxide (rGO). In this regard, GO is reduced to rGO by removing oxygen containing functional groups [33–37]. Conversion of GO to rGO improves various properties, e.g., thermal conductivity, mechanical properties, electron mobility, etc., which are essential for developing highly selective and ultra-fast biosensing devices. The structure of graphene, GO and rGO are shown in Fig. 2.

Several outstanding physical, chemical, and structural properties of graphene and its derivatives make them one of the most interesting materials for the development of biosensors. In this regard, due to extremely flexible and foldable nature, graphene is considered as a suitable material for the fabrication of wearable biosensor devices [38]. Different properties of graphene are summarized in Table 2. Graphite is made up of several sheets of graphene, one sheet is attached to another sheet by van der Waals force with the interplanar spacing of 1.42 Å between two adjacent sheets. A graphite crystal with 1 mm thickness contains around three million layers of stacked graphene sheets [39]. A graphene sheet contains one atom thick layer of sp^2 hybridized carbon atoms where

Table 2 Different properties of graphene

Property	Value	Ref
Electrical (electron mobility)	200,000 cm^2 V^{-1} s^{-1}	[16]
Mechanical (Young's modulus)	0.800 TPa	[22]
Mechanical (breaking strength)	42 N m^{-1}	[22]
Structural (surface area)	2630 m^2 g^{-1}	[23]
Thermal (thermal conductivity)	$(4.84 \pm 0.44) \times 10^3$ to $(5.30 \pm 0.48) \times 10^3$ W m^{-1} K^{-1}	[30]
Optical (light absorption)	2.3%	[31]
Chemical (functionalization)	Wide range of molecules	[32]
Electrochemical (electron transfer)	$0.90 (\pm 0.13) \times 10^{-3}$ cm s^{-1}	[41]
Electroactive (surface area)	0.0800 cm^2	[42]

the bond length between adjacent carbon atoms (the C–C bond length) is 1.42 Å, and the thickness of each layer is 0.35 nm [40].

Graphene shows unique electronic and electrical properties. For example, sp^2 hybridized carbon atoms contain a high degree of π–π conjugation, where electrons move freely, and this property highly facilitates electrochemical sensing. Besides, graphene possesses high charge carrier mobility (around 200,000 cm^2 V^{-1} s^{-1}) at room temperature [43] and high mechanical strength. For instance, the breaking strength of monolayer graphene is 42 N m^{-1}. Moreover, it also exhibits other remarkable mechanical properties such as Young's modulus of 1.0 TPa, intrinsic strength of 130 GPa, and third-order elastic stiffness of − 2.0 TPa [44]. In addition, monolayer graphene has a large specific surface area of 2630 m^2 g^{-1} approximately, which provides scope for the attachment

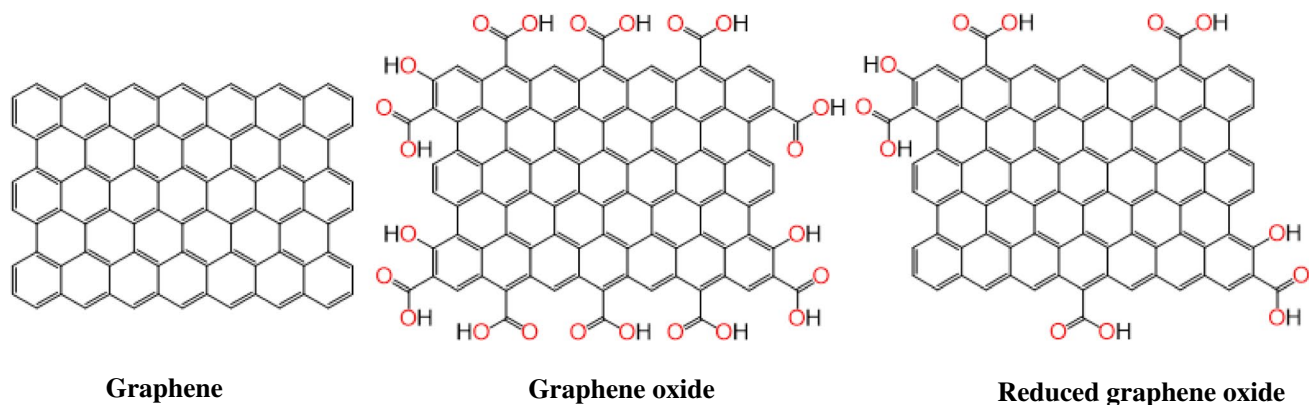**Graphene**   **Graphene oxide**   **Reduced graphene oxide**

Fig. 2 Molecular structure of graphene, graphene oxide, and reduced graphene oxide

of many molecules on its surface. Therefore, it facilitates the development of highly sensitive and miniaturized devices [45]. Furthermore, graphene is also well known for its excellent thermal conductivity. The thermal conductivity of monolayer graphene is found to be in the range from $(4.84 \pm 0.44) \times 10^3$ to $(5.30 \pm 0.48) \times 10^3$ $Wm^{-1} K^{-1}$ at room temperature, which is higher than that of single wall ($\approx 3.5 \times 10^3$ $Wm^{-1} K^{-1}$) and multi-wall ($\approx 3.0 \times 10^3$ $Wm^{-1} K^{-1}$) carbon nanotubes. This high thermal conductivity makes graphene a suitable material for electronics devices [46]. The fine structure constant ($\alpha = e^2/\hbar c$) is used to determine the absorption coefficient of graphene, which means that absorbance and transparency do not depend upon wavelength in this case. A single layer of graphene absorbs approximately 2.3% fraction of incident light over a wide range of wavelength [47]. From the chemistry point of view, pristine graphene is unreactive, but its functionalization with several other elements and materials results in highly increased chemical and electronic properties [48]. Moreover, various layers of graphene show high electrochemical electron transfer rate. The electron transfer occurs due to a redox reaction between graphene surface and a molecule. For example, in case of $[Fe(CN)_6]^{3-/4-}$, the mean electron transfer rates vary from 0.13 (± 0.02) $\times 10^{-3}$ cm s^{-1} for the bilayer to 2.09 (± 1.27) $\times 10^{-3}$ cm s^{-1} for 7 layers, with an overall mean value of 0.90 (± 0.13) $\times 10^{-3}$ cms^{-1} [41]. Electrodes modified with graphene materials demonstrate significant increase in the electroactive surface area. For example, when a glassy carbon electrode surface is modified with GO, for a load of 1.5 mg mL^{-1}, the largest electroactive surface area of 0.0800 cm^2 is achieved. Consequently, this modification results in increase in the sensitivity by fourfold and decrease in the limit of detection (LOD) by tenfold, when the electrode is used as sensor for determination of ascorbate [42]. Owing to the extraordinary multiple properties, graphene

is a promising 2D material especially for the development of wearable sensors [15].

Methods of graphene synthesis

Theoretical knowledge about graphene existed for over 50 years, but it was not practically explored until 2003. In 2004, Novoselov and Geim isolated and characterized graphene using the "Scotch tape" method [49]. Since then, this material has attracted significant attention in research, as proved by an exponential increase in related published literature. So far, many different methods for graphene synthesis have been established to achieve a better quality of graphene suitable for incorporating in wearable devices. These methods have been grouped into two broad categories: the top-down approach and the bottom-up approach [50, 51]. The top-down approach employs breaking of bulk graphene into monolayer/few-layer of graphene, whereas the bottom-up approach produces graphene from carbon precursors on a particular substrate, usually silicon (Si) or silicon carbide (SiC). Depending upon the requirement of the wearable devices, either of the approaches can be followed. These two synthesis processes have both their own advantages and limitations, as summarized in Table 3. Moreover, different methods for graphene synthesis are also elaborated below along with their respective biosensing and other applications.

Micromechanical exfoliation

The first-ever method applied for graphene synthesis was micromechanical exfoliation. In this method, a sticky tape was used to peel off bulk graphite. In order to obtain a monolayer of graphene, several sticking of tape on graphite was performed (Fig. 3a) [49, 57]. Furthermore, many researchers have applied this method to produce graphene and many improvements have been proposed in this method [58].

Table 3 Comparison of different synthesis methods of graphene

| Methods	Advantages	Disadvantages	Application	Ref
Micromechanical exfoliation	High quality and unmodified sheet synthesis, cost efficient, simple	Slow synthesis, small scale	Exploring properties of graphene	[49]
Liquid-phase exfoliation	Faster and large amount of graphene synthesis method	Hazardous solvents, chances of defects	Electrochemical biosensor	[52]
Chemical vapor deposition	Single or few layer graphene synthesis, large area sheets	Complex process, expensive	Biosensors	[53]
Reduction of graphene oxide	Low cost, easy and large-scale production	Unwanted defects, partially reversible	Amperometric biosensor	[54]
Laser scribed graphene	Controllable and inexpensive graphene production	Large number of defects, multilayer production	Electrochemical biosensor	[55]
3D graphene	Porous structure, high quality production, wide range of applications	Requirement of template, large number of defects	Electrochemical biosensor	[56]
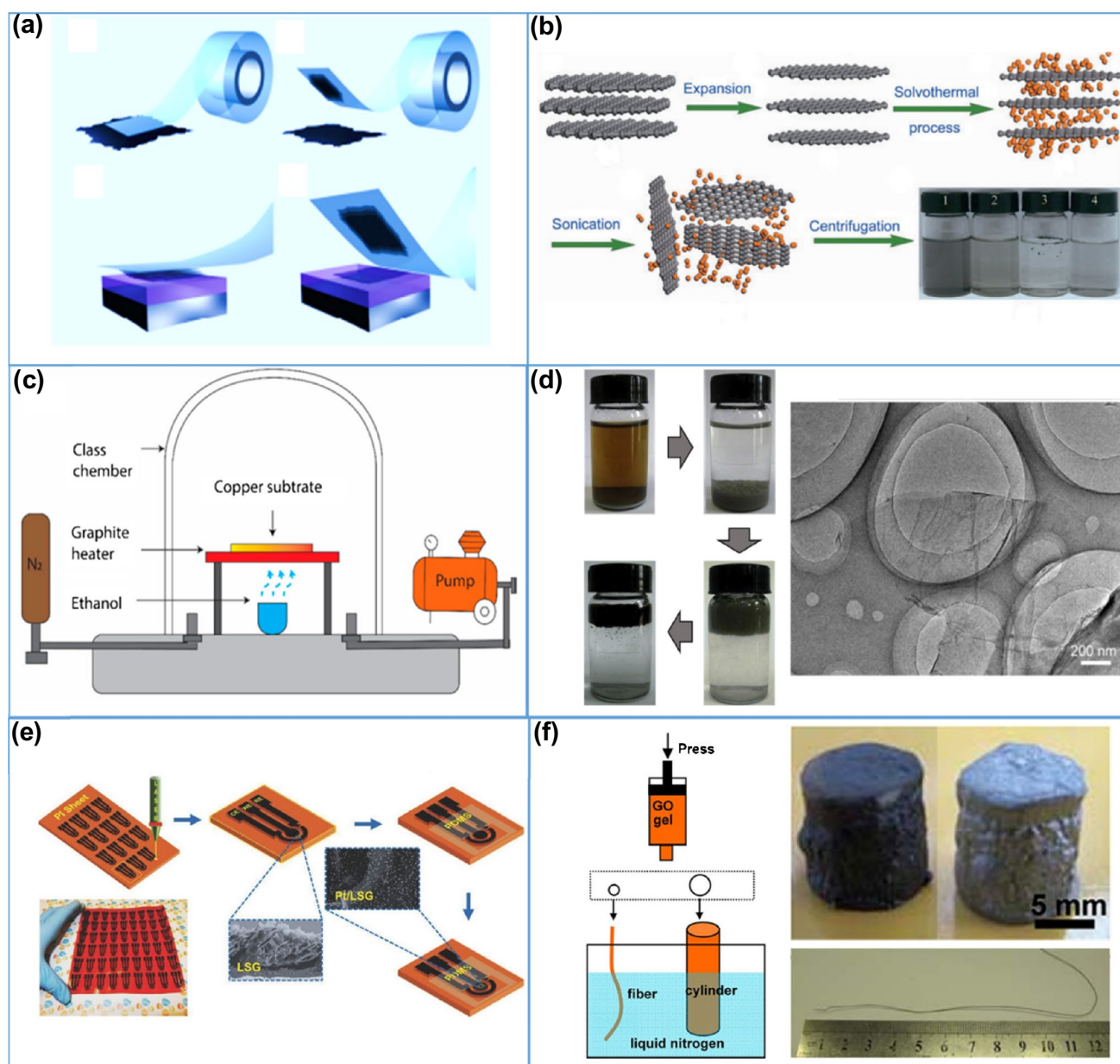
Fig. 3 a Schematic representation of the graphene synthesis by micromechanical exfoliation method. Reprinted with permission from [57]. Copyright 2012 Institute of Physics Publishing. **b** Schematic process of liquid phase exfoliation (LPE) production of graphene. Reprinted with permission from [60]. Copyright 2009 Springer Nature. **c** Schematic of a common chemical vapor deposition setup for synthesis of graphene. Reprinted with permission from [61]. Copyright 2020 Multidisciplinary Digital Publishing Institute. **d** Pho-

tograph of the GO before and after reduction with L-ascorbic acid and HRTEM images of reduced GO. Reprinted with permission from [62]. Copyright 2010 Elsevier. **e** Schematic illustration of fabrication of a laser scribed graphene (LSG) electrodes on a polyimide (PI) sheet. Reprinted with permission from [55]. Copyright 2016Wiley-VCH. **f** Schematic diagram for synthesis of the 3D graphene aerogel fibers. Reprinted with permission from [63]. Copyright 2012 American Chemical Society

Although micromechanical exfoliation is a suitable method to obtain high-quality graphene possessing almost all the properties demonstrated by graphene [59], it is challenging to obtain monolayers of graphene whose lateral dimensions are larger than the order of 10 to 100 μm. Hence, for developing wearable devices, the micromechanical exfoliation method is not viewed as the best choice due to its small-scale limitations.

Liquid-phase exfoliation

For the production of wearable devices, liquid-phase exfoliation (LPE) is an efficient and effective way to fabricate few-layer and multilayer graphene. Different graphitic materials such as graphite oxide, natural graphite, graphite intercalation compound (GIC) can be used as a precursor for

graphene production. LPE follows a top-down approach for graphene synthesis. Also, the LPE method utilizes solvents such as hydrogen peroxide, sulfuric acid, acetic acid, water, and other solvents for exfoliation of graphite using external forces generated from techniques, e.g., stirring, sonication, shearing forces, ball milling [64, 65], etc. Although, graphene fabricated by LPE is usually a little defective due to the use of solvents, it has several advantages such as cost-efficient, suitable for large-scale production, and the ability of the dispersed graphene to be deposited on various substrates. LPE employs mainly four steps for successful synthesis of graphene: firstly, immersion of graphite into the liquid medium, secondly, intercalation of the graphite, thirdly, the exfoliation of graphene flakes, and finally, the stabilization of the exfoliated materials isolated in the medium. Considering the advantages of the LPE method, there are several LPE-based graphene synthesis methods reported previously. For example, graphene was produced in high yield using liquid-phase exfoliation of graphite [66]. For this production, N-methyl-pyrrolidone was used as a solvent and the external force was provided by sonication. Furthermore, characterization performed by transmission electron microscopy (TEM), Raman spectroscopy and electron diffraction confirmed the successful formation of monolayers of graphene. This method produced a very high quality and unoxidized graphene monolayer, with approximately 1 wt% yield. Moreover, produced layers did not show any significant structural defects as confirmed by X-ray photoelectron spectroscopy (XPS), infrared, and Raman spectroscopies. It was proposed that further solution processing of graphene may open many avenues, such as developing functional electronic devices. Furthermore, a liquid-phase exfoliation method called solvothermal-assisted exfoliation process was also used for the production of monolayer as well as bilayer graphene sheets from expanded graphite (EG) precursors using acetonitrile (Fig. 3b) [60]. In this case, the dipole-induced interactions between acetonitrile and graphene caused the exfoliation of graphene. Monolayer as well as bilayer of graphene was further separated by centrifugation. In this regard, during the production of high yield and high-quality graphene, use of any kind of stabilizer or modifier reagent was strongly avoided. Nascimento et al. [65] realized the production of a few-layer of graphene by LPE using 1-cyclohexyl-2-pyrrolidone (CHP)/water mixtures as a medium. The obtained dispersed graphene has flakes which are mostly thinner than that of 5 layers with low defect density (8.3×10^{-3} nm^{-2}) and lateral dimensions in the order of 100 nm. Low et al. [52] demonstrated liquid phase exfoliation as well as solvothermal growth synthesis of graphene/ zinc oxide nanocomposite to develop biosensors. Amperometry and cyclic voltammetry (CV) analysis was used to evaluate the electrochemical performance of graphene/ zinc oxide nanocomposite-modified screen-printed carbon

electrode (SPCE)-based biosensor. The electrode demonstrated enhancement in electrocatalytic activity by reducing hydrogen peroxide (H_2O_2). Furthermore, the nanocomposite was also used to fabricate an electrochemical DNA sensor to detect the Avian Influenza H5 gene.

Chemical vapor deposition

Chemical vapor deposition (CVD) follows the bottom-up approach for graphene synthesis. CVD is considered as the best method for the synthesis of graphene with high quality and large surface areas. Moreover, synthesis strategy by CVD is widely employed due to its simple experimental setup in research laboratories as well as for long-term operation in industrial settings. Moreover, it also has large-scale production capacity. CVD is a chemical process in which a solid thin film of graphene is usually deposited onto transition metal (for example, Cu, Co, Fe, Ni, Pd, and Ir) substrates, with the help of hydrogen (H_2) gas flow as a precursor, at a very high temperature [67]. Many times, methane (CH_4) gas is also used as a reactant. After the discovery of graphene, the first successful production of graphene using the chemical vapor deposition method was reported in 2008 by Coraux et al. [68]. The graphene film was grown on Ir which demonstrated large-scale continuity of its carbon rows with a relatively low density of defects. Furthermore, several studies have been reported on the fabrication of graphene using CVD. For example, a graphene bilayer was prepared on platinum Pt (111) by sequential chemical vapor deposition [69]. This production required a four-step process; in the first step, monolayer graphene was prepared on Pt (111) using thermal decomposition of C_2H_4. The second step involved deposition of thick Pt film, and in the third step, the fabrication of a second layer of graphene was performed. The last step used post-annealing in which the buried monolayer was diffused entirely to the surface, resulting in the formation of extended bilayer domains of graphene. Characterization by scanning tunneling microscopy unraveled the significant growth of graphene. In another study, graphene was deposited by CVD as a durable anticorrosive coating on copper using ethanol as a carbon source (Fig. 3c) [61]. Methane (CH_4) was used as gas precursors to provide stable carbon flow at average growth temperature set around 1000 °C. Consequently, a thin film of double-layered graphene was formed, as confirmed by surface and structural characterization. Graphene-coated copper was kept for more than 1 year at ambient temperature, which exhibited no considerable change in the anticorrosive behavior of graphene.

Graphene has also drawn considerable interest for the development various electronic devices. In this case, for the production of electronic devices, graphene should be grown on a large surface area. In this regard, Li et al. [70] proposed that growing few-layer graphene or large-area graphene films

on metal substrates, e.g., Cu and Ni, was promising by the CVD of hydrocarbons. With the CVD method, high quality of graphene with uniform thickness could be obtained, which demonstrates its potential application in the development of electronic devices. One preferable CVD method was used to fabricate functional devices by transferring of graphene on Si or SiO_2/Si substrate. However, the process shows some degree of contamination. In order to overcome this issue, Ge (001)/Si (001) substrate has been introduced to transfer graphene. Additionally, electron mobility of graphene grown on Ge(001)/Si(001) is quite high [71, 72]. Vyshkvorkina et al. performed a study to compare CVD-grown and exfoliated graphene for its application in biosensors [53]. The results suggested that CVD-grown graphene can be efficient material for the development of surface plasmon resonance (SPR) and surface-enhanced Raman scattering (SERS)-based biosensors, while the exfoliated graphene can be suitable to develop various nanosensors based on nanoelectromechanical systems (NEMS).

Reduction of graphene oxide

GO does not contain all the properties of pristine graphene. Therefore, it is always imperative to reduce GO back to graphene to restore unique properties required for functional wearable devices. For example, GO is an insulator material, which can be converted into a conductor by reduction. However, complete removal of oxygen is not possible, which results in only partial recovery of sp^2 conjugated network of graphene [73]. The obtained material by reduction is called chemically transformed graphene/chemically modified graphene/reduced graphene oxide (rGO). Reduction of GO is performed by many different methods, such as, chemical reduction [33], electrochemical reduction [35], thermal reduction [34, 54], and green reduction [74]. Among the various strategies to reduce GO, the formation of single layer graphene from redried GO by thermal exfoliation or reduction was initially induced by the rapid degradation of epoxy and hydroxyl groups with the generation of gases like CO_2 in the interlayer space [45, 75]. The prime advantage of this methodology is the fast reduction process exceeding the diffusion rate of gases. Besides, high annealing temperature leads to clean the carbon sheet resulting in high electrical conductivity. However, it is well noted that a minimum applied temperature of 550 °C is required to facilitate the reduction phenomena [45]. Moreover, some defects related to topology and vacancy still remains on the reduced sheet even after decomposition of the groups with the release of CO_2 with high annealing temperature [76]. On the other hand, a special thermal reduction method called laser scribing has been widely used over the last decade [77]. Laser scribing is a facile, fast, and cost-efficient method for the production of graphene. The graphene produced from this method is called laser scribed graphene (LSG) method. Numerous studies have been taken to develop biosensors using LSG method. For example, LSG was fabricated as electrode patterns on a polyimide (PI) sheet (Fig. 3e) and utilized as on-chip electrochemical biosensor for the detection of biomarkers, such as ascorbic acid (AA), uric acid (UA), and dopamine (DA) [55]. Moreover, Scardaci et al. have utilized LSG for humidity sensing application [78]. In this regard, continuous wave (CW) laser beam was employed for the reduction of graphene under different controlled atmospheres, such as air, Ar, N_2, and in a 95:5 (v/v) Ar/H_2 mixture. The atmosphere of irradiation highly influences the laser scribing effects, such as degree of reduction, chemical composition, and electrical properties of reduced GO. The materials produced in pure Ar yielded the fastest response and highest sensitivity, whereas mixtures of Ar and Ar-H_2 produced the highest order in humidity sensing. So, the results suggested the importance of controlling the atmosphere in LSG method. LSG method is also an efficient strategy to produced porous graphene structure. Most of the previously reported methodologies to produce porous graphene structure requires high-temperature processing or chemical synthesis routes with several steps which usually rises the graphene synthesis cost. To make the laser scribed graphene production cost-efficient, use of different commercial polymer sheets with cyclic imide group in their molecular chain have been proposed. For example, Lin et al. used a CO_2 infrared laser under ambient conditions to transform polyimide (PI) into porous laser-induced graphene (LIG). Besides, poly(etherimide) could also be converted to porous graphene structure at ambient temperature [79]. Moreover, a laser scribed graphene film could also be produced from polydimethylsiloxane (PDMS) films. The produced graphene films demonstrated excellent flexible properties and high electrical conductivity, thus facilitating its use as flexible conductive layer. A skin-like pressure sensor was also developed using these layers, which exhibited ultrahigh sensitivity (~ 480 K Pa^{-1}) while maintaining excellent cycle stability (> 4000 repetitive cycles) and fast response/relaxation time (2 μs/3 μs) [80].

On the other hand, femtosecond laser direct writing (FsLDW) is another near infrared (NIR) method for the photoreduction of GO. In contrast with LSG method, FsLDW operates in different optical wavelength (790 nm). Moreover, FsLDW technique facilitates complex designable patterning and controllable photo-reduction of GO thin film in comparison with LSG method. In this regard, 100X objective lens (NA:1.4) is employed to concentrate LASER as reported by Zhang et al. [81]. This technique was utilized to directly produce all-graphene-based devices consisting of GO as the sensing material as well as electrodes. Also, the FsLDW technique surpasses the complex manufacturing process by enabling scalable sensor integration on flexible substrates

in a single step which makes it more convenient than that of LSG method.

On the other hand, apart from thermal reduction, some reducing reagents could also be utilized to induce chemical reduction of GO at room temperature by allowing deoxygenation to occur at moderate temperature. In this regard, selective reduction of specific type of oxygen containing group usually takes place. The chemical reduction method is used most frequently for large-scale production of graphene. In this regard, various chemicals, such as borohydrides [82], ascorbic acid [83], hydrohalic acids [84], hydrazine [85], hydroquinone [33], etc., have been utilized for the reduction of graphene oxide. This process takes only 30 min and produces graphene sheets with high bulk electrical conductivity (2.1×10^3 S m^{-1}). Moreover, this reduction results in removal of majority of oxygen-containing functional groups as proved by XPS analysis (Fig. 3d) [62]. Among various chemical reagents, hydrazine can selectively reduce epoxy groups which is initialized by the opening of epoxy ring followed by the generation of amino-aziridine moiety [34, 86]. The amino-aziridine moiety is further transformed to a double carbon bond when di-imide is removed thermally. Strength of chemical reagents play an indispensable role to improve the degree of reduction depending upon the standard reduction potential of the reagents. As an example, standard reduction potential of aluminum powder is quite negative with the value of -1.68 V than that of the well-known reducing agents such as hydrazine and hydride which stood at -1.16 V and -1.24 V, respectively. With the incorporation of hydrochloric acid, aluminum powder can reduce GO more efficiently with high standard reducing potential [62]. In another study, a spontaneous reduction of GO was observed with the incorporation of zinc powder due to the wide gap of standard potential between Zn/Zn^{2+} (-0.76 V) and GO (-0.40 V) [87]. Thus, it is well noted that high standard potential difference between GO and reducing agent plays a prime role to improve the reduction phenomena significantly. Besides, alkaline solution could also play a pivotal role to reduce GO. As an example, in the presence of NaOH, the reduction potential of Al and Zinc are -2.33 V and -1.2 V, respectively, which results in faster reduction of GO in case of Al than that of zinc which usually takes longer time to reduce [88]. Therefore, it is well noted that the strength of the reducing agents to reduce GO depends on their standard reduction potential value. Although, reduction of GO is an indispensable key strategy to eliminate oxygen and restore the original graphene structure, most of the above-mentioned reducing methods exhibit significant number of defects. In addition, different residual functional groups still remain on reduced graphene sheet. Moreover, thermally and chemically reduced sheets have high tendency to agglomerate in the presence of adhesion force between the layers. On the other hand,

high electrical conductivity as well as thermal stability of reduced GO could also be achieved through the reduction by hydrogen arc discharge exfoliation resulting in magnificent electrical conductivity of 200,000 S/m and high thermal stability with oxidation resistance temperature of 601 °C [89]. However, high current density is still necessary to initialize the arc discharge effect. The reduction methods can also be further assessed in terms of degree of reduction. Degree of reduction is one of the prime parameters which modulates thermal and electrical conductivity as well as mechanical strength and chemical performance of the reduced sheet as per the reduction method of GO [90–93]. Moreover, the bandgap, work function, and number of defect sites could be measured in terms of the degree of reduction. Usually, it is determined by the content of residual oxygen remained on the reduced sheets as probed by XPS or EDS (energy-dispersive spectroscopy) [94]. In addition, conductivity test is also an alternative strategy where electrical conductivity of the reduced sheet is directly proportional to reduction degree [95]. In case of thermal and hydrothermal reduction method, the degree of reduction could be enhanced to a certain extent by the virtue of increasing reduction time and temperature [95]. For the further improvement of reduction degree, precise chemical tuning is a prime concern. In addition, thermal reduction methods such as LASER scribed method or other photon induced strategies might be beneficial where light power intensity, exposure time and ambient conditions can be tailored to control reduction degree which results in precise manipulation of the depth and electrical conductivity of reduced GO film. Moreover, precise control over LASER scanning speed and shifting pitch is quite efficient to achieve higher degree of reduction with desired microscopic engineering of GO sheet.

Three-dimensional graphene synthesis

Traditionally, graphene has been utilized as a two-dimensional (2D) material. It also can be synthesized, distributed, hybridized into different 3D materials producing structures, such as aerogels, hydrogels, sponges, and foams. These 3D materials have several outstanding properties, e.g., large surface area, low density, high porosity, stable mechanical properties, fast electron, and mass transport. Moreover, 3D graphene materials widely expand their application into different fields like batteries [96], capacitors [97], biosensors [56], environment [98], and catalysts [99].

Synthesis of 3D graphene follows both the top-down and bottom-up approaches. In the top-down approach, a template is required as a skeleton for the growth of graphene. A 3D graphene foam was grown using the CVD method on a porous Cu/Ni foil, followed by removing the Cu/Ni substrate through etching [100]. In the bottom-up approach, the hydrothermal reduction method is widely applied for 3D

graphene synthesis. Dabiri et al. firstly prepared GO from graphite and then mixed it with ethylenediamine (EDTA) to synthesize 3D graphene hydrogel by hydrothermal treatment. Further, freeze drying was performed to produce 3D graphene aerogel [101] (Fig. 3f).

3D graphene materials could be categorized into several prototypes as per previously reported works. In this regard, in order to ensure interaction scale of 3D graphene, it can be classified into two subcategories, such as (1) 3D graphene macrostructure with dimension more than 100 μm in one or more directions, e.g., 3D graphene foam, sponge, aerogels, microsphere, fiber [63], film, and micropillar [63, 102–106], and (2) 3D graphene microstructure-based materials with dimension less than 100 μm in all direction, which usually looks powder in macroscopic scale [107, 108]. In order to build a macroscopic 3D graphene, GO is utilized as building block which can be assembled through either self-assembly or reduction of GO. There are two types of interactions facilitating self-assembling of GO including (1) binding interaction generated from hydrogen bonding, $\pi - \pi$ interaction, and hydrophobic effect, and (2) 3D interaction from electrostatic repulsion formed by functional groups and hydration [109–111]. During the reduction of GO, the enhancement in $\pi - \pi$ interaction method could be observed where the cross-linking sites with $- CH_2 -$ and $- CH_2O -$ moieties could be transformed into conductive sp2 carbon bridges [112].

Methods for patterning graphene

Since 2004, graphene has given hope for scientists and industrialists with its remarkable properties which has proven its potential in various applications. Many researchers have explored the usage of graphene, and the impact of its patterning methods which is considered as a crucial factor for better performance. Graphene patterning can be conducted after synthesis or along with synthesis based on the application for both single layer and multilayer. The choice of patterning could be depended on various factors, such as application, method of synthesis, layers, etc. Some of the most widely used patterning methods are photolithography, electron-beam (E-beam) lithography, focused ion-beam lithography, laser scribing, inkjet printing, and screen printing which have been discussed in detail in the following section. Moreover, the comparison of different patterning techniques used in graphene-based devices is also summarized in Table 4.

Photolithography

The standard photolithography method is used for graphene patterning. As mentioned earlier, the CVD-grown graphene is typically obtained on a copper sheet, while the synthesized graphene is transferred onto the required surface. The CVD-grown graphene thickness is ideal for photolithography, and thus, graphene patterning can be achieved by coating on a photoresist as per need and then treating with plasma etching [122]. As photolithography is a common technique for graphene patterning, it is considered as an easier way for scale-up [123]. A schematic example of device fabrication based on photolithography is presented in Fig. 4a. The simplicity and broad applicability of photolithography made this technique more acceptable in sensor developments. Zhou et al. developed a label-free detection system for detecting cancer biomarkers using graphene field-effect transistor (GFET) based on photolithography [113]. Throughout the innovative graphene device developments, we can see various examples using photolithography [124–126].

Table 4 Comparison of different patterning techniques used in graphene-based devices

| Methods	Advantages	Limitations	Applications	Ref
Photolithography	High resolution, direct patterning, large area coverage	Usable for mainly 2D structures only	GFET for biomarker detection	[113]
E-beam lithography	Direct patterning, high resolution, fast turnaround time, no need of physical mask	Consumes more time, small area coverage, expensive and complicated	Developing sensors for biomarker detection	[114, 115]
Focused-ion-beam Lithography	Very high resolution, direct patterning	Relatively slow, small area cover-age, 2D technique	Developing biomolecule detection sensors	[116]
Laser scribing	Direct and easy patterning, programmable	Difficult to control quality, low resolution	Developing biosensors for biomolecule/biomarker detection	[117]
Inkjet printing	Adaptable for 3D structures, programmable, direct patterning	Low resolution	Flexible electronics and biosensors	[118, 119]
Screen printing	High flexibility, simplicity	Poor precision, hard to reproduce exact result	Flexible electronics	[120, 121]
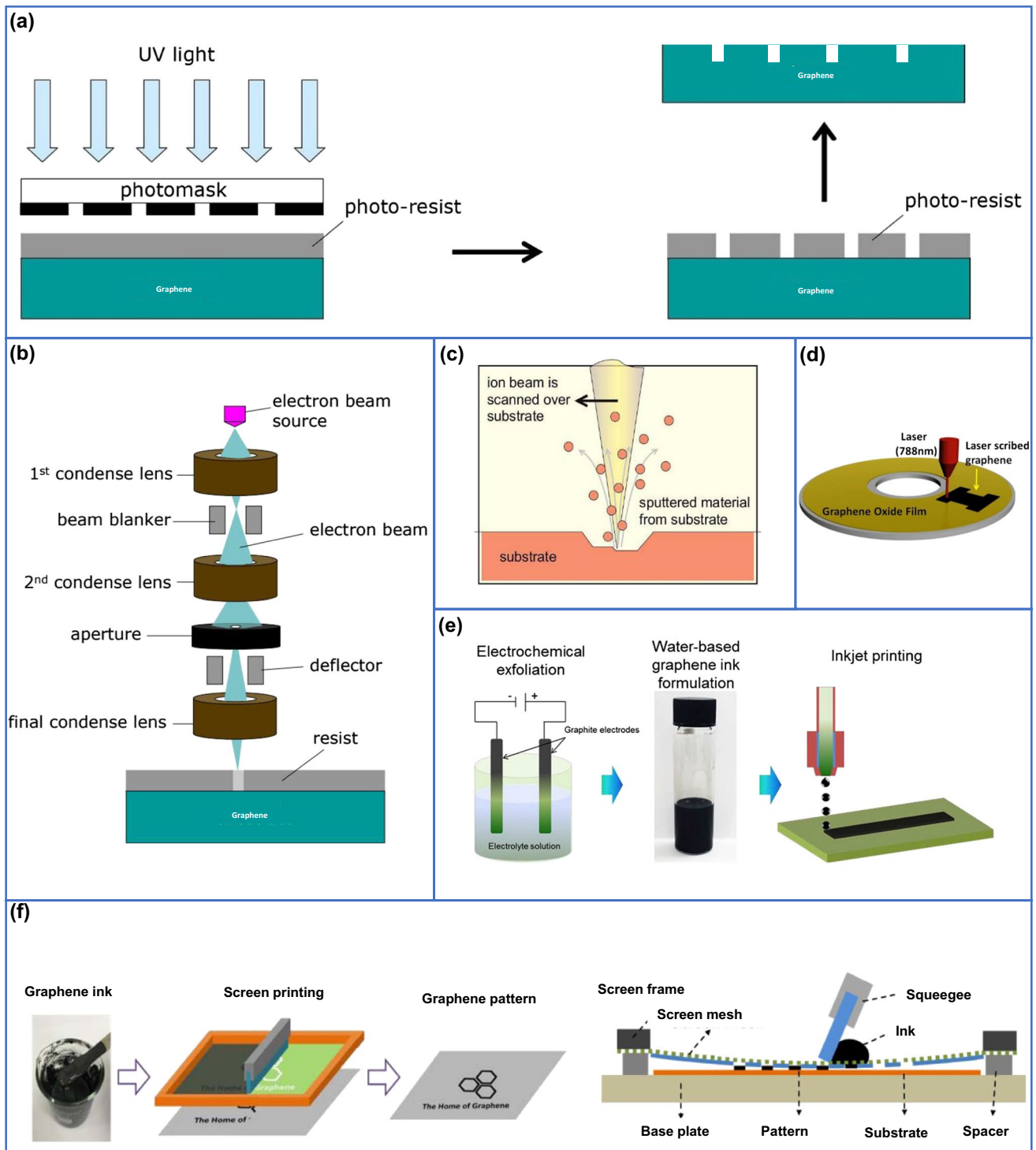
Fig. 4 **a** Schematic diagram of photolithography process. Reprinted with permission from [122]. Copyright Faculty of Engineering, Chulalongkorn University. **b** Schematic diagram of e-beam lithography. Reprinted with permission from [122]. Copyright Faculty of Engineering, Chulalongkorn University. **c** Schematic diagram of focused ion beam lithography used for milling and deposition. Reprinted with permission from [127]. Copyright 2021 Institute of Physics Publish-ing. **d** Schematic diagram of DVD laser scribing for graphene patterning. Reprinted with permission from [128]. Copyright 2013 Springer Nature. **e** Schematic showing water-based inkjet printing of graphene patterning. Reprinted with permission from [129]. Copyright 2021 Elsevier. **f** Schematic diagram of screen printing of graphene. Reprinted with permission from [130]. Copyright 2019 American Chemical Society

Electron-beam lithography

Electron-beam (E-beam) lithography (EBL) is a method that uses a focused electron beam to produce the desired pattern in a suitable recording medium [122]. E-beam lithography provides lithographic resolution in nanometer-scale and makes it possible to write complex patterns for various applications. Fischbein et al. have demonstrated that the technique can be used to create nanometer-scale pores, slits, and gaps on the graphene surface, with the help of e-beam irradiation from a transmission electron microscope [131]. A schematic diagram of e-beam lithography is shown in Fig. 4b. The method is used to develop different graphene-based sensors, such as peptide-enabled biosensors for detecting different biomarkers, especially cancer biomarkers [114, 115].

Focused ion-beam lithography

Focused ion-beam lithography (FIBL) is a site-specific material removal or material deposition technique used to create the desired patterns [127]. The patterning is achieved typically using the collision of gallium ions [132]. This technique is used for nanofabrication processes, such as milling, etching, etc., with excellent controllability of the size and structure (Fig. 4c). To achieve precise nanofabrication with high resolution, helium ions have been proposed to replace conventional gallium ions [133, 134]. The applications of this specific method is explored by many researchers, and they have developed a biomolecule detection sensor using graphene with focused ion-beam lithography (FIBL) [116].

Laser scribing

Laser scribing is a method in which the laser is used to create small cuts over the material (Fig. 4d). This technique helps to reduce micro cracks during patterning [20, 128]. As this technique is a more efficient method to directly modify graphene, it is widely used for patterning. The pattern is loaded and developed with the help of lasers over carbon sources or polymers. Being an efficient and easier method, this technique is adapted in the development of various biosensors. Vanegas et al. used laser scribed graphene to create a biosensor for the detection of biogenic amines in food samples [117].

Inkjet printing

Inkjet printing is a widely employed technique that uses a programmable controller to spray ink through a well-controlled ejection of ink droplets to obtain the desired pattern [20, 135]. The ink, which can contain various chemicals such as graphene, is sprayed through a nozzle to the substrate. The technique could be used for a lot of applications all around the world with digital and additive patterning. The schematic diagram of inkjet printing is shown in Fig. 4e [129]. Graphene inks could be an excellent replacement for conventional carbon-based inks, as the latter shows limited conductivity [136]. Secor et al. has developed and demonstrated the usage of graphene ink to print highly conductive graphene patterns for flexible electronics [137]. The inkjet printing is highly usable in bio sensing also, such as Xiang et al. developed a biosensor based on FET fabricated by inkjet-based graphene printing on a flexible substrate [118]. Kudr et al. developed a HT-2 mycotoxin immunosensor from graphene oxide printed by inkjet [119].

Screen printing

Screen printing is similar to other printing methods such as inkjet printing and gravure printing [130]. However, the process requires a printable ink, a stencil mesh, and a squeegee as the main elements. The ink is deposited on the stencil in front of the squeegee. Thereafter, the ink is emptied and evenly spread using the squeegee to form the patterns (Fig. 4f). Even though a major part of the ink will be transferred onto the substrate, some parts of the ink will still remain in the mesh. The concept of screen printing is applied also majorly in textile industry [138] and flexible electronics production [120, 121].

For flexible electronics production, mainly conductive inks are used. Therefore, as graphene has really good conductive properties, it is an excellent choice for ink production and screen printing [130]. The prepared graphene ink is transferred on to the substrate to produce thick film patterns for the developments of biosensors and flexible electronics.

Other patterning methods

There are many other conventional and non-conventional patterning methods used by different researchers for the effective patterning according to their need. Some of these techniques are derivatives of the abovementioned methods and some are entirely unconventional. Oliveira et al. has used self-assembly method to develop a graphene-based biosensor to detect urea and penicillin in which they observed improved sensing performance in comparison to the conventional sensors [139]. Secor et al. demonstrated gravure printing technique to directly pattern the surface which removes the need for etching, to develop flexible electronics using graphene [140]. Ameri et al. used direct dry patterning, i.e., direct patterning using a mechanical cutter to develop patterns of graphene for developing epidermal tattoo like sensor [141]. Zhao et al. explored the usage of microwaves for patterning graphene [141]. New patterning methods will likely be introduced according to the need and structure of the pattern. The patterning of graphene layers and graphene

derivatives are highly usable to modify the performance of various sensors.

Sensing strategies used in wearable graphene-based biosensors

There are several biosensing strategies followed in graphene-based biosensors such as colorimetry, surface plasmon resonance (SPR), fluorescence spectrometry, mass spectrometry, and gas chromatography. However, most of those techniques require cumbersome or expensive instruments with complex operating or transduction methodology which are not suitable for wearable application of graphene-based biosensors. In order to avoid this major bottleneck, electrochemical-based sensing strategies have been mostly followed in wearable application of graphene-based biosensors owing to their adaptability in wearable format, sensitive response, selectivity, and fast response. Different electrochemical sensing strategies employed in wearable sensors have been discussed in the following.

Chronoamperometry

Amperometry is an electrochemical approach in which variations in current caused by electrochemical oxidation and reduction are recorded directly with time while a constant potential is determined at the working electrode in relation to the reference electrode (Fig. 5a (i, ii)) [142–145]. In amperometry, platinum is often used as the working electrode to measure oxygen reduction while Ag/AgCl is employed as the reference electrode to measure current at a constant potential [146]. The current generated by the faradaic reaction is proportional to the concentration of the electroactive species in the sample [147, 148]. At constant potential, electron transfer takes place at a diffusion-controlled pace; hence, the process is now governed by mass transfer. The diffusion regulated current I is determined by the diffusion layer thickness δ, the analyte diffusion coefficient D, the electron transfer number n, the electrode surface area A, the analyte concentration C, and the Faraday number F (96,480 C mol^{-1}) as illustrated in Eq. (1):

$$i = \frac{nFAD(C_{bulk} - C_{x=0})}{\delta} \tag{1}$$

where C_{bulk} and $C_{x=0}$ represent the analyte concentration in the bulk solution and concentration of the surface of the electrode, respectively.

Chronoamperometry employs pulsed amperometric detection with a few microliters of solution without stirring. For an instance, a wearable sweat sensor has been proposed which was based on rGO/SiO$_2$ nanocomposite, glucose oxidase

(GOx) and Nafion (NF) coated conductive and flexible substrate comprised of a carbon nanotube film and polydimethylsiloxane (C-PDMS). Sensing performance of NF/GOx/rGO/SiO$_2$/C-PDMS was evaluated by using amperometric $I - T$ curve analysis for different concentration of glucose at an operating potential of 0.4 V and after 100 s, the equilibrium current values were fitted [149]. The biosensor exhibits glucose detection range of 0.1–9 mM with sensitivity of 60.8 μA mM^{-1} cm^{-2}. In this regard, one benefit of chronoamperometric analysis is that it can determine the diffusion coefficient even when sluggish heterogeneous electron transfer kinetics are present, because the potential may be stepped to a suitably positive or negative value where the process is under diffusion control. As in this case, mass transport is exclusively regulated by diffusion under these conditions, the current as a function of time reflects the concentration gradient near the electrode surface. As a result, according to the Cottrell equation, the current diminishes with time where n, F, A, C, D, and t are the number of electrons transformed, Faraday's constant, the surface area, the concentration, the diffusion coefficient, and time, respectively. The current can be related to the concentration of electroactive species as [158] follows by Eq. (2):

$$i(t) = \frac{nFACD^{1/2}}{\pi^{1/2} + t^{1/2}} = K^{1/2} \tag{2}$$

Cyclic voltammetry

Voltammetry is an electrochemical technique that measures current by altering potential. There are several types of voltammetry including polarography (DC voltage) [159], linear sweep, differential staircase, normal pulse, reverse pulse, differential pulse, and others [160]. The voltage is measured between the reference and working electrodes, while the current is measured between the working and counter electrodes as shown in (Fig. 5b (i, ii)) [150, 151]. The Nernst equation governs cyclic voltammetry (CV) and an electrochemical method is used for measuring current under high voltage. The Nernst equation is used to calculate the cell potential in relation to the standard potential and the activities of electroactive species [150, 161] by applying the following equation (Eq. (3)) (where E = reduction potential, E^0 = standard potential, R = universal gas constant, T = temperature in Kelvin, n = mole of electrons, F = Faraday constant):

$$E = E^0 - \frac{RT}{NF} lnQ \tag{3}$$

Potentiometry

Potentiometry is a technique to measure the potential difference between working electrode and reference
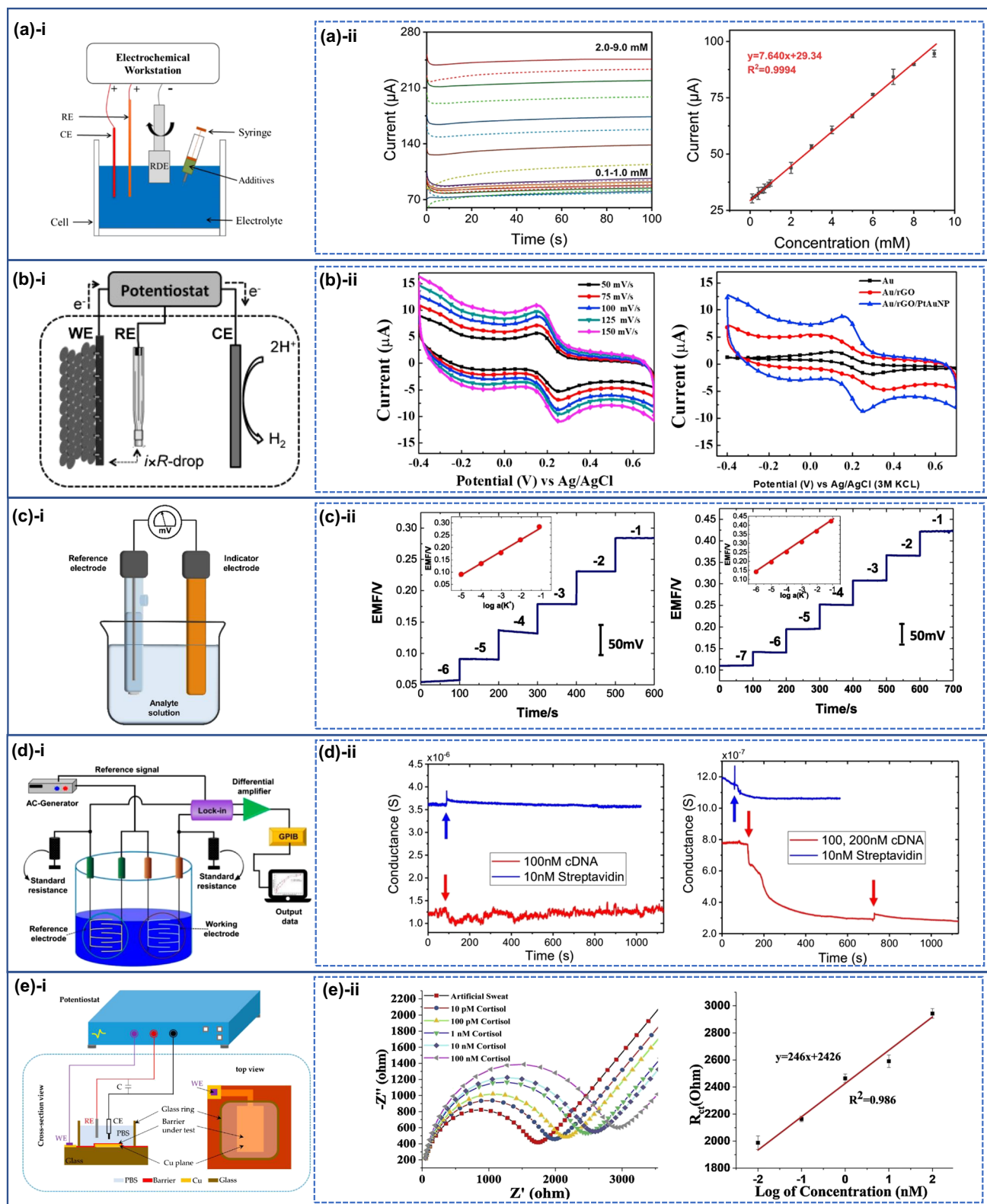
electrode (Fig. 5c (i, ii)) in an electrochemical cell when no or little current flows between them [142, 146, 152, 153, 162]. The Nernst equation already explains the link between concentration and potential. Direct measurement of analyte ion concentration using the Nernst equation is referred to as direct potentiometry. The ion selective electrode (ISE) achieves the lowest detection limit and also functions as a transducer, which is an electrochemical

sensor based on a thin film or selective membrane as a recognition element [163]. Potentiometry can readily measure small sample volumes and pH electrode is the most frequent potentiometric device, however other ions such as F^-, I^-, CN^-, Na^+, K^+, Ca^{2+}, and NH_4^+ could also detected. Many potentiometric devices use various types of field effect transistor (FET) devices to monitor pH changes, selective ion concentration, and the kinetics of biocatalytic and reaction processes.

Conductometry

Conductometric measurements are connected to a solution's capacity to conduct an electric current (Fig. 5d (i, ii)) [154]. It is a universal approach for detecting ions that is used to examine ionic species and monitor a chemical reaction by evaluating the electrolytic conductivity of reacting species and the resulting product. It is the most commonly employed to examine enzymatic reactions and various biological membrane receptors using interdigitated microelectrodes, ion conductometric and impedimetric devices [162, 164]. The electrolytic conductance, G, of a medium is equal to the reciprocal of its electrical resistance R in ohms can be expressed as

$$G = \frac{1}{R} \tag{4}$$

If we consider the electrolytic cell with two electrodes having cross-sectional area A in m^2 and separated by a distance l in m, then the resistance R of electrolytes solution present between the electrodes is

$$R = \rho \frac{l}{A} \tag{5}$$

where ρ is the proportionality constant called specific resistivity. Substituting the value of R from (5)

$$G = \frac{1}{\rho(A/l)} = K\frac{A}{l} \tag{6}$$

where K is reciprocal of specific resistance called specific conductivity and is measured in $\Omega^{-1}\ m^{-1}$. In the SI system, the unit of conductance is "Siemens" (S). Hence, the unit of specific conductivity will be [$S\ m^{-1}$], where A is the area of cross section (m^2), l is the length (m), and G is the conductance (Ω^{-1}).

Electrochemical impedance spectroscopy

Electrochemical impedance spectroscopy (EIS) is a strong tool for material characterization in electrochemical systems. It is helpful for the monitoring of changes in electrical characteristics caused by biorecognition processes at the surface of modified electrodes. Protein immobilization and antibody-antigen reactions on the electrode surface can be used to evaluate the changes in conductance [165, 166]. The basic strategy of the EIS method is to apply a small amplitude of sinusoidal excitation signal and to measure the response as current, voltage, or another signal of interest (Fig. 5e (i, ii)) [156, 157, 167]. Moreover, it is often monitored with a modest excitation pulse, resulting in a pseudo-linear cell response. The current response to a sinusoidal potential in a linear system will be sinusoidal at the same frequency but displaced in phase, as illustrated below. The excitation signal has shape when expressed as a function of time.

$$E_t = E_0\sin(\omega t) \tag{7}$$

where E_t is the potential dependent on time, E_0 is the amplitude of signal, and ω is the radial frequency. The relationship between radial frequency ω (expressed in radians/second) and frequency f (expressed in Hertz) is:

$$\omega = 2\pi f \tag{8}$$

In linear system, the response signal, I_t, is shifted in phase (Φ) and has different amplitude

$$I_t = I_0\sin(\omega t + \Phi) \tag{9}$$

An expression analogous to ohm's law allows us to calculate impedance of system as:

$$Z = \frac{E_t}{I_t} = \frac{E_0\sin(wt)}{I_0\sin(wt+\Phi)} = Z_0\frac{\sin(wt)}{\sin(wt+\Phi)} \tag{10}$$

As a result, the impedance (Z) is represented in terms of a magnitude, Z_0, and a phase shift Φ as mentioned above.
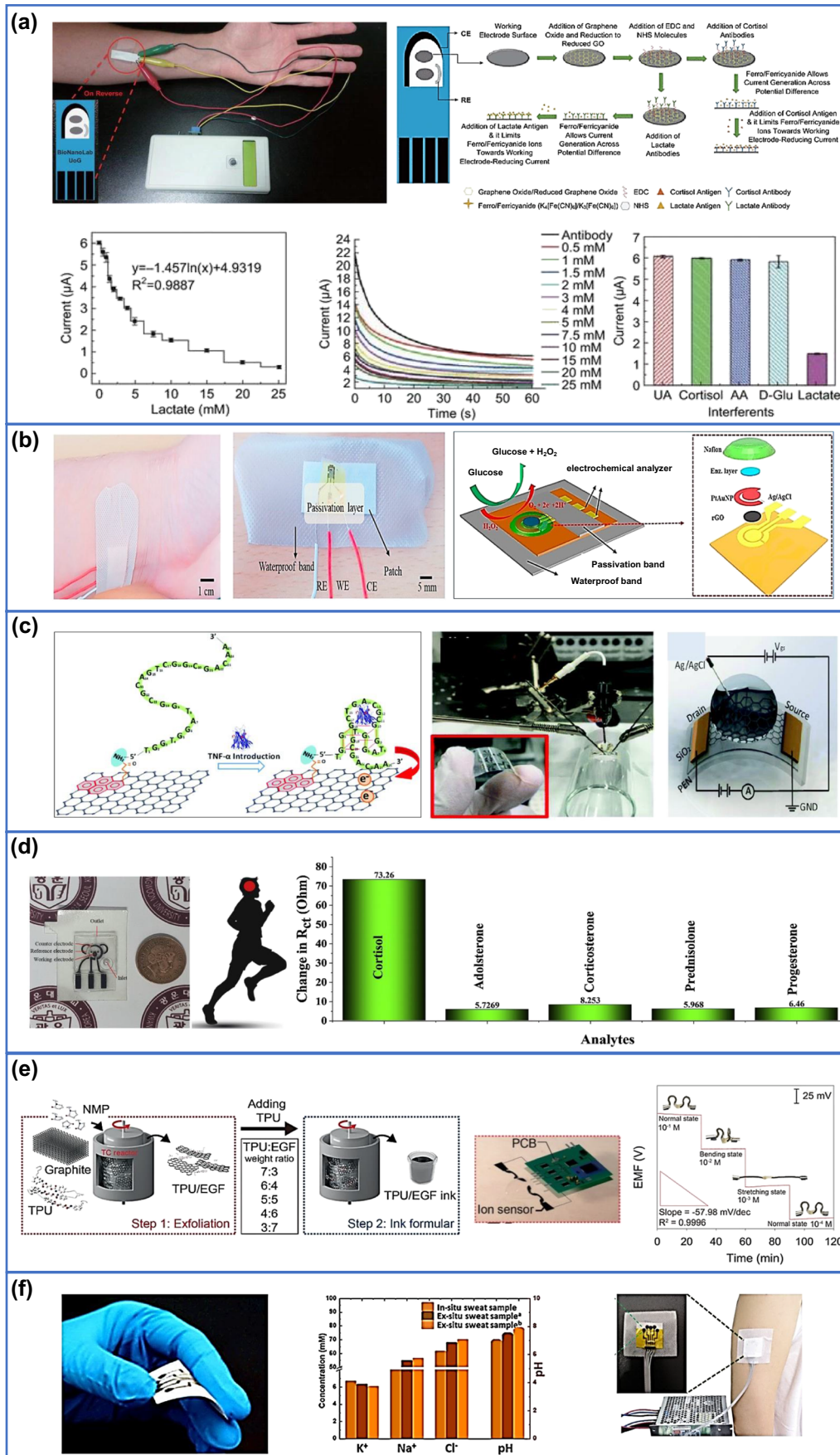
◄**Fig. 6 a** Detection of lactate using graphene embedded screen-printed electrode. Reprinted with permission from. [145]. Copyright 2018 Springer Nature. **b** Au/rGO/AuPtNP/GOx/Nafion-based miniaturized hybrid working electrode-based wearable biosensor to monitor glucose in real human sweat. Reprinted with permission from [151]. Copyright 2018 Elsevier. **c** Detection of cytokine using graphene-Nafion biosensor. Reprinted with permission from [194]. Copyright 2021 Wiley–VCH. **d** Wearable immuno-sensor based on laser-burned graphene with incorporation of $Ti_3C_2T_x$ MXene for non-invasive sweat cortisol detection. Reprinted with permission from [157]. Copyright 2021 Elsevier. **e** Flexible wearable electronic devices to measure Na^+ ion detection. Reprinted with permission from [195]. Copyright 2021 Wiley–VCH. **f** A multi-ion sensing system based on multichannel electrochemical all-solid-state wearable potentiometric sensor for real-time sweat ion monitoring. Reprinted with permission from [153]. Copyright 2019 Elsevier

Classification of graphene-based wearable biosensors

Human skin is the most accessible organ of body fluids related to the current health conditions [168]. Body fluids are broadly classified into two categories, such as intracellular and extracellular. Biofluids secreted through the human body are saliva, sweat, tears, and intestinal fluid (ISF). These biofluids are considered as an important source of biomarkers for disease diagnosis as well as monitoring, since it is easy to collect them to provide rapid results. Concentration of different biomolecules depends on the type of the sampled biofluids. For instance, sweat contains high concentration of proteins, hormones, and DNA, making it an attractive biofluid for non-invasive health monitoring [169, 170]. Intestinal fluid is another chemically rich biofluid and contains many molecules similar to those found in blood [171]. On the other hand, saliva is the easiest to obtain biofluid. Moreover, it contains variety of electrolytes including sodium potassium, calcium, magnesium, bicarbonate, and phosphate [172]. However, the concentration of the available biomolecules in saliva are mostly low. Similarly, tear composition also includes high concentration of salts, proteins, lipids etc. In this regard, by detecting the protein level, syndrome such as dry eye can be identified [173]. In addition, exhaled breath is an excellent source for detecting various biomarkers and moisture content [174]. Therefore, wearable sensors based on these biofluids and exhaled breath are the most promising candidate for the next generation diagnosis system and in present [175].

Biofluid sensors and breath sensing devices

Sweat sensing devices

Sweat plays an important role in continuous disease progression monitoring, non-invasive detection, effective data gathering and reading. Sweat as biofluid performs an important excretory role by removing excess micronutrients, metabolic waste, and toxicants from the body [176]. The body has three types of sweat glands, i.e., eccrine, apocrine and apoeccrine [177]. Eccrine sweat glands are found almost everywhere on the body's surface and are responsible for the majority of sweat output. Apocrine and apo-eccrine glands, on the other hand, have a minor influence on general sweat production [178]. Human body contains 2–4 million eccrine sweat glands on both glabrous (palms, soles) and non-glabrous (hairy) skin [4]. Sweating can be produced by physical exertion, thermal heating, and stress or iontophoretic activation. Sweat contains metabolites (lactate, glucose, urea, ethanol, or cortisol) along with electrolytes (sodium, potassium, chloride, or ammonium), trace elements (zinc or copper), and a small number of large molecules (proteins, nucleic acid, neuropeptides, or cytokines) [4]. In addition to glucose, lactate is also one of the most important metabolites found in sweat [179]. It is a waste product formed during glycolysis process. Under the normal condition, liver absorbs 70% of the lactate but under abnormal condition, such as liver necrosis, the liver fails to absorb lactate, and it cause muscle fatigue and acidosis. A sensitive and specific immunosensor has been developed for detection of lactate in sweat sample where lactate antibodies were bio-conjugated to the electro reduced graphene oxide (e-RGO) using carbodiimide chemistry (Fig. 6a) [145]. Moreover, sweat lactate is also useful in reflecting the poor oxidative metabolism and in pressure ischemia as reported by few groups [180]. On the other hand, diabetes is a chronic disease related to inadequate insulin synthesis in the cell and is difficult to cure or prevent after being diagnosed. By proper glucose monitoring, measurement technique one can increase treatment efficiency and simplify patient lifestyle [181–183]. The classic glucose testing method, "finger pricking," is a well-known method for detecting blood glucose, but it has a major drawback that leads to patient non-compliance. As a result, there is an urgent need to develop non-invasive glucose monitoring methods since human sweat samples contain a variety of analytes [184–187]. Skin worn GOx/Pt-modified graphite-based stretchable biosensor has been successfully applied to monitor glucose in human perspiration through the quantification of hydrogen peroxide (H_2O_2) reduction by chronoamperometry at -0.35 V vs pseudo-Ag/AgCl. The sensor have a linear range between 0 and 0.9 mM with limit of detection of 0.010 mM [188]. On the other hand, the CVD-grown graphene-based FET sensor hold great promise in continuous glucose monitoring based on wearable platform. In this regard, PET was used as a substrate, and CVD-grown graphene was functionalized on PET with a linker molecule. The fabricated sensor could detect glucose level in the range of 3.3–10.9 mM with limit of detection of 3.3 mM by the precise quantification of Dirac point shift and differential source current [189]. Patch-based flexible and miniaturized electrochemical glucose biosensor comprising of a hybrid working electrode which consists of

electrochemically deposited gold/platinum nanoparticles and platinum alloy nanoparticles (AuPt NPs) onto rGO surface and chitosan-glucose oxidase composites was successfully developed to measure glucose in a solution of human sweat. The fabricated biosensor exhibited excellent amperometric response for glucose detection at a detection range of 0–2.4 mM (within the clinical range if glucose in sweat), with a sensitivity of 48 µA/mM cm^2, a short response time (20 s), and high linearity (99%). The limit of detection for glucose was calculated as 5 µM (Fig. 6b) [151]. On the other hand, hybrid hydrogel nanocomposites have also shown great potential in glucose level detection. A recent example of the hydrogel-based prototype of glucose biosensor device was fabricated by deposition of polyaniline (PANI) on rGO. The thermally exfoliated graphene oxide (TEGO) helps in the formation of additional crosslink, thereby increasing electrochemical property. The sensor exhibits glucose detection range of 0.2 µM–10 mM with limit of detection of 0.2 µM [190]. Furthermore, it was well noted that graphene doped with gold and combined with a gold mesh has improved electrochemical activity over bare graphene which was sufficient to form a wearable patch for sweat-based diabetes. In this regard, a stretchable device was developed which features a serpentine bilayer of gold mesh with glucose detection range of 10 µM–0.7 mM and limit of detection of 10 µM [191]. Furthermore, a simple and easily wearable device was also developed for simultaneous monitoring of glucose and lactate in human sweat without direct contact of the active part with skin. In this method, glucose oxidase and lactate oxidase were anchored to graphene oxide and chitosan composite (GO-Ch) to achieve stable deposition of the bio-receptors on the electrochemical platform. The device was integrated with the capillary flow system activated by a nitrocellulose strip to collect and deliver sweat on the sensor platform with limit of detection of 9.6 µM and 20 µM for glucose and lactate, respectively [192]. Besides, non-enzymatic and simultaneous detection of glucose and lactate have also attracted considerable interest. In this regard, metal-based organic framework (MOF) electrodes were used as non-enzymatic electrochemical biosensors for detection of glucose and lactate. In this method, the electrode was functionalized by aminofunctionalized graphene paper modified with 2D oriented assembly of Cu$_3$(btc)$_2$ (BTC = benzenen 1,3,5-tricarboxylate) nanocubes via facile interfacial synthesis and effective dipcoating. The biosensor shows a linear dynamic range of 0.05 to 22.6 mM with a detection limit down to 5 µM for lactate and 0.05–1775.5 µM with a detection limit down to 30 nM for glucose [193].

Hormones are secreted by a special group of cells called endocrine glands. They play a pivotal in controlling and regulating the activity of certain cells, and organs in the human body [196–201]. Various diseases such as osteoporosis, cardiovascular, adenoma, hyperplasia, and cancer are related to hormone imbalance. Therefore, detection of hormone through the human sweat is an interesting tool in biomarker [202, 203]. Due to psychological and emotional stress, hormones such as cortisol are secreted in human body [204, 205]. A pleiotropic cytokine produced by activating monocytes/macrophages in inflammatory response such as tumor necrosis factor-alpha (TNF-α) is an important biomarker of autoimmune diseases [206–209]. In this regard, a flexible wearable aptameric graphene–Nafion field-effect transistor-based sensor has been developed for the detection of cytokine biomarker in undiluted sweat sample of human as shown in Fig. 6c. The graphene-Nafion composite film effectively eliminate non-specific adsorption interferences and biosensor has sensitive detection of IFN-γ, a representative inflammatory cytokine with detection range from 0.015 to 250 nM and LOD down to 740 fM [194]. Besides, Ti$_3$C$_2$T$_x$-MXene nanosheet was successfully incorporated in porous laser burned graphene (LBG) to develop wearable electrochemical immuno-sensor patch with a microfluidic channel to detect cortisol (Fig. 6d). The stretchable patch sensor exhibited linearity and limit of detection of 0.01–100 nM and 88 pM, respectively. The sensor was attached to human skin, and the secreted sweat was passed to the microfluidic channel through a hole under natural pressure [157]. Continuous monitoring of diabetes and kidney failure from wearer sweat was also visualized using cellulose nanofiber/chitosan-graphene oxide-based wearable sensor devices. This colorimetric sensor can readily differentiate glucose and urea level by the naked eye. The sensor exhibit a linear range of 0.1–3 mM with detection limit of 0.1 mM for glucose and a linear range of 30–180 mM with detection limit of 30 mM for urea, respectively [210]. In addition to metabolites and hormones, Na$^+$ and Cl$^-$ are the most abundant ions responsible for the production of sweat among all the electrolytes [211].

In this regard, a modification of CFTR protein facilitates the transportation of Na$^+$ and Cl$^-$ ion in epithelial secreting cells [212, 213]. Consequently, muscle cramps, dehydration, hyponatremia, and hypokalemia usually occurs owing to the variation of Na$^+$ and K$^+$ ions concentration in sweat [214]. In order to develop graphene-based wearable biosensor for Na$^+$ ion detection, highly conductive, stretchable, and printable ink was fabricated through the incorporation of exfoliated graphene flakes into viscoelastic thermoplastic polyurethane. The wearable biosensor was further employed to measure Na$^+$ ion concentration from the perspiration of a volunteer during physical stretching. The sensing performance was maintained under an extremely high strain level of 300% over 10,000 cycles in a fatigue test. The sensor exhibits detection range from 10^{-1} to 10^{-4} M with limit of detection of 2.5×10^{-6} M (Fig. 6e) [195]. In another study, the ion-selective membrane (ISM) on a 3D porous structure comprising a MOF/graphene network is used to monitor

ammonium NH_4^+ ion content. The hydrophobic property of the ion-selective membrane gives an excellent sensing response to NH_4^+ ion concentration with detection range $10^{-6} \sim 10^{-1}$ M (Fig. 6e) [215]. On the other hand, a multi-ion sensing system based on flexible, all-solid-state, ion-selective electrode (ISE) wearable potentiometric sensor provides information about the quality of persons' health by monitoring K^+, Na^+, Cl^-, and pH ion concentration in sweat. It could be integrated with a self-powered unit as well as combined with mobile devices for in situ analysis in the field of healthcare and clinical research. The integrated solid ISE has four channels which can detect K^+, Na^+, Cl^-, and pH simultaneously with limit of detection of ~ 6.5 Mm, ~ 49.5, ~ 61.4, and ~ 6.91 for K^+ Na^+, Cl^-, and pH, respectively (Fig. 6f) [153]. Finally, Table 5 summarizes the detection of different analytes in sweat along with the respective sensing strategy.

Interstitial fluid sensing devices

The human body is a treasure of various biofluids such as urine, sweat, saliva, blood, cerebrospinal fluid, gastric juices, and blood [216]. These biofluids contain a complex mixture of substances and are attractive sources for disease diagnosis. However, withdrawing biofluids such as blood by inserting a needle is very painful, sometimes tedious, and makes patients discomfort; therefore, recent emphasis is given on externally secreted biofluids (sweat, saliva,

tear). A major component of these non-invasive collected biofluids is water. Thus, analysis of human body fluid has become one of the most promising approaches to discover biomarkers or reveal a path for physiological mechanisms of human disease [217, 218]. Sweat and saliva are easily obtainable biofluid, but they have some limitations and lead to contamination, while other biofluids such as interstitial fluid serve as unique biomarkers in disease diagnosis [219, 220]. ISF is most prevalent accessible fluid in the body, constituting 75% of extracellular fluid and 15 to 25% of body weight. It acts as bridge between blood and cells [221]. ISF is mostly present in the lowermost skin layer of dermis, which is 70% by volume [222]. Some studies have shown that interstitial fluid act as a rich source of information compared to blood. Spaces between cells is filled with ISF, and it is formed by extravasation of plasma from capillaries [223] (Fig. 7a), and which is modified due to metabolic process. ISF fluid flow from blood plasma through endothelial cell wall into interstitial compartments (region between the vasculature and cells) and then return to the blood [221–225]. It acts as mediator between blood vessels and cells in constant supply of nutrients and waste product [226]. Flexible electrochemical glucose sensor integrated with the ISF extraction is used to form wearable devices and which is further utilized for the extraction, dilution, collection, and detection of ISF to realize continuous glucose monitoring. Graphene layer was modified with gold nanoparticles to improve electron transfer rate between

Table 5 Summary of the detection of various analytes by different sensing strategies in sweat

| Analyte	Sensing material	Mechanism	Detection range	Detection limit	Ref
Glucose	CVD-grown graphene	Field effect	3.3–10.9 mM	3.3 mM	[189]
Glucose	Prussian blue/gold-doped graphene hybrid /GOx	Cyclic voltammetry/patch	10 µM ~ 0.7 mM	10 µM	[191]
Glucose	GOx/Pt-graphite biosensor	Chronoamperometry	0–0.9 mM	0.010 mM	[188]
Glucose	PtAuNP/rGO/CHIT/GOx	Amperometry/patch	0 ~ 2.4 mM	5 µM	[151]
Glucose	Amino-functionalized graphene paper/$Cu_3(btc)_2$ nanocubes	Electrochemical	0.05 ~ 1775.5 mM	5 µM	[151]
Glucose	Cellulose nanofiber/chitosan-graphene oxide	Colorimetry	0.1–3 mM	0.1 mM	[210]
Glucose	PANI/TEGO/PVA	Electrochemical	0.2 µM ~ 10 mM	0.2 µM	[190]
Lactate	Amino-functionalized graphene paper/$Cu_3(btc)_2$ nanocubes	Electrochemical	0.5 ~ 25 mM	5 µM	[193]
Lactate	SPE/PB/GO-Ch/GO-xf	Amperometry	1.0–50.0 mM	28 nM	[192]
Urea	Cellulose nanofiber/chitosan-graphene oxide	Colorimetry	30–180 mM	30 mM	[210]
Cortisol	Ti_3C_2x MXene/LBG/PDMS	Impedimetric immunosensor	0.01–100 nM	88 pM	[157]
Cytokine	Graphene-Nafion	Field effect	0.015–250 nM	740 fM	[194]
K^+	Paper-based ion selective electrode/fluorinated alkyl silane/GO	Potentiometry	~6.5 mM	NM	[153]
Na^+	Paper-based ion selective electrode/fluorinated alkyl silane /GO	Potentiometric	~49.5 mM	NM	[153]
Cl^-	Paper-based ion selective electrode/fluorinated alkyl silane/GO	Potentiometric	~61.4 mM	NM	[153]
pH	Paper-based ion selective electrode/fluorinated alkyl silane /GO	Potentiometric	~6.91 mM	NM	[153]

NM not mentioned
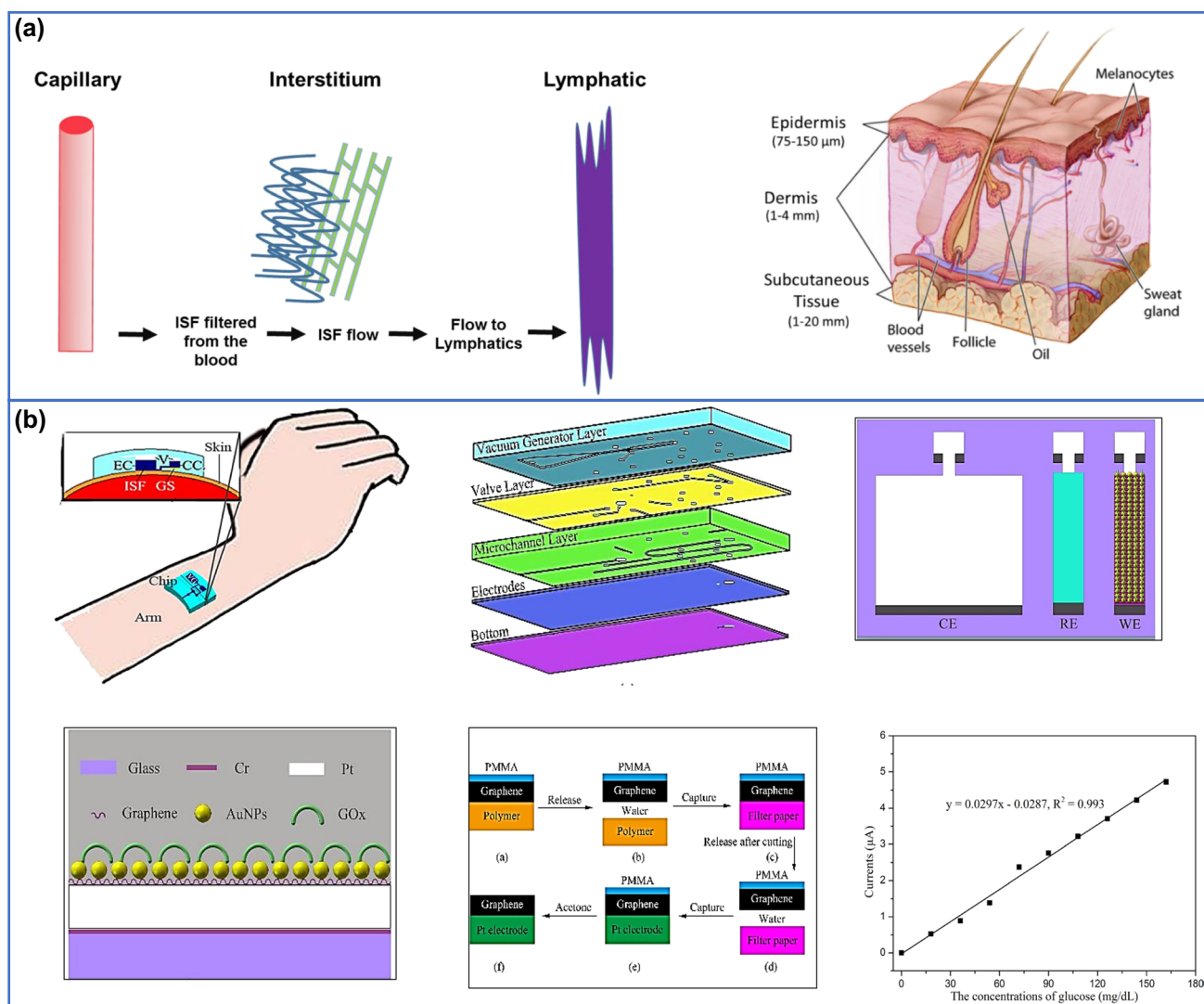
Fig. 7 **a** Interstitial fluid moment and skin anatomy showing the outermost epidermal layer the epidermis, dermis, and subcutaneous. Reprinted with the permission from [223]. Copyright 2020 Elsevier.

b Transdermal extraction system of ISF fluid for continuous glucose monitoring. Reprinted with the permission from [227]. Copyright 2015 American institute of publishing

the activity center of enzyme and electrode to enhance sensitivity of sensor [227].

Saliva sensing devices

Saliva is considered one of the vital biofluids due to its easy accessibility and large availability [228]. It is proved to be an alternative to blood analysis due to its good correlations with available blood analytes [229]. Also, the presence of a wide range of biomarkers makes it an ideal biofluid for monitoring various kinds of human diseases [230]. It is composed of several kinds of biomarkers such as microbes, antibodies, DNA, RNA, metabolites, lipids, and proteins [231]. The biomarkers present in saliva can originate from different sources such as inflammatory cells that contribute to

chronic diseases [232, 233] and molecules produced by the immune system, etc. [234, 235] Various types of portable, non-invasive, and wearable biosensors have been developed to detect different biomarkers in saliva [236–239].

In the past few years, the production of wearable biosensors by graphene and its derivatives has caught significant attention. For example, Mannoor et al. developed the first graphene-based wearable saliva sensing biosensor [240]. The graphene was firstly printed onto water-soluble silk, and the transfer of biosensors was easily facilitated onto different biomaterials and tooth enamel to detect bacteria. Integration of the oral-cavity biosensors with a resonant coil provided battery-free operation. Antimicrobial peptides were immobilized onto graphene, making the sensors capable of detecting bacteria present in saliva at the single-cell level.

This biosensor can be modified to detect some other salivary biomarkers as well.

In a recent study, Mercante et al. designed a biosensor-bioelectronic tongue using zinc oxide (ZnO) nanofibers (NFZ) and graphene derivatives to detect glucose in saliva [241]. Firstly, ZnO nanofibers were fabricated and combined with graphene quantum dots (GQDs) and rGO. Then, glucose oxidase (GOx) was immobilized on this platform to prepare the biosensor. Two biosensor units NFZ-GQDs@GOx and NFZ-rGO@Gox were developed. Both the biosensors utilized electrical impedance measurements and detected glucose in the concentration range of 0.1–6 mM. The NFZ-GQDs@GOx and NFZ-rGO@Gox units showed 32 μM and 14 μM LOD, respectively. Also, the prepared biosensors were employed efficiently to determine glucose in small volumes of artificial saliva. Furthermore, an enzymatic bioelectronic tongue was developed by assembling three different sensing units (NFZ@GOx, NFZ-GQDs@GOx, and NFZ-rGO@GOx) into an array. The bioelectronic tongue was successfully used to detect different glucose concentration levels and the discrimination of glucose from other compounds present in saliva. This study suggested that the bioelectronic tongue could be potentially used to detect other biomarkers associated with various diseases (Fig. 8a).

Although saliva has been proved to be an interesting biofluid candidate, few oral-cavities-based wearable biosensors are developed for non-invasive human health monitoring. However, some issues need to be addressed for wide-scale acceptance and saliva sensing biosensors. For example, a low concentration of salivary biomarkers compared with blood biomarkers will require developing a biosensor with high sensitivity. The purity of the biofluid sample is one of the essential things for its continuous and errorless monitoring. A saliva sample is quite easy to obtain compared to other biofluids, but there are always high chances of contamination by exogenously sourced analytes such as from foods and drinks. In such a case, a biosensor should employ an immobilized receptor with high specificity towards the analyte of interest. Contamination of saliva by mouth wounds and gum bleeding also can lead to interference in analyte sensing. Further, one more issue which might arise easily in salivary-based biosensors is biofouling. Various contaminants of saliva (for instance, food residues and oral-cavity bacteria) can accumulate on the surface of the transducer through non-specific interaction, which might affect the biosensor's performance. Making a protective coating around the biosensor might overcome the issue of biofouling. Moreover, rigorous analysis of saliva will reveal the presence of many more different biomarkers. Developing oral-cavity biosensors to detect multi analytes will be a further advancement in saliva-based wearable devices. Incorporating graphene in the saliva sensing biosensors could be beneficial over other materials in many aspects. It may provide improved mechanical stability and flexibility so that biosensors can withstand the stress due to mouth muscle movements while talking, eating, and drinking.

Tear sensing devices

The biofluid accumulated in the eyes is called tear. Human tears are secreted by the lachrimal gland and act as a protecting film covering the eye. The tears can be exploited to monitor physiological status due to the presence of a wide range of analytes such as salts, proteins, enzymes, peptides, lipids, electrolytes, metabolites, and more than 98% of water [247–249]. Several analytes of tears act as biomarkers to reveal much crucial information regarding different systematic diseases and ocular conditions [250–252]. Moreover, many tear biomarkers exhibit a good correlation with blood biomarkers. For example, glucose concentrations of tears correlate well with blood glucose levels [253, 254]. However, analysis of tear samples is challenging, and it shows several errors such as easily volatile in natures, less secretion compare to other biofluids (secretion rate of sweat is 2 μL min^{-1}, saliva is 0.5 mL min^{-1}, and tear is 0.9 μL min^{-1} in healthy person), non-uniform tear production among individuals, difficult in collection, and handling methods [255–260]. To overcome these issues, the development of wearable tear sensing platforms has garnered attention in the past few decades. Contact lens-based wearable platforms are considered as most suitable, as they can collect the tears without any damage and irritation to the eyes [261, 262]. Interestingly, contact lenses can easily integrate all the necessary components in the platform, such as biosensing elements, transducer, data processing, and power sources. Initially, a tear-sensing contact lens-based device was produced to measure optical phenomenon. This biosensor, concanavalin-A or phenylboronic acid derivatives, was used as an immobilized receptor on transducer for detecting tear glucose [263–265]. The introduction of graphene has revolutionized the field of wearable sensors, most notably in the development of contact lenses. Graphene-based contact lenses offer many advantages such as minimal eye irritation, nil damage to any eye part, better biocompatibility, and avoiding almost all kind of discomfort to wearers.

Kim et al. prepared a graphene-based highly transparent and stretchable wearable contact lens biosensor [242]. The contact lens provided clear vision without any discomfort when worn by users. It showed the multifunctional ability to monitor the tear fluid and intraocular pressure simultaneously and independently using the RLC circuit. A composite/hybrid of silver nanowire and graphene was utilized as stretchable and transparent electrodes, resistors, and antenna because of its increased mechanical and electrical properties without any loss in transparency. The silver nanowire-graphene hybrid was used as a source/drain of electrodes,
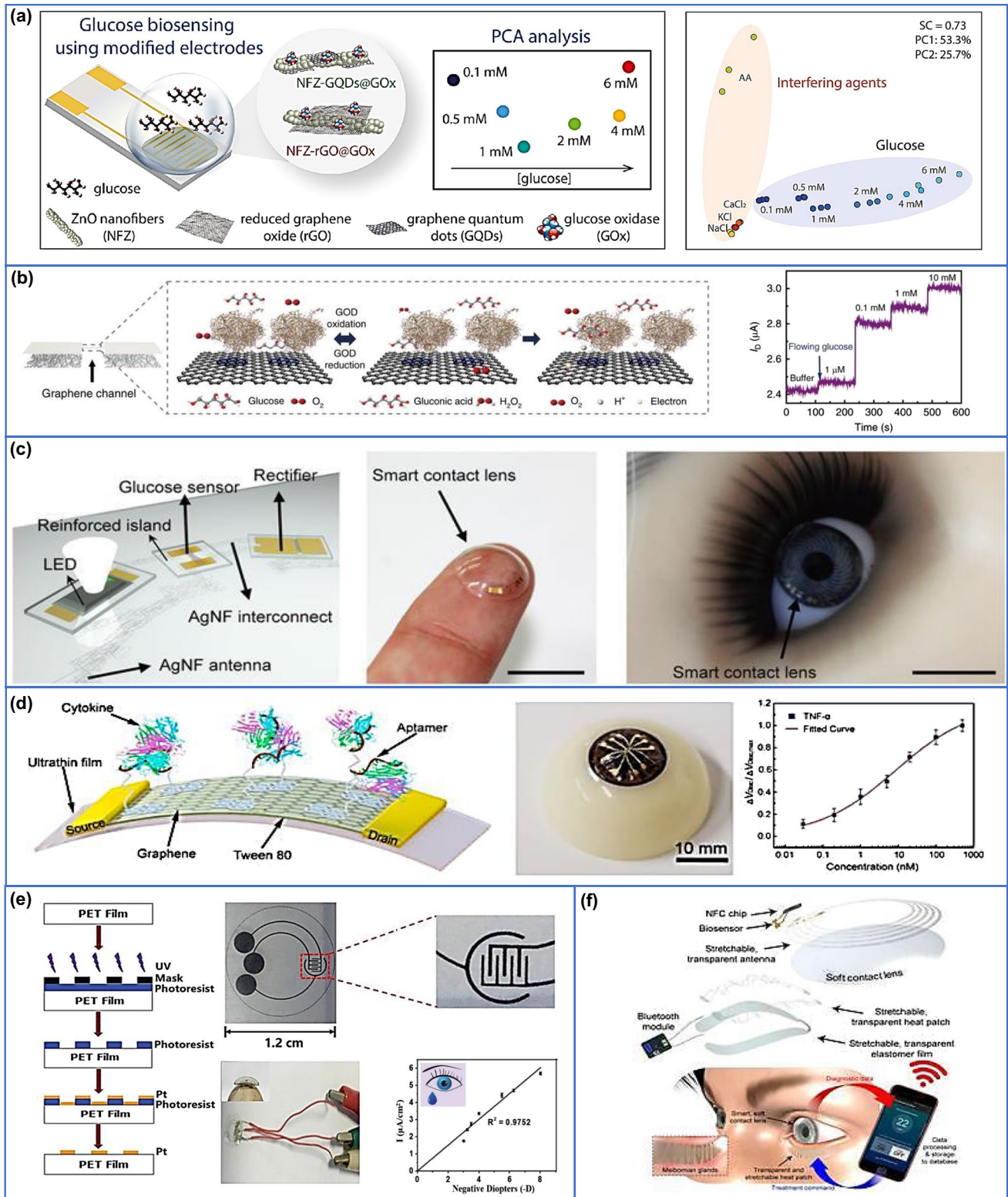
and the graphene/glucose oxidase acted as a channel in a FET, which continuously and wirelessly detected the glucose in tears. The contact lens biosensor exhibited wireless monitoring of glucose concentrations from 1 μM to 10 mM. This multiplexed contact lens biosensor showed solid promise for next-generation ocular diagnostics, which can monitor disease-related markers and evaluate ocular and overall health conditions of the human body (Fig. 8b)

◄**Fig. 8 a** Schematic of a bioelectronic tongue developed using zinc oxide and graphene derivatives (rGO and GQDs) for monitoring of glucose present in saliva. Reprinted with permission from [241]. Copyright 2021 Elsevier. **b** Diagram of a graphene-based wearable contact lens sensor showing glucose sensing with graphene-AgNW. Reprinted with permission from [242]. Copyright 2017 Springer Nature. **c** The schematic picture of the graphene-based soft, smart contact lens for glucose detection. Reprinted with the permission from [243]. Copyright 2018 American Association for the Advancement of Science. **d** Schematic of the flexible graphene field-effect transistor (GFET) biosensor fabricated on an ultrathin film, and the device attached onto the artificial eyeball for detection of cytokine. Reprinted with the permission from [244]. Copyright 2020 Multidisciplinary Digital Publishing Institute. **e** Fabrication process and photographs of corneal microelectrode of corneal biosensors for the in vivo tears testing. Reprinted with the permission from [245]. Copyright 2020 Wiley–VCH. **f** Schematic illustration of integrated and therapeutic devices for chronic OSI. Reprinted with the permission from [246]. Copyright 2021 American Association for the Advancement of Science

[242]. Further, Park et al. demonstrated a soft, smart contact lens for a wireless and real-time operation to analyze the in-vivo glucose concentration in tears with sensing results displayed together [243]. For glucose detection, catalase (CAT) and glucose oxidase (GOx) were immobilized on the surface of the transducer made up of graphene, and a pyrene linker facilitated immobilization for π-π stacking interaction. In this biosensor, different components such as the light-emitting diode (LED), pixel, glucose sensor, and rectifier circuit were fixed on a mechanical stress-tunable hybrid substrate. The interconnected electrodes produced by sliver nanofibers and stretchable transparent antenna were positioned on elastic regions. The stretchable and transparent antenna combined with a rectifier which helped to turn on LED display and real-time sensing results. The detection range of 0.1 ~ 0.9 mM was demonstrated by the contact lens, with detection limit of 12.57 μM. The response time was measured as ~ 1.3 s, and the sensitivity was calculated as approximately 22.72%/mM. For application, the contact lens was applied onto the eyes of a live rabbit to perform an in vivo test. The sensor along with glucose monitoring also measures the temperature change, demonstrating a bright future of contact-lens-based tear sensing wearable biosensors for non-invasive motoring of human health (Fig. 8c) [243]. Wang et al. developed another graphene-based tear sensing wearable biosensor based on FET [244]. The biosensor uses aptamer (polymethyl methacrylate)-modified graphene as the conducting channel for the consistent, sensitive, and time-resolved detection of cytokines (TNF-α and IFN-γ) in artificial tears. Additionally, a non-ionic surfactant Tween 80 was employed to modify the surface of the graphene in order to avoid any kind of non-specific binding for specific detection of the cytokines. To fabricate this GFET biosensor, firstly biosensor's substrate was developed by placing ultrathin mylar film (2.5 μm) on a glass slide.

Further, a lithography technique was used to pattern drain, source, and gate electrodes (4/46 nm of Cr/Au) on the film. Then, conducting channel was produced by transferring the monolayer graphene sheet onto electrodes. The ultrathin substrate provided the biosensor with high mechanical stability to withstand large deformations, including bending and stretching, and also makes the sensor capable of fitting to non-planar surfaces such as the eyeball or human skin. The biosensor showed highly sensitive and consistent detection of TNF-α and IFN-γ, with limits of detection down to 2.75 pM and 2.89 pM, respectively. Ultimately, this biosensor demonstrated good potential as a wearable electronic for human health monitoring by predicting the attack of chronic diseases (Fig. 8d) [244]. Zhang et al. demonstrated an electrochemical corneal biosensor used to detect dopamine (DA) in tears for monitoring myopia diopter [245]. For fabrication of biosensor, firstly, a vapor phase polymerization (VPP) enhanced ball milling method was applied to prepare electroactive nanoelectrodes from poly (3,4-ethylene dioxythiophene) (PEDOT) functionalized sulfur-doped graphene (PEDOT-graphene). Then, the enzyme tyrosinase (TYR) receptor was immobilized covalently onto the thin PEDOT-graphene nanosheets. Further, a wearable corneal biosensor was assembled by electrodeposition of PEDOT-graphene-TYR and shaped to fit the eye's anatomical structure. The biosensor showed excellent performance by detecting DA in both in vivo and in vitro tests and presented high stability and excellent selectivity. The sensitivity of 12.9 μA $\times$ 10^{-3} M^{-1} cm^{-2} and detection limit of 101 $\times$ 10^{-9} M was demonstrated by the biosensor. Additionally, the human tear samples from defocus-induced myopia patients were tested by the corneal biosensor. The biosensor showed good sensitivity to myopia diopters which proved an underlying relationship between myopia diopters and DA content in tears. It was concluded based on the results that this corneal biosensor might prove a potential device for early, real-time detection, and prevention of myopia (Fig. 8e) [245].

Recently, soft, smart contact lens wearable biosensor was reported for non-invasive diagnosis and monitoring of chronic ocular surface inflammation [246]. This contact lens incorporated graphene FET to sense tears for remote and quantitative measurement of a biomarker matrix metalloproteinase-9 (MMP-9) present in chronic ocular surface inflammation. Apart from graphene FET, other components integrated to this device were wireless antenna, capacitors, resistors, and a nearfield communication (NFC) chip. The smart contact lens showed good biocompatibility and functioned adequately without any complication in wearer's vision. The contact lens biosensor responded to detection from 1 to 500 ng mL^{-1} of MMP-9 concentration in tear fluids, with the 0.74 ng mL^{-1} of limit of detection. The sensitivity and response time of the biosensor was reported as 11.1 ng mL^{-1} and ~ 2.5 s, respectively. The contact lens also

enabled real-time wireless transmission of the sensing data to the user's portable device (smartwatch or smartphone). The advantage of this contact lens over previously developed contact lenses is that an eyelid-attachable heat patch was developed for hyperthermia treatment and integrated with this contact lens. So, this system provides both the diagnosis and continuous treatment of OSI. Finally, in vivo studies were performed on human subjects and live animals. Many promising results obtained from the experiments proved the reliability and wearability of this device for sustainable personal health management (Fig. 8f) [246].

Graphene-based tear sensing wearable biosensors have proved crucial in providing a point of care, non-invasive diagnosis, though the majority of the biosensors developed so far are for the detection of glucose monitoring for diabetes. In the past few years, tear-based biosensors have been reported to detect other biomarkers, such as cytokines (TNF-α and IFN-γ), matrix metalloproteinase-9, and DA, expanding the area to diagnose other diseases as well. The scope of these biosensors can be further increased to detect other analytes, which shows good correlations with blood's analytes. For example, detecting amyloid-beta peptides could be helpful for the diagnosis of Alzheimer's disease [266, 267]. Many other proteins, most notably lactoferrin, lysozyme, and albumin can be detected in tears to diagnose different diseases [268]. Also, most of the current tear-based biosensors are being used to detect single analytes. Developing an advanced multifunctional device that detects two or more analytes together would help monitor more than one disease simultaneously, which would reduce cost, diagnosis time, and treatment process. In addition, the selectivity of the biosensors also should be increased to an optimum level for detection ultralow concentration of tear analytes. Furthermore, comprehensive and efficient studies will be needed to explore the tear chemistry in detail and establish the correlation between the concentration of analyte in tears and blood for improving the reliability. Moreover, a large scale of experimental repetition and validation studies will be needed before using them clinically. Table 6 summarizes the graphene-based biosensors used for detection of biomarkers in saliva and tear.

Breath sensors

Detection of diseases from exhaled breath has been shown in different fields of medicine [246]. However, the breath analysis needs to be moved to the next stage to facilitate diseases diagnosis. Breath, a critical physiological sign, contains various molecules that help diagnose various diseases and body functions [269, 270]. Wearable breath sensors have become an international research interest because of their huge potential to detect various biomarkers and humidity levels [271]. It is observed that the presence of various volatile organic compounds will differ in a healthy human being and an infected person [272–274]. The humidity level in breath is also an indicator of the state of well-being [275, 276]. The move towards portability has shifted the development of the wearable sensors towards graphene. Since its invention, researchers have been looking for more and more graphene-based technology to improve existing systems. Graphene plays a huge role in enhancing various sensor's detection capabilities, which makes them better than the existing sensors [15].

Table 6 Summary of graphene-based wearable biosensors for detection of biomarkers in saliva and tear

Wearable device	Receptor system (s)	Detection mechanism	Biomarker	Biofluid	Disease	LOD	Ref
Patch	Graphene/AMP	LC resonant	Bacteria	Saliva	Infectious disease	Single bacterium	[240]
Bioelectronic tongue	NFZ-GQDs@ GOx and NFZ-rGO@ GOx	Electrical impedance	Glucose	Artificial saliva	Diabetes	14 μM and 32 μM	[241]
Contact lens	Graphene/GOx	Electrochemical	Glucose	Tears	Diabetes	1 μM	[242]
Contact lens	Graphene/GOx/ CAT	Electrochemical	Glucose	Tears	Diabetes	12.7 μM	[243]
Ultrathin film	Graphene/PMMA/ PASE	Field effect	TNF-α and IFN-γ	Artificial tears	Chronic diseases	2.75 pM	[244]
Corneal electrode	Graphene/PEDOT/ TYR	Electrochemical	Dopamine	Tears	Myopia	101×10^{-9} M	[245]
Contact lens	Graphene/AgNWs/ IgG	Field effect	MMP-9	Tears	OSI	0.74 ng mL^{-1}	[246]

Abbreviations: AMP, antimicrobial peptides; NFZ, nanofibers; GQDs, glucose quantum dots; GOx, Glucose oxidase; rGO, reduced graphene oxide; CAT, catalase; PMMA, polymethyl methacrylate; PASE, 1-pyrenebutanoic acid succinimidyl ester; OSI, ocular surface inflammation; MMP-9, Matrix metalloproteinase-9; PEDOT, poly (3,4-ethylenedioxythiophene); TYR, tyrosinase

Volatile organic compound detection

The breath of human being is a complex mixture of various compounds, such as nitrogen, oxygen, CO_2, and water vapor, along with a lot of volatile organic compounds (VOC) [21]. Commonly, the VOCs present in breath are acetone, ethanol, CO etc., which could tell us about various medical conditions of the body, such as diabetes [277], hypoglycemia [278], cancer [279], etc. The graphene-based sensors will analyze the breath to identify the presence of specific volatile organic compounds for diagnostics [280]. The easy detection of these volatile compounds as biomarkers has made the sensor industry moves into a more wearable breath sensing approach. Graphene and its derivatives are excellent materials that could be used in volatile biomarker detection and help to develop a sustainable wearable technology [281]. Liu et. al has developed an electronic nose using functionalized rGO, which has a high sensitivity of 25 ppm (Fig. 9a). They used rGO and eight functionalized rGO to detect different VOCs such as ethanol, 2-ethylhexanol, nonanal, and ethylebenzene, which are known cancer biomarkers. In the proposed sensor amine ligands are working as the organic sensing layer which in turn provides different adsorption capacity for VOCs where they have functionalized rGO with ethylamine, hexylamine, octylamine, benzylamine, 2-(4-chloropenyl) ethylamine, 1-(2-aminoethyl) piperidine, 1,3-diaminopropane, and tyramine. They have used principal component analysis to distinguish the sensor performance among VOCs. The main advantage discussed is that the sensor's enhanced performance is not the result of hybridization or doping but the chemistry of rGO which helped to build a rGO library with eight functionalized rGO. They observed linear response to the detection of various cancer biomarkers, which in the structure of an electronic nose is useful in a wearable environment (Fig. 9a) [282]. The developed sensor shows a fast response for detecting acetone in breath, which is an easy method for diabetes detection and also high selectivity towards acetone was observed. The sensor is a biocompatible one as the chitosan template is produced with knight butterfly wings, on which the honeycomb structure is still retained after processing. This was one of the first few researches in which the chemical composition, unique biological functions, and topographical features of butterfly wings along with graphene is observed in the use of wearable biosensors. Chitosan has several -NH_2 groups that remain exposed, specifically interacting with the carbonyl groups in acetone. The sensing capability of this device is tested under different acetone concentrations and observed a fast response (< 1 s) with a small limit of detection (20 ppb). Xu. et al. also explored the usage of graphene in biosensors to detect diabetes biomarkers in breath and to identify various physiological signals [280]. They proposed multifunctional sensing devices which employ porphyrin-modified rGO arrays as the sensor (Fig. 9b) [280] to monitor volatile compounds in breath along with a strain sensing matrix with porous rGO films to detect physiological signals. The sensor was successfully able to distinguish between varieties of human physiological signals and various VOCs in breath, which could benefit the wearable health monitoring of the individual. It was tested on analyzing simulated breath samples with diabetes, nephrotic breath samples, and breath sample of a healthy individual and based on the output pattern, the condition of the patient could be determined. This sensor was able to successfully obtain data based on the wearer's health while operating in a multifunctional manner without signal interference. The idea researched by Xu. et al. bears an important role, since the sensors attached should be multifunctional and efficient while minimizing the number of wearable instruments. Sanchez-Vicente et al. developed an innovative sensor that can detect ethanol, acetone, NO, and CO in the breath, which could relate to many diseases such as chronic obstructive pulmonary disease, cystic fibrosis, asthma, and even diabetes (Fig. 9c) [283]. The detection was carried out at 0% humidity as well as 50% humidity under which the following equation was implied to find the sensor's performance:

$$\text{Response} = (R_a - R) \times 100/R \qquad (11)$$

where R_a and R represent the resistance at exposure to air and the gas, respectively. However, the sensor has shown a lower response under higher humidity for the detection of ethanol and acetone. Under these conditions, the response was observed to increase for CO and NO. In this work, graphene increases the detection capability of the sensor at low temperature and also it increases the response to the gases due to the n-p heterojunction. However, the experiments are done in simulated breath, which implies that there's a need for real life scenario testing. The ability to detect multiple biomarkers strongly recommends the usage of this system in an electronic nose sensor. Tung et. al demonstrated the usage of hybridized graphene in metal organic frameworks (MOF) which helps to tune the sensitivity and selectivity of the VOC sensors (Fig. 9d) [284]. The proposed sensor was used to detect various major biomarkers such as acetone, methanol, and ethanol. They prepared three different hybrid nanocomposites with pristine graphene and MOFs, namely, copper-benzene-1,3,5-tricarboxylate (pG-Cu BTC), zirconium 1,4 dicarboxybenzene (pG-UiO 66), and 2-methylimidazole zinc salt (pG-ZIF 8). The usage of pristine graphene sensor and the hybrid sensor is tested. The hybrid sensor is observed to have a higher response to VOCs, which indicated that the proper hybridisation could help to improve the results of sensing. In the case of pG-Cu-BTC, the result was three times higher than pristine graphene sensor. The addition of metal organic frameworks increased the number
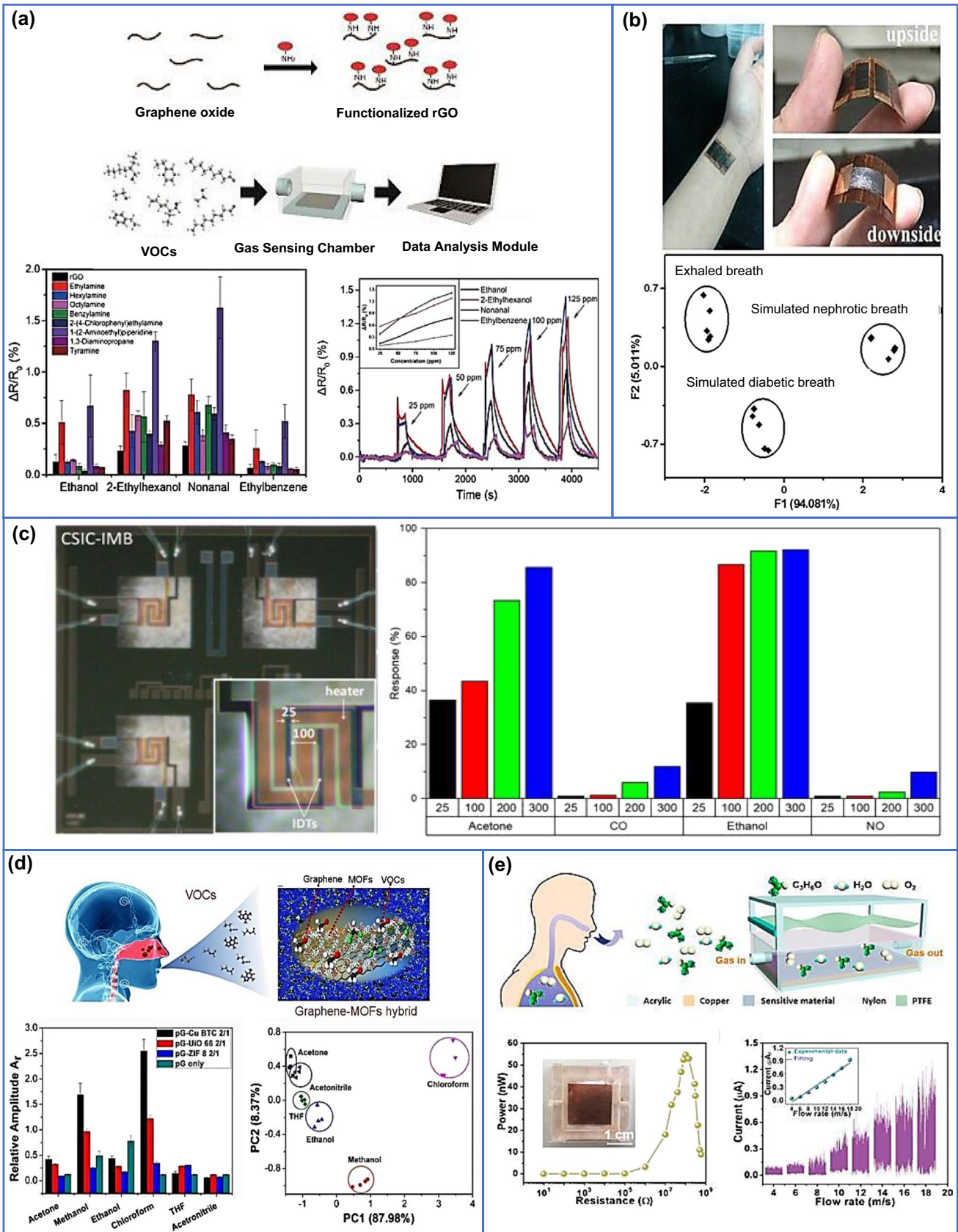
◀**Fig. 9 a** Schematic representation of the functionalized graphene composite sensor with the observed responses to various VOCs. Reprinted with permission from [282]. Copyright 2019 Elsevier. **b** Multifunctional sensing device with the pattern of detection. Reprinted with permission from [280]. Copyright 2018 American Chemical Society. **c** The silicon substrates with micro hot plates and the sensor response to various VOCs. Reprinted with permission from [283]. Copyright 2020 Multidisciplinary Digital Publishing Institute. **d** Schematic representation of the VOC sensor along with the observed response to various VOCs. Reprinted with permission from [284]. Copyright 2020 Elsevier. **e** Schematic representation of triboelectric powered pre-diabetics detection. Reprinted with permission from [286]. Copyright 2020 Elsevier

of adsorption sites, which in turn increased the coordination of VOC molecules with the sensor. Among the three types of sensors tested, pG-Cu BTC has shown superior performance to detect methanol, ethanol and chloroform and pG-UiO 66 has also shown good response towards methanol and chloroform but lower than the response of pG-Cu BTC. However, pG-ZIF8 was observed to have lower or similar performance to pristine graphene sensor (Fig. 9d). To develop sensors that are entirely reliable on its own, the main problem is that it requires a power source. Technology is constantly evolving, and there is always room for improvement. The main problem with wearable technology is that it requires a power source. The need for self-powered systems or highly efficient energy storage structures which are compact is ever increasing. Bio-energy harvesting is a key development that could help power these sensors [285]. Su et al. demonstrated the triboelectric powered sensor for detection of pre-diabetic condition with the sensing of acetone content in the breath (Fig. 9e) [286]. It consists of two parts, an energy developing part and a sensor part. The sensor is self-powered with triboelectricity and chemisorption sensing, which helps the sensor to easily adapt to the wearable environment. The airflow-induced vibration of PTFE (polytetrafluoroethylene) films induces periodic contact with nylon film and due to their difference in triboelectric series, it generates the required power for the sensor. The sensor developed using rGO and chitosan shows a sensing ability of 27.89% under 97.5% relative humidity, which is a much-improved result than when using chitosan alone. This is due to the addition of rGO the surface-to-volume ratio is increased and allows more acetone to participate in the reaction. The sensor also exhibits higher selectivity towards acetone in comparison with other VOCs. However, real human breath is not analyzed since all breath samples were in a simulated condition.

Breath humidity detection

Water is an inevitable part of life and can be identified in the human body with breath humidity. The humidity of breath is an important factor that helps determine the individual's health condition [287]. Humidity variations could

be observed on exhalation and inhalation. With the thorough monitoring of humidity, we can obtain even the water consumption rate of that specific individual [288]. Graphene or graphene derivatives have excellent sensitivity towards humidity. For example, if GO reacted with water molecules to release protons, a decrease in the electrical impedance could be observed [289]. The humidity detection sensors could greatly benefit various peoples who regularly check their water intake. Borini et al. developed one of the first breath humidity sensors using graphene (Fig. 10a) [290]. The sensor observes ultrafast response time and fast recovery (~ 30 ms) at a 15 nm GO film thickness. This was one of the fastest humidity sensors reported during that time. The application of these sensors could go beyond healthcare and could be used in user interfaces in wearables.

Compared with commercially available sensors, they have observed that their sensor works better with easy production as GO can be spray coated to develop the sensor while keeping the sensitivity to relative humidity. The ease of production and ultrafast operation makes this sensor stand out. While being highly efficient, wearable sensors also need to be cost-effective. Selamneni et al. have proposed a straightforward approach towards low-cost wearables with potential applications in human health monitoring [288]. The proposed design consists of a simple solvent-free graphene pencil coating on biodegradable cellulose paper. The sensor can easily detect the moisture in the breath by increasing the sensor resistance, resulting in reduced current. Under NIR (near infrared), a current response increase could be observed due to the photoconductivity and bolometric effect. Under normal conditions, the healthy individual who consumed enough water has shown a massive reduction of 25–35% in the current value, while those with insufficient water consumption has shown 5–10% decrement in current. This proposes an easy to fabricate sensor along with good performance. Looking more into the different material combinations, He et al. [291] explored the tunable application of graphene-polymer nanosensing junctions to detect the moisture content of breath (Fig. 10b). The proposed graphene nanochannels confined poly(dopamine) (GNCP) presented fast capture and release of water molecules according to the conditions, which leads to fast operation and enables recording the humidity variation on different activities such as speaking, singing, etc. It enables to capture even the slightest differences in relative humidity. The technology was adapted to develop a smart mask which can assess the humidity level in breath, which could differentiate between inhalation, exhalation, and also slow-medium-, and fast-paced breathing. The smart mask could be used for athletes training purposes since the processed data could be used to analyze patterns and generate predictive algorithm about the person's health status. Iyengar et al. has demonstrated a humidity sensor with high sensing ability and low response time (~ 1 s),
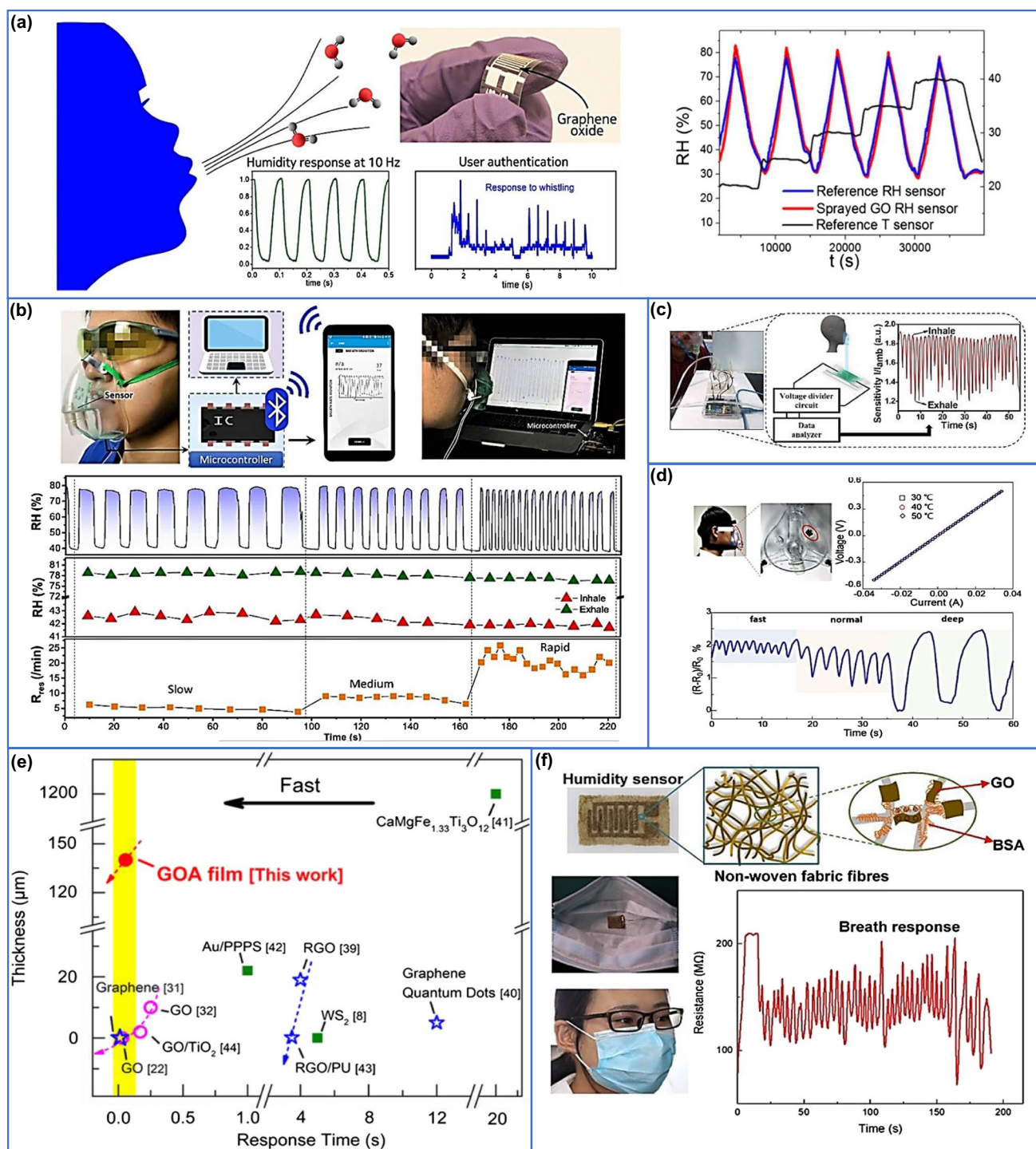
Fig. 10 **a** Graphene oxide-based humidity sensors from exhaled breath. Reprinted with permission from [290]. Copyright 2013 American Chemical Society. **b** Bio-inspired atomic precise tunable graphene for humidity detection from breath. Reprinted with permission [291]. Copyright 2018 American Chemical Society. **c** Schematic representation of PVDF/rGO nanofibers and polyaniline-based wearable sensor for humidity detection. Reprinted with permission from [292]. Copyright 2019 American Chemical Society. **d** Porous graphene coated with PEDOT: PSS, GO, and Ag colloids for respiration monitoring. Reprinted with permission from [275]. Copyright 2018 Elsevier. **e** GO and aniline-based humidity sensor. Reprinted with permission from [293]. Copyright 2020 Wiley–VCH. **f** Non-woven fabric and graphene oxide-based respiration monitoring with the application demonstrated in a mask. Reprinted with permission from [294]. Copyright 2020 American Chemical Society

which is also flexible (Fig. 10c) [292]. It used PVDF/rGO nanofibers and polyaniline (PANi) to develop the sensor. The sensor could successfully detect both oral and nasal respiration. After each oral exhalation, the calibrated response was observed to be at > 95%. The sensor could provide breath rate analysis as well as distinguish between artificial breath and natural breath. The proposed sensor can be used to identify only the humidity in breath as volatile compounds have a negligible effect on this. The sensor offers high performance with minimal circuitry and low working voltage and also is suitable for mass production. However, the need for external power limits the usage in wearable applications. Breath humidity sensors are under constant development and different surface modifications, and many materials are being tried out. Pang et al. developed a sensor based on porous graphene on which poly(3, 4-ethylene dioxythiophene)-poly(styrene sulfonate) (PEDOT: PSS), GO, and Ag colloids were used to modify the surface to enhance the detection [275]. The sensor could also identify the respiration pattern as fast, normal, or deep breath (Fig. 10d). Graphene/Ag colloids sensor has shown better performance than the rest with good linearity. The signal variations could identify the subject's water intake, which helps to identify dehydration. The humidity sensor developed by Tang et al. has a response/recovery time of about 50 ms, which was developed using graphene oxide and aniline.

They explored the developed sensor's ability compared to existing materials used in sensors (Fig. 10e) [293]. The quick recovery observed even at high humidity, and easy production aids for mass production. Wang et al. adapted a new approach to integrating wearable technology with various designs proposed for flexible humidity [294]. The sensor uses non-woven fabric and graphene oxide to detect the moisture content in breath which could help determine patient's respiratory condition. The dependency of sensing over the bovine serum albumin concentration is also discussed. The prepared sensor is kept inside a normal surgical mask or could be attached to the nose tip to monitor the humidity levels in breath while exhaling and inhaling (Fig. 10f). The resistance variation is detected to analyze the humidity of the breath and even fast breathing and deep breathing can be classified according to the sensor output. Also, the sensor helps to determine whether the breathing was through the nose or mouth.

Conclusion and future perspectives

This review systematically discussed the recent developments of graphene, classifying the developments into sensors for different sources of detection at different body sections. With the increasing life expectancy and developing healthcare infrastructure, people tend to put their faith in hospitals, but with the updated technology and data processing, diagnostics are coming over to the people's hands. With a steady increase in wearable technology usage over the years, industries are looking for optimization of their wearable products. As summarized in this review, graphene is an excellent candidate from different perspectives for developing a wearable biosensor. The promised graphene revolution is still underway, but that does not mean the usage of graphene will be limited. While critically analyzing the present graphene biosensors, the data suggests graphene has a promising future for development in this sector. Especially materials with such unique properties like graphene will aid in wearable device developments with increasing performance. The advantages of using graphene in wearable sensors are its high conductivity, strength, flexibility, optical transparency, etc. As of now, graphene is used for all kinds of sensors with excellent performances; however, some major challenges need to be addressed to gain even better performances and wide usage. A major issue with graphene is its mass production. Until now, only a few industries have taken up the challenge for the mass production of graphene. However, the production of graphene on a global scale has seen a good increase from year to year. Even, with a technique to produce graphene on a large scale, it will have to be cheap to replace existing materials. Presently large consortiums such as "Graphene Flagship" are supporting the commercialization of graphene. Graphene has already been tested and applied in sporting goods, anti-corrosion coatings, some sensors, etc., but the proper understanding of the properties of graphene in the wearable industry is yet on the research phase rather than mass commercialization. Even with the understanding of all properties and analyzing the potential product markets, graphene still needs to bridge the gap between laboratory and industry development for developing wearable technologies, but few companies such as "NanoMed" are developing and promoting agile biosensors developed with graphene, which is a huge milestone. As graphene does not have a bandgap, more research is needed to be done to properly use it at a nanoelectronic device development level. To develop graphene as a material that can be used in a wearable system, i.e., a completely independent wireless system, which can monitor various areas of the human body for healthcare, it needs proper development of energy storage systems or self-powering mechanisms. A few mechanisms, such as triboelectricity, piezoelectricity, enzymatic, and non-enzymatic biofuel cells, etc., could potentially be used to power these kinds of sensors. Even though there are devices that are working on the basis of these technologies, most of them are not entirely wearable as they still need to be attached to measuring instruments to properly detect the sensor outputs. Even though graphene is expected to have good material life, the loss of material and performance caused by human movements are not properly studied for graphene-based wearable sensor production. The effect of combining various biological samples, which is discussed previously, is also a major

section that is quite often overlooked. The detection sensitivity of graphene biosensors should be improved by considering above mentioned characteristics. Proper validation between the sensor responses to the analyte concentration in the blood will increase the accuracy and dependability of the sensor. To have a genuinely integrated sensor for everyday use, one of the main factors that needs to be properly studied is the biofouling of graphene-based biosensors such as micro-organisms functionalized over the sensor and components could affect the sensor outputs, leading to false signals. The developed sensors need to be tested in a real-world environment to understand the effects of prolonged usage and the durability of the sensors. Otherwise, proper encapsulation techniques that separate the sensor's functions, which still manages to let the sensor work properly, is required to be developed. However, these issues of graphene pave the road for new and further research towards the graphene revolution in biosensors.

The boom in automation around us is growing, every technology being developed is key to making life simpler than before. The same goes for biosensors, too; the ability to diagnose at home or one's own will has caught attention in the market. However, the technology is not full-fledged at present. Some hiccups create opportunities for future research, even in graphene-based biosensors. One such example will be to create a data management system integrated with machine learning for individuals, as there will be streams of data flowing in from all different sensors or wearables from all parts of the body; thus, data management is a priority. As most of the biosensor data are confidential medical information, the need for a secure and private data processing system is of utmost importance, and if needed, the obtained data could be used for personalizing the home automation. The integration of various components for making the graphene sensor is a challenge that will arise in the near future. The development of miniaturized components that are bio-compatible will help to realize fully wearable systems. With the sensor being fully wearable, the functionalities should also increase, i.e., the same sensor should be multi-functional in the application, rather than one sensor is applied for one specific application, the obtained biofluid samples should be analyzed for multiple components by the same sensor. The possibilities of real-time analysis of other biofluids such as urine, semen, and mucus should be further examined. The doping of various components such as nitrogen, boron, etc., are observed to improve the performance. However, fabrication process should be simplified so that the system can be adapted easily onto large scale.

Declarations

References

1. Bandodkar AJ, Jeerapan I, Wang J (2016) Wearable chemical sensors: present challenges an future prospects. ACS Sensors 1:482. https://doi.org/10.1021/acssensors.6b00250
2. Heikenfeld J, Jajack A, Rogers J, Gutruf P, Tian L, Pan T, Li R, Khine M, Kim J, Wang J, Kim J (2018) Wearable sensors: modalities, challenges, and prospects. Lab Chip 18:217–248. https://doi.org/10.1039/c7lc00914c
3. Morales NE, Baptista PL, Zamora GA, Merkoçi A (2017) Graphene-based biosensors: going simple. Adv Mater 29:1604905. https://doi.org/10.1002/adma.201604905
4. Salim A, Lim S (2019) Recent advances in noninvasive flexible and wearable wireless biosensors. Biosens Bioelectron 141:111422. https://doi.org/10.1016/j.bios.2019.111422
5. Lin Y, Bariya M, Javey A (2021) Wearable biosensors for body computing. Adv Funct Mater 31:2008087. https://doi.org/10.1002/adfm.202008087
6. Yetisen AK, Martinez-Hurtado JL, Ünal B, Khademhosseini A, Butt H (2018) Wearables in medicine. Adv Mater 30:1706910–1706910. https://doi.org/10.1002/adma.201706910
7. Wei X, Zhu M, Li J, Liu L, Yu J, Li Z, Ding B (2021) Wearable biosensor for sensitive detection of uric acid in artificial sweat enabled by a fiber structured sensing interface. Nano Energy 85:106031. https://doi.org/10.1016/j.nanoen.2021.106031
8. Bian S, Zhu B, Rong G, Sawan M (2021) Towards wearable and implantable continuous drug monitoring: a review. J Pharm Anal 11:1–14. https://doi.org/10.1016/j.jpha.2020.08.001
9. Kim J, Campbell AS, De BEF, Wang J (2019) Wearable biosensors for healthcare monitoring. Nat Biotechnol 37:389–406. https://doi.org/10.1038/s41587-019-0045-y
10. Kim SJ, Choi SJ, Jang JS, Cho HJ, Kim ID (2017) Innovative nanosensor for disease diagnosis. Acc Chem Res 50:1587–1596. https://doi.org/10.1021/acs.accounts.7b00047
11. Ashammakhi N, Hernandez AL, Unluturk BD, Quintero SA, de Barros NR, Hoque AE, Bin Shams A, Ostrovidov S, Li J, Contag C, Gomes AS, Holgado M (2021) Biodegradable implantable sensors: materials design, fabrication, and applications. Adv Funct Mater 31:2104149. https://doi.org/10.1002/adfm.202104149
12. Narayan RJ, Verma N (2017) Nanomaterials as implantable sensors. Mater Chem Sens 123–139. https://doi.org/10.1007/978-3-319-47835-7_6
13. Matzeu G, Florea L, Diamond D (2015) Advances in wearable chemical sensor design for monitoring biological fluids. Sensors Actuators B Chem 211:403–418. https://doi.org/10.1016/j.snb.2015.01.077
14. Liu Y, Pharr M, Salvatore GA (2017) Lab-on-skin: a review of flexible and stretchable electronics for wearable health monitoring. ACS Nano 11:9614–9635. https://doi.org/10.1021/acsnano.7b04898
15. Huang H, Su S, Wu N, Wan H, Wan S, Bi H, Sun L (2019) Graphene-based sensors for human health monitoring. Front Chem 7:399. https://doi.org/10.3389/fchem.2019.00399
16. Krishnan SK, Singh E, Singh P, Meyyappan M, Nalwa HS (2019) A review on graphene-based nanocomposites for electrochemical and fluorescent biosensors. Rsc Adv 9:8778–8881. https://doi.org/10.1039/c8ra09577a

17. Chauhan N, Maekawa T, Kumar DNS (2017) Graphene based biosensors—accelerating medical diagnostics to new-dimensions. J Mater Res 32:2860–2882. https://doi.org/10.1557/jmr.2017.91

18. Kim H, Ahn JH (2017) Graphene for flexible and wearable device applications. Carbon 120:244–257. https://doi.org/10.1016/j.carbon.2017.05.041

19. Singh E, Meyyappan M, Nalwa HS (2017) Flexible graphene-based wearable gas and chemical sensors. ACS Appl Mater Interfaces 9:34544–34586. https://doi.org/10.1021/acsami.7b07063

20. Qiao Y, Li X, Hirtz T, Deng G, Wei Y, Li M, Ji S, Wu Q, Jian J, Wu F, Shen Y, Tian H, Yang Y, Ren TL (2019) Graphene-based wearable sensors. Nanoscale 11:18923–18945. https://doi.org/10.1039/c9nr05532k

21. Yang Y, Gao W (2019) Wearable and flexible electronics for continuous molecular monitoring. Chem Soc Rev 48:1465–1491. https://doi.org/10.1039/c7cs00730b

22. Wang B, Sun Y, Ding H, Zhao X, Zhang L, Bai J, Liu K (2020) Bioelectronics-related 2D materials beyond graphene: fundamentals, properties, and applications. Adv Funct Mater 30:2003732. https://doi.org/10.1002/adfm.202003732

23. Seo G, Lee G, Kim MJ, Baek S-H, Choi M, Ku KB, Lee C-S, Jun S, Park D, Kim HG, Kim S-J, Lee JO, Kim BT, Park EC, Kim S (2020) Rapid detection of covid-19 causative virus (SARS-COV-2) in human nasopharyngeal swab specimens using field-effect transistor-based biosensor. ACS Nano 14:5135–5142. https://doi.org/10.1021/acsnano.0c02823

24. Zhang Y, Bai Y, Jia J, Gao N, Li Y, Zhang R, Jiang G, Yan B (2014) Perturbation of physiological systems by nanoparticles. Chem Soc Rev 43:3762–3809. https://doi.org/10.1039/c3cs60338e

25. Pelin M, Fusco L, León V, Martín C, Criado A, Sosa S, Vázquez E, Tubaro A, Prato M (2017) Differential cytotoxic effects of graphene and graphene oxide on skin keratinocytes. Sci Rep 7:1–12. https://doi.org/10.1038/srep40572

26. Fadeel B, Bussy C, Merino S, Vázquez E, Flahaut E, Mouchet F, Evariste L, Gauthier L, Koivisto AJ, Vogel U, Martín C, Delogu LG, Buerki-Thurnherr T, Wick P, Beloin-Saint-Pierre D, Hischier R, Pelin M, Candotto Carniel F (2018) Safety assessment of graphene-based materials: focus on human health and the environment. ACS Nano 12:10582–10620. https://doi.org/10.1021/acsnano.8b04758

27. Li Y, Yuan H, Von Dem Bussche A, Creighton M, Hurt RH, Gao KAB, H, (2013) Graphene microsheets enter cells through spontaneous membrane penetration at edge asperities and corner sites. Proc Natl Acad Sci U S A 110:12295–12300. https://doi.org/10.1073/pnas.1222276110

28. Liu TC, Chuang MC, Chu CY, Huang WC, Lai HY, Wang CT, Chu WL, Chen SY, Chen YY (2016) Implantable graphene-based neural electrode interfaces for electrophysiology and neurochemistry in in vivo hyperacute stroke model. ACS Appl Mater Interfaces 8:187–196. https://doi.org/10.1021/acsami.5b08327

29. Liu S, Wu X, Zhang D, Guo C, Wang P, Hu W, Li X, Zhou X, Xu H, Luo C, Zhang J, Chu J (2017) Ultrafast dynamic pressure sensors based on graphene hybrid structure. ACS Appl Mater Interfaces 9:24148–24154. https://doi.org/10.1021/acsami.7b07311

30. Hummers WS, Offeman RE (1958) Preparation of graphitic oxide. J Am Chem Soc 80:1339. https://doi.org/10.1021/ja01539a017

31. Marcano DC, Kosynkin DV, Berlin JM, Sinitskii A, Sun Z, Slesarev A, Alemany LB, Lu W, Tour JM (2010) Improved synthesis of graphene oxide. ACS Nano 4:4806–4814. https://doi.org/10.1021/nn1006368

32. Sun L, Fugetsu B (2013) Mass production of graphene oxide from expanded graphite. Mater Lett 109:207–210. https://doi.org/10.1016/j.matlet.2013.07.072

33. Guoxiu W, Juan Y, Jinsoo P, Xinglong G, Bei W, Hao L, Jane Y (2008) Facile synthesis and characterization of graphene nanosheets. J Phys Chem C 112:8192–8195. https://doi.org/10.1021/jp710931h

34. Gao X, Jang J, Nagase S (2010) Hydrazine and thermal reduction of graphene oxide: reaction mechanisms, product structures, and reaction design. J Phys Chem C 114:832–842. https://doi.org/10.1021/jp909284g

35. Pei S, Cheng HM (2012) The reduction of graphene oxide. Carbon 50:3210–3228. https://doi.org/10.1016/j.carbon.2011.11.010

36. Lima AH, Mendonça JP, Duarte M, Stavale F, Legnani C, De Carvalho GSG, Maciel IO, Sato F, Fragneaud B, Quirino WG (2017) Reduced graphene oxide prepared at low temperature thermal treatment as transparent conductors for organic electronic applications. Org Electron 49:165–173. https://doi.org/10.1016/j.orgel.2017.05.054

37. Goldoni R, Farronato M, Connelly ST, Tartaglia GM, Yeo WH (2021) Recent advances in graphene-based nanobiosensors for salivary biomarker detection. Biosens Bioelectron 171:112723. https://doi.org/10.1016/j.bios.2020.112723

38. Yang H, Xue T, Li F, Liu W, Song Y (2019) Graphene: diversified flexible 2D material for wearable vital signs monitoring. Adv Mater Technol 4:1–20. https://doi.org/10.1002/admt.201800574

39. Lonkar SP, Deshmukh YS, Abdala AA (2015) Recent advances in chemical modifications of graphene. Nano Res 8:1039–1074. https://doi.org/10.1007/s12274-014-0622-9

40. Castro NH, Guinea F, Peres NMR, Novoselov KS, Geim AK (2009) The electronic properties of graphene. Rev Mod Phys 81:109–162. https://doi.org/10.1103/RevModPhys.81.109

41. Velický M, Bradley DF, Cooper AJ, Hill EW, Kinloch IA, Mishchenko A, Novoselov KS, Patten HV, Toth PS, Valota AT, Worrall SD, Dryfe RAW (2014) Electron transfer kinetics on mono- and multilayer graphene. ACS Nano 8:10089–10100. https://doi.org/10.1021/nn504298r

42. Celiesiute R, Grinciene G, Vaitekonis S, Venckus T, Rakickas T (2013) Application of carbon electrodes modified with graphene and chitosan to electrochemical sensing of ascorbate. Chemija 24:296–306

43. Bolotin KI, Sikes KJ, Jiang Z, Klima M, Fudenberg G, Hone J, Kim P, Stormer HL (2008) Ultrahigh electron mobility in suspended graphene. Solid State Commun 146:351–355. https://doi.org/10.1016/j.ssc.2008.02.024

44. Lee C, Wei X, Kysar JW, Hone J (2008) Measurement of the elastic properties and intrinsic strength of monolayer graphene. Science 321:385–388. https://doi.org/10.1126/science.1157996

45. Mcallister MJ, Li JL, Adamson DH, Schniepp HC, Abdala AA, Liu J, Herrera-Alonso M, Milius DL, Car R, Prudhomme RK, Aksay IA (2007) Single sheet functionalized graphene by oxidation and thermal expansion of graphite. Chem Mater 19:4396–4404. https://doi.org/10.1021/cm0630800

46. Balandin AA, Ghosh S, Bao W, Calizo I, Teweldebrhan D, Miao F, Lau CN (2008) Superior thermal conductivity of single-layer graphene. Nano Lett 8:902–907. https://doi.org/10.1021/nl0731872

47. Nair RR, Blake P, Grigorenko AN, Novoselov KS, Booth TJ, Stauber T, Peres NMR, Geim AK (2008) Fine structure constant defines visual transparency of graphene. Science 320:1308. https://doi.org/10.1126/science.1156965

48. Georgakilas V, Otyepka M, Bourlinos AB, Chandra V, Kim N, Kemp KC, Hobza P, Zboril R, Kim KS (2012) Functionalization of graphene: covalent and non-covalent approaches, derivatives and applications. Chem Rev 112:6156–6214. https://doi.org/10.1021/cr3000412

49. Novoselov KS, Geim AK, Morozov SV, Jiang D, Zhang Y, Dubonos SV, Grigorieva IV, Firsov AA (2004) Electric field in atomically thin carbon films. Science 306:666–669. https://doi.org/10.1126/science.1102896

50. Zhang J, Zhang X, Hou Z, Zhang L, Li C (2019) Uniform SiOx/graphene composite materials for lithium ion battery anodes. J Alloys Compd 809:151798. https://doi.org/10.1016/j.jallcom.2019.151798

51. Tour JM (2014) Top-down versus bottom-up fabrication of graphene-based electronics. Chem Mater 26:163–171. https://doi.org/10.1021/cm402179h

52. Low SS, Tan MTT, Loh HS, Khiew PS, Chiu WS (2016) Facile hydrothermal growth graphene/ZnO nanocomposite for development of enhanced biosensor. Anal Chim Acta 903:131–141. https://doi.org/10.1016/j.aca.2015.11.006

53. Vyshkvorkina IM, Stebunov YV, Arsenin AV, Volkov VS, Novikov SM (2021) Comparison of CVD-grown and exfoliated graphene for biosensing applications. AIP Conf Proc 2359:020035. https://doi.org/10.1063/5.0054960

54. Razumiene J, Gureviciene V, Sakinyte I, Rimsevicius L, Laurinavicius V (2020) The synergy of thermally reduced graphene oxide in amperometric urea biosensor: application for medical technologies. Sensors 20:1–16. https://doi.org/10.3390/s20164496

55. Nayak P, Kurra N, Xia C, Alshareef HN (2016) Highly efficient laser scribed graphene electrodes for on-chip electrochemical sensing applications. Adv Electron Mater 2:1600185. https://doi.org/10.1002/aelm.201600185

56. Xu J, Xu K, Han Y, Wang D, Li X, Hu T, Yi H, Ni Z (2020) A 3D porous graphene aerogel@GOx based microfluidic biosensor for electrochemical glucose detection. Analyst 145:5141–5147. https://doi.org/10.1039/d0an00681e

57. Novoselov KS, Castro Neto AH (2012) Two-dimensional crystals-based heterostructures: materials with tailored properties. Phys Scr 2012:014006. https://doi.org/10.1088/0031-8949/2012/T146/014006

58. Sinclair RC, Suter JL, Coveney PV (2019) Micromechanical exfoliation of graphene on the atomistic scale. Phys Chem Chem Phys 21:5716–5722. https://doi.org/10.1039/c8cp07796g

59. Cao Y, Fatemi V, Demir A, Fang S, Tomarken SL, Luo JY, Sanchez-Yamagishi JD, Watanabe K, Taniguchi T, Kaxiras E, Ashoori RC, Jarillo HP (2018) Correlated insulator behaviour at half-filling in magic-angle graphene superlattices. Nature 556:80–84. https://doi.org/10.1038/nature26154

60. Qian W, Hao R, Hou Y, Tian Y, Shen C, Gao H, Liang X (2009) Solvothermal-assisted exfoliation process to produce graphene with high yield and high quality. Nano Res 2:706–712. https://doi.org/10.1007/s12274-009-9074-z

61. Ji D, Wen X, Foller T, You Y, Wang F, Joshi R (2020) Chemical vapour deposition of graphene for durable anticorrosive coating on copper. Nanomaterials 10:1–9. https://doi.org/10.3390/nano10122511

62. Fan Z, Wang K, Wei T, Yan J, Song L, Shao B (2010) An environmentally friendly and efficient route for the reduction of graphene oxide by aluminum powder. Carbon 48:1686–1689. https://doi.org/10.1016/j.carbon.2009.12.063

63. Xu Z, Zhang Y, Li P, Gao C (2012) Strong, conductive, lightweight, neat graphene aerogel fibers with aligned pores. ACS Nano 6:7103–7113. https://doi.org/10.1021/nn3021772

64. Cui X, Zhang C, Hao R, Hou Y (2011) Liquid-phase exfoliation, functionalization and applications of graphene. Nanoscale 3:2118–2126. https://doi.org/10.1039/c1nr10127g

65. Nascimento JP, Serodre T, Santos JCC, Paulinelli LR, Santos AP, Aparício S, Costa LT, Furtado CA (2021) Molecular insights into the production of few-layer graphene in n-cyclohexylpyrrolid and water mixtures. Carbon 171:723–738. https://doi.org/10.1016/j.carbon.2020.09.034

66. Hernandez Y, Nicolosi V, Lotya M, Blighe FM, Sun Z, De S, McGovern IT, Holland B, Byrne M, Gun'ko YK, Boland JJ, Niraj P, Duesberg G, Krishnamurthy S, Goodhue R, Hutchison J, Scardaci V, Ferrari AC, (2008) High-yield production of graphene by liquid-phase exfoliation of graphite. Nat Nanotechnol 3:563–568. https://doi.org/10.1038/nnano.2008.215

67. Xu S, Zhang L, Wang B, Ruoff RS (2021) Chemical vapor deposition of graphene on thin-metal films. Cell Rep Phys Sci 2:100372. https://doi.org/10.1016/j.xcrp.2021.100372

68. Coraux J, Diaye AT, Busse C, Michely T (2008) Structural coherency of graphene on Ir (111). Nano Lett 8:565–570. https://doi.org/10.1021/nl0728874

69. Halle J, Mehler A, Néel N, Kröger J (2019) Preparation of graphene bilayers on platinum by sequential chemical vapour deposition. Phys Chem Chem Phys 21:3140–3144. https://doi.org/10.1039/c8cp07569g

70. Li X, Cai W, Colombo L, Ruoff RS (2009) Evolution of graphene growth on Ni and Cu by carbon isotope labeling. Nano Lett 9:4268–4272. https://doi.org/10.1021/nl902515k

71. Lukosius M, Dabrowski J, Kitzmann J, Fursenko O, Akhtar F, Lisker M, Lippert G, Schulze S, Yamamoto Y, Schubert MA, Krause HM, Wolff A, Mai A, Schroeder T, Lupina G (2016) Metal-free CVD graphene synthesis on 200 mm Ge/Si(001) substrates. ACS Appl Mater Interfaces 8:33786–33793. https://doi.org/10.1021/acsami.6b11397

72. Pasternak I, Dabrowski P, Ciepielewski P, Kolkovsky V, Klusek Z, Baranowski JM, Strupinski W (2016) Large-area high-quality graphene on Ge(001)/Si(001) substrates. Nanoscale 8:11241–11247. https://doi.org/10.1039/c6nr01329e

73. Eda G, Chhowalla M (2010) Chemically derived graphene oxide: towards large-area thin-film electronics and optoelectronics. Adv Mater 22:2392–2415. https://doi.org/10.1002/adma.200903689

74. Feng Y, Feng N, Du G (2013) A green reduction of graphene oxide via starch-based materials. RSC Adv 3:21466–21474. https://doi.org/10.1039/c3ra43025a

75. Schniepp HC, Li JL, Mcallister MJ, Sai H, Herrera-Alonson M, Adamson DH, Prud'homme RK, Car R, Seville DA, Aksay IA (2006) Functionalized single graphene sheets derived from splitting graphite oxide. J Phys Chem B 110:8535–8539. https://doi.org/10.1021/JP060936F

76. Bagri A, Mattevi C, Acik M, Chabal YJ, Chhowalla M, Shenoy VB (2010) Structural evolution during the reduction of chemically derived graphene oxide. Nat Chem 27(2):581–587. https://doi.org/10.1038/nchem.686

77. ScardaciV, (2021) Laser synthesized graphene and its applications. Appl Sci 11:6304. https://doi.org/10.3390/app11146304

78. Scardaci V, Fichera L, Fragalà ME, Tuccitto N, Marletta G, Compagnini G (2020) Reduction of graphene oxide by laser scribing in different atmospheres and application in humidity sensing. J Nanomater 2020.https://doi.org/10.1155/2020/4946954

79. Lin J, Peng Z, Liu Y, Ruiz ZF, Ye R, Samuel ELG, Yacaman MJ, Yakobson BI, Tour JM (2014) Laser-induced porous graphene films from commercial polymers. Nat Commun 5:1–8. https://doi.org/10.1038/ncomms6714

80. Zhu Y, Cai H, Ding H, Pan N, Wang X (2019) Fabrication of low-cost and highly sensitive graphene-based pressure sensors by direct laser scribing polydimethylsiloxane. ACS Appl Mater Interfaces. https://doi.org/10.1021/acsami.8b17085

81. An J, Le TSD, Huang Y, Zhan Z, Li Y, Zheng L, Huang W, Sun G, Kim YJ (2017) All-graphene-based highly flexible noncontact electronic skin. ACS Appl Mater Interfaces 9:44593–44601. https://doi.org/10.1021/acsami.7b13701

82. Chua CK, Pumera M (2013) Reduction of graphene oxide with substituted borohydrides. J Mater Chem A 1:1892–1898. https://doi.org/10.1039/c2ta00665k

83. Zhang J, Yang H, Shen G, Cheng P, Zhang J, Guo S (2010) Reduction of graphene oxide via-ascorbic acid. Chem Commun 46:1112–1114. https://doi.org/10.1039/b917705a

84. Pei S, Zhao J, Du J, Ren W, Cheng HM (2010) Direct reduction of graphene oxide films into highly conductive and flexible graphene films by hydrohalic acids. Carbon 48:4466–4474. https://doi.org/10.1016/j.carbon.2010.08.006

85. Zhu Y, Cai W, Piner RD, Velamakanni A, Ruoff RS (2009) Transparent self-assembled films of reduced graphene oxide platelets. Appl Phys Lett 95:103104. https://doi.org/10.1063/1.3212862

86. Kim MC, Hwang GS, Ruoff RS (2009) Epoxide reduction with hydrazine on graphene: a first principles study. J Chem Phys 131:064704. https://doi.org/10.1063/1.3197007

87. Mei X, Ouyang J (2011) Ultrasonication-assisted ultrafast reduction of graphene oxide by zinc powder at room temperature. Carbon 49:5389–5397. https://doi.org/10.1016/j.carbon.2011.08.019

88. Pham VH, Pham HD, Dang TT, Hur SH, Kim EJ, Kong BS, Kim S, Chung JS (2012) Chemical reduction of an aqueous suspension of graphene oxide by nascent hydrogen. J Mater Chem 22:10530–10536. https://doi.org/10.1039/c2jm30562c

89. Wu ZS, Ren W, Gao L, Zhao J, Chen Z, Liu B, Tang D, Yu B, Jiang C, Cheng HM (2009) Synthesis of graphene sheets with high electrical conductivity and good thermal stability by hydrogen arc discharge exfoliation. ACS Nano 3:411–417. https://doi.org/10.1021/nn900020u

90. Zhiqiang NC, Chen J, Hoon HH, Ma J, Chen X, Niu ZQ, Hng HH, Ma J, Chen XD, Chen J (2012) A Leavening Strategy to prepare reduced graphene oxide foams. Adv Mater 24:4144–4150. https://doi.org/10.1002/adma.201200197

91. Chen W, Yan L (2011) In situ self-assembly of mild chemical reduction graphene for three-dimensional architectures. Nanoscale 3:3132–3137. https://doi.org/10.1039/c1nr10355e

92. Korkut S, Roy JD, Dabbs DM, Milius DL, Aksay IA (2011) High surface area tapes produced with functionalized graphene. ACS Nano 5:5214–5222. https://doi.org/10.1021/nn2013723

93. Renteria JD, Ramirez S, Malekpour H, Alonso B, Centeno A, Zurutuza A, Cocemasov AI, Nika DL, Balandin AA, Renteria JD, Ramirez S, Malekpour H, Cocemasov AI, Nika DL, Balandin AA, Alonso B, Centeno A, Zurutuza A (2015) Strongly anisotropic thermal conductivity of free-standing reduced graphene oxide films annealed at high temperature. Adv Funct Mater 25:4664–4672. https://doi.org/10.1002/adfm.201501429

94. Pham HD, Pham VH, Cuong TV, Nguyen PTD, Chung JS, Shin EW, Kim S (2011) Synthesis of the chemically converted graphene xerogel with superior electrical conductivity. Chem Commun 47:9672–9674. https://doi.org/10.1039/c1cc13329b

95. Wu Y, Yi N, Huang L, Zhang T, Fang S, Chang H, Li N, Oh J, Lee JA, Kozlov M, Chipara AC, Terrones H, Xiao P, Long G, Huang Y, Zhang F, Zhang L, Lepró X (2015) Three-dimensionally bonded spongy graphene material with super compressive elasticity and near-zero Poisson's ratio. Nat Commun 6141:1–9. https://doi.org/10.1038/ncomms7141

96. Li G, Huang B, Pan Z, Su X, Shao Z, An L (2019) Advances in three-dimensional graphene-based materials: configurations, preparation and application in secondary metal (Li, Na, K, Mg, Al)-ion batteries. Energy Environ Sci 12:2030–2053. https://doi.org/10.1039/c8ee03014f

97. Tang W, Peng L, Yuan C, Wang J, Mo S, Zhao C, Yu Y, Min Y, Epstein AJ (2015) Facile synthesis of 3D reduced graphene oxide and its polyaniline composite for super capacitor application. Synth Met 202:140–146. https://doi.org/10.1016/j.synthmet.2015.01.031

98. Wang Y, Guo L, Qi P, Liu X, Wei G (2019) Synthesis of three-dimensional graphene-based hybrid materials for water purification: a review. Nanomaterials 9:1123. https://doi.org/10.3390/nano9081123

99. Ji X, Zhang X, Zhang X (2015) Three-dimensional graphene-based nanomaterials as electrocatalysts for oxygen reduction reaction. J Nanomater 2015:1–9. https://doi.org/10.1155/2015/357196

100. Huang M, Wang C, Quan L, Nguyen THY, Zhang H, Jiang Y, Byun G, Ruoff RS (2020) CVD growth of porous graphene foam in film form. Matter 3:487–497. https://doi.org/10.1016/j.matt.2020.06.012

101. Dabiri M, Kasmaei M, Salari P, Movahed SK (2016) Copper nanoparticle decorated three dimensional graphene with high catalytic activity for Huisgen 1,3-dipolar cycloaddition. RSC Adv 6:57019–57023. https://doi.org/10.1039/c5ra25317a

102. Zhang Y, Huang Y, Zhang T, Chang H, Xiao P, Chen H, Huang Z, Chen ZYY, Huang Y, Zhang T, Chang H, Xiao P, Chen H, Huang Z, Chen Y (2015) Broadband and tunable high-performance microwave absorption of an ultralight and highly compressible graphene foam. Adv Mater 27:2049–2053. https://doi.org/10.1002/adma.201405788

103. Zhao Y, Liu J, Hu Y, Cheng H, Hu C, Jiang C, Jiang L, Cao A, Qu L (2013) Highly compression-tolerant supercapacitor based on polypyrrole-mediated graphene foam electrodes. Adv Mater 25:591–595. https://doi.org/10.1002/adma.201203578

104. Kou L, Liu Z, Huang T, Zheng B, Tian Z, Deng Z, Gao C (2015) Wet-spun, porous, orientational graphene hydrogel films for high-performance supercapacitor electrodes. Nanoscale 7:4080–4087. https://doi.org/10.1039/c4nr07038k

105. Yang C, Xu Y, Zhang C, Sun Z, Chen C, Li X, Jiang S, Man B (2014) Facile synthesis 3D flexible core-shell graphene/glass fiber via chemical vapor deposition. Nanoscale Res Lett 9:1–6. https://doi.org/10.1186/1556-276x-9-394/figures/4

106. Zhao X, Yao W, Gao W, Chen H, Gao C, Zhao XL, Yao WQ, Gao WW, Chen H, Gao C (2017) Wet-spun superelastic graphene aerogel millispheres with group effect. Adv Mater 29:1701482. https://doi.org/10.1002/adma.201701482

107. Wang H, Sun K, Tao F, Stacchiola DJ, Hang HY, Wang H, Hu YH, Sun K, Tao F, Stacchiola DJ (2013) 3D honeycomb-like structured graphene and its high efficiency as a counter-electrode catalyst for dye-sensitized solar cells. Angew Chemie Int Ed 52:9210–9214. https://doi.org/10.1002/anie.201303497

108. Wei W, Sun K, Hu YH (2014) Synthesis of 3D cauliflower-fungus-like graphene from CO_2 as a highly efficient counter electrode material for dye-sensitized solar cells. J Mater Chem A 2:16842–16846. https://doi.org/10.1039/c4ta03909b

109. Chen Z, Jin L, Hao W, Ren W, Cheng HM (2019) Synthesis and applications of three-dimensional graphene network structures. Mater Today Nano 5:100027. https://doi.org/10.1016/j.mtnano.2019.01.002

110. Bai H, Li C, Wang X, Shi G (2011) On the gelation of graphene oxide. J Phys Chem C 115:5545–5551. https://doi.org/10.1021/JP1120299

111. Wu X, Zhou J, Xing W, Wang G, Cui H, Zhuo S, Xue Q, Yan Z, Qiao SZ (2012) High-rate capacitive performance of graphene aerogel with a superhigh C/O molar ratio. J Mater Chem 22:23186–23193. https://doi.org/10.1039/c2jm35278h

112. Worsley MA, Kucheyev SO, Mason HE, Merrill MD, Mayer BP, Lewicki J, Valdez CA, Suss ME, Stadermann M, Pauzauskie PJ, Satcher JH, Biener J, Baumann TF (2012) Mechanically robust 3D graphene macroassembly with high surface area. Chem Commun 48:8428–8430. https://doi.org/10.1039/c2cc33979j

113. Zhou L, Mao H, Wu C, Tang L, Wu Z, Sun H, Zhang H, Zhou H, Jia C, Jin Q, Chen X, Zhao J (2017) Label-free graphene biosensor targeting cancer molecules based on non-covalent modification. Biosens Bioelectron 87:701–707. https://doi.org/10.1016/j.bios.2016.09.025

114. Khatayevich D, Page T, Gresswell C, Hayamizu Y, Grady W, Sarikaya M (2014) Selective detection of target proteins by peptide-enabled graphene biosensor. Small 10:1505–1513. https://doi.org/10.1002/SMLL.201302188

115. Teixeira S, Burwell G, Castaing A, Gonzalez D, Conlan RS, Guy OJ (2014) Epitaxial graphene immunosensor for human chorionic gonadotropin. Sensors Actuators B Chem 190:723–729. https://doi.org/10.1016/j.snb.2013.09.019

116. Md Ibrahim NNN, Hashim AM (2021) High sensitivity of deoxyribonucleic acid detection via graphene nanohole/silicon micronanopore structure fabricated by focused ion beam. Mater Lett 305:130740. https://doi.org/10.1016/j.matlet.2021.130740

117. Vanegas DC, Patiño L, Mendez C, De Oliveira DA, Torres AM, Gomes CL, McLamore ES (2018) Laser scribed graphene biosensor for detection of biogenic amines in food samples using locally sourced materials. Biosensors 8:42. https://doi.org/10.3390/bios8020042

118. Xiang L, Wang Z, Liu Z, Weigum SE, Yu Q, Chen MY (2016) Inkjet-printed flexible biosensor based on graphene field effect transistor. IEEE Sens J 16:8359–8364. https://doi.org/10.1109/jsen.2016.2608719

119. Kudr J, Zhao L, Nguyen EP, Arola H, Nevanen TK, Adam V, Zitka O, Merkoçi A (2020) Inkjet-printed electrochemically reduced graphene oxide microelectrode as a platform for HT-2 mycotoxin immunoenzymatic biosensing. Biosens Bioelectron 156:112109. https://doi.org/10.1016/j.bios.2020.112109

120. Suikkola J, Bjorninen T, Mosallaei M, Kankkunen T, Iso-Ketola P, Ukkonen L, Vanhala J, Mantysalo M (2016) Screen-printing fabrication and characterization of stretchable electronics. Sci Rep 6:1–8. https://doi.org/10.1038/srep25784

121. Marra F, Minutillo S, Tamburrano A, Sarto MS (2021) Production and characterization of graphene nanoplatelet-based ink for smart textile strain sensors via screen printing technique. Mater Des 198:109306. https://doi.org/10.1016/j.matdes.2020.109306

122. Pimpin A, Srituravanich W (2011) Review on micro- and nanolithography techniques and their applications. Eng J 16:37–56. https://doi.org/10.4186/ej.2012.16.1.37

123. Shi R, Xu H, Chen B, Zhang Z, Peng LM (2013) Scalable fabrication of graphene devices through photolithography. Appl Phys Lett 102:113102. https://doi.org/10.1063/1.4795332

124. Wimalananda MDSL, Kim JK, Lee JM (2019) Selective growth of monolayer and bilayer graphene patterns by a rapid growth method. Nanoscale 11:6727–6736. https://doi.org/10.1039/c9nr01011d

125. Yuan J, Ma LP, Pei S, Du J, Su Y, Ren W, Cheng HM (2013) Tuning the electrical and optical properties of graphene by ozone treatment for patterning monolithic transparent electrodes. ACS Nano 7:4233–4241. https://doi.org/10.1021/nn400682u

126. Kang M, Kang M, Han C, Han C, Jeon H, Jeon H, Jeon H (2020) Submicrometer-scale pattern generation via maskless digital photolithography. Optica 7:1788–1795. https://doi.org/10.1364/optica.406304

127. Reyntjens S, Puers R (2001) A review of focused ion beam applications in microsystemtechnology. J Micromech Microeng 11:287. https://doi.org/10.1088/0960-1317/11/4/301

128. Tian H, Yang Y, Xie D, Cui YL, Mi WT, Zhang Y, Ren TL (2014) Wafer-scale integration of graphene-based electronic, optoelectronic and electroacoustic devices. Sci Rep 4:1–9. https://doi.org/10.1038/srep03598

129. Parvez K, Worsley R, Alieva A, Felten A, Casiraghi C (2019) Water-based and inkjet printable inks made by electrochemically exfoliated graphene. Carbon 149:213–221. https://doi.org/10.1016/j.carbon.2019.04.047

130. He P, Cao J, Ding H, Liu C, Neilson J, Li Z, Kinloch IA, Derby B (2019) Screen-printing of a highly conductive graphene ink for flexible printed electronics. ACS Appl Mater Interfaces 11:32225–32234. https://doi.org/10.1021/acsami.9b04589

131. Fischbein MD, Drndić M (2008) Electron beam nanosculpting of suspended graphene sheets. Appl Phys Lett 93:113107. https://doi.org/10.1063/1.2980518

132. Lucot D, Gierak J, Ouerghi A, Bourhis E, Faini G, Mailly D (2009) Deposition and FIB direct patterning of nanowires and nanorings into suspended sheets of graphene. Microelectron Eng 86:882–884. https://doi.org/10.1016/j.mee.2009.01.023

133. Abbas AN, Liu G, Liu B, Zhang L, Liu H, Ohlberg D, Wu W, Zhou C (2014) Patterning, characterization, and chemical sensing applications of graphene nanoribbon arrays down to 5 nm using helium ion beam lithography. ACS Nano 8:1538–1546. https://doi.org/10.1021/nn405759v

134. Bell DC, Lemme MC, Stern LA, Williams JR, Marcus CM (2009) Precision cutting and patterning of graphene with helium ions. Nanotechnology 20:455301. https://doi.org/10.1088/0957-4484/20/45/455301

135. Li J, Ye F, Vaziri S, Muhammed M, Lemme MC, Östling M (2013) Efficient inkjet printing of graphene. Adv Mater 25:3985–3992. https://doi.org/10.1002/adma.201300361

136. Tobjork D, Osterbacka R (2011) Paper electronics. Adv Mater 23:1935–1961. https://doi.org/10.1002/adma.201004692

137. Secor EB, Prabhumirashi PL, Puntambekar K, Geier ML, Hersam MC (2013) Inkjet printing of high conductivity, flexible graphene patterns. J Phys Chem Lett 4:1347–1351. https://doi.org/10.1021/jz400644c

138. Kasikovic N, Stancic M, Vladic G, Grujic D, Novakovic D, Milosevic R, Pincjer I (2017) The influence of heat treatment on the quality of screen printed textile substrates. Revista Materia 22.https://doi.org/10.1590/s1517-707620170001.0123

139. Oliveira DA, Molinnus D, Beging S, Siqueira JR, Schöning MJ (2021) Biosensor based on self-assembled films of graphene oxide and polyaniline using a field-effect device platform. Phys status solidi 218:2000747. https://doi.org/10.1002/pssa.202000747

140. Secor EB, Lim S, Zhang H, Frisbie CD, Francis LF, Hersam MC (2014) Gravure printing of graphene for large-area flexible electronics. Adv Mater 26:4533–4538. https://doi.org/10.1002/adma.201401052

141. Kabiri AS, Ho R, Jang H, Tao L, Wang Y, Wang L, Schnyer DM, Akinwande D, Lu N (2017) Graphene electronic tattoo sensors. ACS Nano 11:7634–7641. https://doi.org/10.1021/acsnano.7b02182

142. Eggins BR (2002) Chemical sensors and biosensors. Wiley

143. Luppa PB, Sokoll LJ, Chan DW (2001) Immunosensors principles and applications to clinical chemistry. Clin Chim Acta 314:1–26. https://doi.org/10.1016/s0009-8981(01)00629-5

144. Wu H, Wang Y, Li Z (2020) Investigations of the electrochemical performance and filling effects of additives on electroplating process of TSV. Sci Rep 10:9204. https://doi.org/10.1038/s41598-020-66191-7

145. Tuteja SK, Ormsby C, Neethirajan S (2018) Noninvasive label-free detection of cortisol and lactate using graphene embedded screen-printed electrode. Nano-Micro Lett 10:1–10. https://doi.org/10.1007/s40820-018-0193-5/figures/6

146. Chaubey A, Malhotra BD (2002) Mediated biosensors. Biosens Bioelectron 17:441–456. https://doi.org/10.1016/s0956-5663(01)00313-x

147. Goldsmith JG (2000) Modern analytical chemistry. J Chem Educ 77:705. https://doi.org/10.1021/ed077p705.2

148. Wang J (2006) Analytical electrochemistry, 3rd edn. Hoboken, Wiley

149. Xu M, Zhu Y, Gao S, Zhang Z, Gu Y, Liu X (2021) Reduced graphene oxide-coated silica nanospheres as flexible enzymatic biosensors for detection of glucose in sweat. ACS Appl Nano Mater 4:12442–12452. https://doi.org/10.1021/acsanm.1c02887

150. Harnisch F, Freguia S (2012) A basic tutorial on cyclic voltammetry for the investigation of electroactive microbial biofilms. Chem Asian 7:466–475. https://doi.org/10.1002/asia.201100740

151. Xuan X, Yoon HS, Park JY (2018) A wearable electrochemical glucose sensor based on simple and low-cost fabrication

supported micro-patterned reduced graphene oxide nanocomposite electrode on flexible substrate. Biosens Bioelectron 109:75–82. https://doi.org/10.1016/j.bios.2018.02.054

152. Gil RL, Amorim CG, Montenegro MCBSM, Araujo AN (2019) Potentiometric detection in liquid chromatographic systems: An overview. J Chromatogr A 1602:326–340. https://doi.org/10.1016/j.chroma.2019.06.006

153. An Q, Gan S, Xu J, Bao Y, Wu T, Kong H, Zhong L, Ma Y, Song Z, Niu L (2019) A multichannel electrochemical all-solid-state wearable potentiometric sensor for real-time sweat ion monitoring. Electrochem Commun 107:106553. https://doi.org/10.1016/j.elecom.2019.106553

154. Naresh V, Lee N (2021) Review on biosensors and recent development of nanostructured materials-enabled biosensors. Sensors 21:1109. https://doi.org/10.3390/s21041109

155. Danielson E, Dhamodharan V, Porkovich A, Kumar P, Jian N, Ziadi Z, Grammatikopoulos P, Sontakke VA, Yokobayashi Y, Sowwan M (2019) Gas-phase synthesis for label-free biosensors: zinc-oxide nanowires functionalized with gold nanoparticles. Sci Rep 9:17370. https://doi.org/10.1038/s41598-019-53960-2

156. Li C, Cauwe M, Yang Y, Schaubroeck D, Mader L, de Beeck M (2019) Ultra-long-term reliable encapsulation using an atomic layer deposited $HFO_2/Al_2O_3/HFO_2$ triple-interlayer for biomedical implants. Coatings 9:579. https://doi.org/10.3390/coatings9090579

157. Nah JS, Barman SC, Zahed MA, Sharifuzzaman M, Yoon H, Park C, Yoon S, Zhang S, Park JY (2021) A wearable microfluidics-integrated impedimetric immunosensor based on $Ti_3C_2T_x$ MXene incorporated laser-burned graphene for noninvasive sweat cortisol detection. Sensors Actuators B Chem 329:129206. https://doi.org/10.1016/j.snb.2020.129206

158. Amine A, Mohammadi H (2019) Amperometry. Encycl Anal Sci 85–98. https://doi.org/10.1016/b978-0-12-409547-2.14204-0

159. Heyrovský J (1956) The development of polarographic analysis. Analyst 81:189–192. https://doi.org/10.1039/AN9568100189

160. Katz E, Willner I (2003) Probing biomolecular interactions at conductive and semiconductive surfaces by impedance spectroscopy: routes to impedimetric immunosensors, DNA-sensors, and enzyme biosensors. Electroanalysis 15:913–947. https://doi.org/10.1002/elan.200390114

161. Mabbott GA (1983) An introduction to cyclic voltammetry. J Chem Educ 60:697. https://doi.org/10.1021/ed060p697

162. D'Orazio P (2003) Biosensors in clinical chemistry. Clin Chim Acta 334:41–69. https://doi.org/10.1016/s0009-8981(03)00241-9

163. Bakker E, Pretsch E (2005) Potentiometric sensors for trace-level analysis. Trends Analyt Chem 24:199–207. https://doi.org/10.1016/j.trac.2005.01.003

164. Cullen DC, Sethi RS, Lowe CR (1990) Multi-analyte miniature conductance biosensor. Anal Chim Acta 231:33–40. https://doi.org/10.1016/S0003-2670(00)86394-1

165. Patolsky F, Zayats M, Katz EE, Willner I (1999) Precipitation of an insoluble product on enzyme monolayer electrodes for biosensor applications: characterization by faradaic impedance spectroscopy, cyclic voltammetry, and microgravimetric quartz crystal microbalance analyses. Anal Chem 71:3171–3180. https://doi.org/10.1021/ac9901541

166. Bakker E (2004) Electrochemical sensors. Anal Chem 76:3285–3298. https://doi.org/10.1021/ac049580z

167. Baltes H, Brand O, Fedder GK, Hierold C, Korvink JG, Tabata O, Kumar CSSR, Hormes J, Leuschner C, Advincula RC, Brittain WJ, Caster KC, Uhe JR, Ohler MK, Fritzsche W (2005) Bioelectronics: from theory to applications. Wiley-VCH 1:1–475. https://doi.org/10.1002/352760376x

168. Swann G (2010) Editorial. J Vis Commun Med 33:148–149. https://doi.org/10.3109/17453054.2010.525439

169. Nakata S, Shiomi M, Fujita Y, Arie T, Akita S, Takei K (2018) A wearable pH sensor with high sensitivity based on a flexible charge-coupled device. Nat Electron 1:596–603. https://doi.org/10.1038/s41928-018-0162-5

170. Alizadeh A, Burns A, Lenigk R, Gettings R, Ashe J, Porter A, Mccaul M, Barrett R, Diamond D, White P, Skeath P, Tomczak M (2018) A wearable patch for continuous monitoring of sweat electrolytes during exertion. Lab Chip 18:2632–2641. https://doi.org/10.1039/c8lc00510a

171. Samant PP, Niedzwiecki MM, Raviele N, Tran V, Mena-Lapaix J, Walker DI, Felner EI, Jones DP, Miller GW, Prausnitz MR (2020) Sampling interstitial fluid from human skin using a microneedle patch. Sci Transl Med 12. https://doi.org/10.1126/scitranslmed.aaw0285

172. Lin Y, Bariya M, Nyein HYY, Kivimäki L, Uusitalo S, Jansson E, Ji W, Yuan Z, Happonen T, Liedert C, Hiltunen J, Fan Z, Javey A (2019) Porous enzymatic membrane for nanotextured glucose sweat sensors with high stability toward reliable noninvasive health monitoring. Adv Funct Mater 29:1902521. https://doi.org/10.1002/adfm.201902521

173. Dartt DA (1994) Regulation of tear secretion. Adv Exp Med Biol 350:1–9. https://doi.org/10.1007/978-1-4615-2417-5_1

174. Broza YY, Zhou X, Yuan M, Qu D, Zheng Y, Vishinkin R, Khatib M, Wu W, Haick H (2019) Disease detection with molecular biomarkers: from chemistry of body fluids to nature-inspired chemical sensors. Chem Rev 119:11761–11817. https://doi.org/10.1021/acs.chemrev.9b00437

175. Buszewski B, Kęsy M, Ligor T, Amann A (2007) Human exhaled air analytics: biomarkers of diseases. Biomed Chromatogr 21:553–566. https://doi.org/10.1002/bmc.835

176. Baker LB (2019) Physiology of sweat gland function: the roles of sweating and sweat composition in human health. Temperature (Austin) 3:211–259. https://doi.org/10.1080/23328940.2019.1632145

177. Sato K, Kang WH, Saga K, Sato KT (1989) Biology of sweat glands and their disorders. I. normal sweat gland function. J Am Acad Dermatol 20:713–726. https://doi.org/10.1016/S0190-9622(89)70063-3

178. Best A, Kamilar JM (2018) The evolution of eccrine sweat glands in human and nonhuman primates. J Hum Evol 117:33–43. https://doi.org/10.1016/j.jhevol.2017.12.003

179. Derbyshire PJ, Barr H, Davis F, Higson SPJ (2012) Lactate in human sweat: a critical review of research to the present day. J Physiol Sci 62:429–440. https://doi.org/10.1007/s12576-012-0213-z

180. Onor M, Gufoni S, Lomonaco T, Ghimenti S, Salvo P, Sorrentino F, Bramanti E (2017) Potentiometric sensor for non invasive lactate determination in human sweat. Anal Chim Acta 989:80–87. https://doi.org/10.1016/j.aca.2017.07.050

181. Cui G, Yoo JH, Woo BW, Kim SS, Cha GS, Nam H (2001) Disposable amperometric glucose sensor electrode with enzyme-immobilized nitrocellulose strip. Talanta 54:1105–1111. https://doi.org/10.1016/S0039-9140(01)00377-0

182. Harborn U, Xie B, Venkatesh R, Danielsson B (1997) Evaluation of a miniaturized thermal biosensor for the determination of glucose in whole blood. Clin Chim Acta 267:225–237. https://doi.org/10.1016/S0009-8981(97)00151-4

183. Zhu J, Zhu Z, Lai Z, Wang R, Guo X, Wu X, Zhang G, Zhang Z, Wang Y, Chen Z (2002) Planar amperometric glucose sensor based on glucose oxidase immobilized by Chitosan film on prussian blue layer. Sensors 2:127–136. https://doi.org/10.3390/s20400127

184. Liu C, Sheng Y, Sun Y, Feng J, Wang S, Zhang J, Xu J, Jiang D (2015) A glucose oxidase-coupled DNA enzyme sensor for glucose detection in tears and saliva. Biosens Bioelectron 70:455–461. https://doi.org/10.1016/j.bios.2015.03.070

185. Ladgotra A, Verma P, Raj SS (2016) Estimation of salivary and serum biomarkers in diabetic and non diabetic patients - a comparative study. J Clin Diagn Res 10:56–61. https://doi.org/10.7860/jcdr/2016/19135.7995

186. Rabti A, Argoubi W, Raouafi N (2016) Enzymatic sensing of glucose in artificial saliva using a flat electrode consisting of a nanocomposite prepared from reduced graphene oxide, chitosan, nafion and glucose oxidase. Microchim Acta 183:1227–1233. https://doi.org/10.1007/s00604-016-1753-3

187. Labroo P, Cui Y (2013) Flexible graphene bio-nanosensor for lactate. Biosens Bioelectron 41:852–856. https://doi.org/10.1016/j.bios.2012.08.024

188. Abellán LA, Jeerapan I, Bandodkar A, Vidal L, Canals A, Wang J, Morallón E (2017) A stretchable and screen-printed electrochemical sensor for glucose determination in human perspiration. Biosens Bioelectron 91:885–891. https://doi.org/10.1016/j.bios.2017.01.058

189. Kwak YH, Choi DS, Kim YN, Kim H, Yoon DH, Ahn S-S, Yang J-W, Yang WS, Seo S (2012) Flexible glucose sensor using CVD-grown graphene-based field effect transistor. Biosens Bioelectron 37:82–87. https://doi.org/10.1016/j.bios.2012.04.042

190. Garg V, Gupta T, Rani S, Bandyopadhyay GS, Ghosh SB, Qiao L, Liu G (2021) A hierarchically designed nanocomposite hydrogel with multisensory capabilities towards wearable devices for human-body motion and glucose concentration detection. Compos Sci Technol 213:108894. https://doi.org/10.1016/j.compscitech.2021.108894

191. Lee H, Choi TK, Lee YB, Cho HR, Ghaffari R, Wang L, Choi HJ, Chung TD, Lu N, Hyeon T, Choi SH, Kim DH (2016) A graphene-based electrochemical device with thermoresponsive microneedles for diabetes monitoring and therapy. Nat Nanotechnol 11:566–572. https://doi.org/10.1038/nnano.2016.38

192. Poletti F, Zanfrognini B, Favaretto L, Quintano V, Sun J, Treossi E, Melucci M, Palermo V, Zanardi C (2021) Continuous capillary-flow sensing of glucose and lactate in sweat with an electrochemical sensor based on functionalized graphene oxide. Sensors Actuators B Chem 344:130253. https://doi.org/10.1016/j.snb.2021.130253

193. Wang Z, Gui M, Asif M, Yu Y, Dong S, Wang H, Wang W, Wang F, Xiao F, Liu H (2018) A facile modular approach to the 2D oriented assembly MOF electrode for non-enzymatic sweat biosensors. Nanoscale 10:6629–6638. https://doi.org/10.1039/C8NR00798E

194. Wang Z, Hao Z, Wang X, Huang C, Lin Q, Zhao X, Pan Y (2021) A flexible and regenerative aptameric graphene–nafion biosensor for cytokine storm biomarker monitoring in undiluted biofluids toward wearable applications. Adv Funct Mater 31:2005958. https://doi.org/10.1002/adfm.202005958

195. Park HJ, Jeong JM, Son SG, Kim SJ, Lee M, Kim HJ, Jeong J, Hwang SY, Park J, Eom Y, Choi BG (2021) Fluid-dynamics-processed highly stretchable, conductive, and printable graphene inks for real-time monitoring sweat during stretching exercise. Adv Funct Mater 31:2011059. https://doi.org/10.1002/adfm.202011059

196. Neave N (2007) Hormones and behaviour: a psychological approach. Cambridge University Press.https://doi.org/10.1017/CBO9780511808203

197. Lubke K, Schillinger E, Topert M (1976) Hormone receptors. Angew Chem Int Ed Engl 15:741–748. https://doi.org/10.1002/anie.197607411

198. Schauer R (1972) The mode of action of hormones. Angew Chem Int Ed Engl 11:7–16. https://doi.org/10.1002/anie.197200071

199. Hodsman AB, Bauer DC, Dempster DW, Dian L, Hanley DA, Harris ST, Kendler DL, McClung MR, Miller PD, Olszynski WP, Orwoll E, Yuen CK (2005) Parathyroid hormone and teriparatide for the treatment of osteoporosis: a review of the evidence and suggested guidelines for its use. Endocr Rev 26:688–703. https://doi.org/10.1210/er.2004-0006

200. Hagström E, Hellman P, Larsson TE, Ingelsson E, Berglund L, Sundström J, Melhus H, Held C, Lind L, Michaëlsson K, Arnlöv J (2009) Plasma parathyroid hormone and the risk of cardiovascular mortality in the community. Circulation 119:2765–2771. https://doi.org/10.1161/circulationaha.108.808733

201. Downs TM, Burton DW, Araiza FL, Hastings RH, Deftos LJ (2011) PTHrP stimulates prostate cancer cell growth and upregulates aldo-keto reductase 1C3. Cancer Lett 306:52–59. https://doi.org/10.1016/j.canlet.2011.02.007

202. Zafrani B, Aubriot MH, Mouret E, De Crémoux P, De Rycke Y, Nicolas A, Boudou E, Vincent-Salomon A, Magdelénat H, Sastre-Garau X (2000) High sensitivity and specificity of immunohistochemistry for the detection of hormone receptors in breast carcinoma: comparison with biochemical determination in a prospective study of 793 cases. Histopathology 37:536–545. https://doi.org/10.1046/j.1365-2559.2000.01006.x

203. Hsu SM, Raine L, Fanger H (1981) A comparative study of the peroxidase-antiperoxidase method and an avidin-biotin complex method for studying polypeptide hormones with radioimmunoassay antibodies. Am J Clin Pathol 75:734–738. https://doi.org/10.1093/ajcp/75.5.734

204. Kaushik A, Yndart A, Jayant RD, Sagar V, Atluri V, Bhansali S, Nair M (2015) Electrochemical sensing method for point-of-care cortisol detection in human immunodeficiency virus-infected patients. Int J Nanomedicine 10:677–685. https://doi.org/10.2147/IJN.S75514

205. Kinnamon D, Ghanta R, Lin K-C, Muthukumar S, Prasad S (2017) Portable biosensor for monitoring cortisol in low-volume perspired human sweat. Sci Rep 7:13312. https://doi.org/10.1038/s41598-017-13684-7

206. Arya SK, Estrela P (2020) Electrochemical ELISA protein biosensing in undiluted serum using a polypyrrole-based platform. Sensors 20:2857. https://doi.org/10.3390/s20102857

207. Ali MM, Ibrahim K, Hamad OS, Eisa MH, Faraj MG, Azhari F (2010) Deposited Indium Tin Oxide (ITO) thin films by DC-Magnetron sputtering on polyethylene terephthalate substrate (PET). Rom J Phys 56:730–741

208. Altintas Z, Fakanya WM, Tothill IE (2014) Cardiovascular disease detection using bio-sensing techniques. Talanta 128:177–186. https://doi.org/10.1016/j.talanta.2014.04.060

209. Kalliolias GD, Ivashkiv LB (2016) TNF biology, pathogenic mechanisms and emerging therapeutic strategies. Nat Rev Rheumatol 12:49–62. https://doi.org/10.1038/nrrheum.2015.169

210. Promphet N, Hinestroza JP, Rattanawaleedirojn P, Soatthiyanon N, Siralertmukul K, Potiyaraj P, Rodthongkum N (2020) Cotton thread-based wearable sensor for non-invasive simultaneous diagnosis of diabetes and kidney failure. Sensors Actuators B Chem 321:128549. https://doi.org/10.1016/j.snb.2020.128549

211. Bariya M, Nyein HYY, Javey A (2018) Wearable sweat sensors. Nat Electron 1:160–171. https://doi.org/10.1038/s41928-018-0043-y

212. Reddy MM, Quinton PM (2006) Cytosolic potassium controls CFTR deactivation in human sweat duct. Am J Physiol Cell Physiol 291:122–129. https://doi.org/10.1152/ajpcell.00134.2005

213. Brothers MC, DeBrosse M, Grigsby CC, Naik RR, Hussain SM, Heikenfeld J, Kim SS (2019) Achievements and challenges for real-time sensing of analytes in sweat within wearable platforms. Acc Chem Res 52:297–306. https://doi.org/10.1021/acs.accounts.8b00555

214. Speedy DB, Noakes TD, Schneider C (2001) Exercise-associated hyponatremia: a review. Emerg Med (Fremantle) 13:17–27. https://doi.org/10.1046/j.1442-2026.2001.00173.x

215. Hua Y, Kwok SCTT, Wang X, Lee Y-KK, Yuen MM-FMF (2019) Flexible Sweat monitoring based on all-solid-state

metal-organic frameworks/graphene composite sensors. IEEE Sensors 1–4. https://doi.org/10.1109/sensors43011.2019.8956516

216. Su SB, Poon TCW, Thongboonkerd V (2013) Human body fluid. Biomed Res Int 2013:918793. https://doi.org/10.1155/2013/918793

217. Chu JYS, Cheng CYY, Lee VHY, Chan YS, Chow BKC (2011) Secretin and body fluid homeostasis. Kidney Int 79:280–287. https://doi.org/10.1038/ki.2010.397

218. Colon LA (1997) Analysis of body fluids: urine, blood, saliva and tears. Polonsky J (eds) Handbook of capillary electrophoresis applications. Springer Netherlands, Dordrech, 486–498

219. Humphrey SP, Williamson RT (2001) A review of saliva: normal composition, flow, and function. J Prosthet Dent 85:162–169. https://doi.org/10.1067/mpr.2001.113778

220. Heikenfeld J (2016) Non-invasive analyte access and sensing through eccrine sweat: challenges and outlook circa 2016. Electroanalysis 28:1242–1249. https://doi.org/10.1002/elan.201600018

221. Fogh AN, Altura BM, Altura BT, Siggaard AO (1995) Composition of interstitial fluid. Clin Chem 41:1522–1525. https://doi.org/10.1093/clinchem/41.10.1522

222. Fanian F, Maibach HI, Agache P, Humbert P (2017) Agache's measuring the skin. https://doi.org/10.1007/978-3-319-32383-1

223. Madden J, O'Mahony C, Thompson M, O'Riordan A, Galvin P (2020) Biosensing in dermal interstitial fluid using microneedle based electrochemical devices. Sens Bio-Sensing Res 29:100348. https://doi.org/10.1016/j.sbsr.2020.100348

224. Heikenfeld J, Jajack A, Feldman B, Granger SW, Gaitonde S, Begtrup G, Katchman BA (2019) Accessing analytes in biofluids for peripheral biochemical monitoring. Nat Biotechnol 37:407–419. https://doi.org/10.1038/s41587-019-0040-3

225. Muller AC, Breitwieser FP, Fischer H, Schuster C, Brandt O, Colinge J, Superti FG, Stingl G, Elbe BA, Bennett KL (2012) A comparative proteomic study of human skin suction blister fluid from healthy individuals using immunodepletion and ITRAQ labeling. J Proteome Res 11:3715–3727. https://doi.org/10.1021/pr3002035

226. Luijf YM, Mader JK, Doll W, Pieber T, Farret A, Place J, Renard E, Bruttomesso D, Filippi A, Avogaro A, Arnolds S, Benesch C, Heinemann L, Devries JH (2013) Accuracy and reliability of continuous glucose monitoring systems: a head-to-head comparison. Diabetes Technol Ther 15:722–727. https://doi.org/10.1089/dia.2013.0049

227. Pu Z, Zou C, Wang R, Lai X, Yu H, Xu K, Li D (2016) A continuous glucose monitoring device by graphene modified electrochemical sensor in microfluidic system. Biomicrofluidics 10:011910. https://doi.org/10.1063/1.4942437

228. Boroumand M, Olianas A, Cabras T, Manconi B, Fanni D, Faa G, Desiderio C, Messana I, Castagnola M (2021) Saliva, a bodily fluid with recognized and potential diagnostic applications. J Sep Sci 44:3677–3690. https://doi.org/10.1002/jssc.202100384

229. Ngamchuea K, Batchelor MC, Cowen PJ, Williams C, Gonçalves LM, Compton RG (2016) Can saliva testing replace blood measurements for health monitoring? Insights from a correlation study of salivary and whole blood glutathione in humans. Analyst 141:4707–4712. https://doi.org/10.1039/c6an01139j

230. Haji MM, Mulder S, Khashayar P, Kalbasi A, Azimzadeh M, Aref AR (2021) Saliva Lab-on-a-chip biosensors: recent novel ideas and applications in disease detection. Microchem J 168:106506. https://doi.org/10.1016/j.microc.2021.106506

231. Yoshizawa JM, Schafer CA, Schafer JJ, Farrell JJ, Paster BJ, Wong DTW (2013) Salivary biomarkers: toward future clinical and diagnostic utilities. Clin Microbiol Rev 26:781–791. https://doi.org/10.1128/cmr.00021-13

232. Prasad S, Tyagi AK, Aggarwal BB (2016) Detection of inflammatory biomarkers in saliva and urine: potential in diagnosis, prevention, and treatment for chronic diseases. Exp Biol Med 241:783–799. https://doi.org/10.1177/1535370216638770

233. Rathnayake N, Gieselmann DR, Heikkinen A, Tervahartiala T, Sorsa T (2017) Salivary diagnostics—point-of-care diagnostics of MMP-8 in dentistry and medicine. Diagnostics 7:7. https://doi.org/10.3390/diagnostics7010007

234. Choromanska M, Klimiuk A, Kostecka SP, Wilczynska K, Kwiatkowski M, Okuniewska N, Waszkiewicz N, Zalewska A, Maciejczyk M (2017) Antioxidant defence, oxidative stress and oxidative damage in saliva, plasma and erythrocytes of dementia patients. Can salivary AGE be a marker of dementia? Int J Mol Sci 18:2205. https://doi.org/10.3390/ijms18102205

235. Khurshid Z, Naseem M, Sheikh Z, Najeeb S, Shahab S, Zafar MS (2016) Oral antimicrobial peptides: types and role in the oral cavity. Saudi Pharm J 24:515–524. https://doi.org/10.1016/j.jsps.2015.02.015

236. Garcia CL, Martin A, Sempionatto JR, Moreto JR, Gonzalez MC, Wang J, Escarpa A (2019) Pacifier Biosensor: toward noninvasive saliva biomarker monitoring. Anal Chem 91:13883–13891. https://doi.org/10.1021/acs.analchem.9b03379

237. Petropoulos K, Piermarini S, Bernardini S, Palleschi G, Moscone D (2016) Development of a disposable biosensor for lactate monitoring in saliva. Sensors Actuators B Chem 237:8–15. https://doi.org/10.1016/j.snb.2016.06.068

238. Soni A, Surana RK, Jha SK (2018) Smartphone based optical biosensor for the detection of urea in saliva. Sensors Actuators, B Chem 269:346–353. https://doi.org/10.1016/j.snb.2018.04.108

239. Stevenson H, Bacon A, Joseph KM, Gwandaru WRW, Bhide A, Sankhala D, Dhamu VN, Prasad S (2019) A rapid response electrochemical biosensor for detecting Thc In Saliva. Sci Rep 9:1–11. https://doi.org/10.1038/s41598-019-49185-y

240. Mannoor MS, Tao H, Clayton JD, Sengupta A, Kaplan DL, Naik RR, Verma N, Omenetto FG, McAlpine MC (2012) Graphene-based wireless bacteria detection on tooth enamel. Nat Commun 3:763. https://doi.org/10.1038/ncomms1767

241. Mercante LA, Andre RS, Facure MHM, Fugikawa-SL CDS (2021) Design of a bioelectronic tongue for glucose monitoring using zinc oxide nanofibers and graphene derivatives. Sensors Actuators Rep 3:100050. https://doi.org/10.1016/j.snr.2021.100050

242. Kim J, Kim M, Lee MS, Kim K, Ji S, Kim YT, Park J, Na K, Bae KH, Kim HK, Bien F, Lee CY, Park JU (2017) Wearable smart sensor systems integrated on soft contact lenses for wireless ocular diagnostics. Nat Commun 8:1–8. https://doi.org/10.1038/ncomms14997

243. Park J, Kim J, Kim SY, Cheong WH, Jang J, Park YG, Na K, Kim YT, Heo JH, Lee CY, Lee JH, Bien F, Park JU (2018) Soft, smart contact lenses with integrations of wireless circuits, glucose sensors, and displays. Sci Adv 4:1–12. https://doi.org/10.1126/sciadv.aap9841

244. Wang Z, Hao Z, Yu S, Huang C, Pan Y, Zhao X (2020) A wearable and deformable graphene-based affinity nanosensor for monitoring of cytokines in biofluids. Nanomaterials 10:1–9. https://doi.org/10.3390/nano10081503

245. Zhang W, Dong G, Feng H, Shan S, Huang L, Yuan F, Bao B, Yan L, Xia Z, Lawson T, Chen J, Qu J, Liu Y (2020) Wearable Corneal Biosensors Fabricated from PEDOT functionalized sulfur-doped graphene for use in the early detection of myopia. Adv Mater Technol 5:1–7. https://doi.org/10.1002/admt.2020000682

246. Jang J, Kim J, Shin H, Park YG, Joo BJ, Seo H, Won JE, Kim DW, Lee CY, Kim HK, Park JU (2021) Smart contact lens and transparent heat patch for remote monitoring and therapy of

chronic ocular surface inflammation using mobiles. Sci Adv 7:1–11. https://doi.org/10.1126/sciadv.abf7194

247. Pankratov D, Gonzalez AE, Blum Z, Shleev S (2016) Tear based bioelectronics. Electroanalysis 28:1250–1266. https://doi.org/10.1002/elan.201501116

248. Ponzini E, Santambrogio C, De Palma A, Mauri P, Tavazzi S, Grandori R (2021) Mass spectrometry-based tear proteomics for noninvasive biomarker discovery. Mass Spectrom Rev 1–19.https://doi.org/10.1002/mas.21691

249. Jacob JT, Ham B (2008) Compositional profiling and biomarker identification of the tear film. Ocul Surf 6:175–185. https://doi.org/10.1016/S1542-0124(12)70178-7

250. Bachhuber F, Huss A, Senel M, Tumani H (2021) Diagnostic biomarkers in tear fluid: from sampling to preanalytical processing. Sci Rep 11:1–9. https://doi.org/10.1038/s41598-021-89514-8

251. Di Zazzo A, Micera A, De Piano M, Cortes M, Bonini S (2019) Tears and ocular surface disorders: usefulness of biomarkers. J Cell Physiol 234:9982–9993. https://doi.org/10.1002/jcp.27895

252. Jalbert I (2013) Diet, nutraceuticals and the tear film. Exp Eye Res 117:138–146. https://doi.org/10.1016/j.exer.2013.08.016

253. Aihara M, Kubota N, Minami T, Shirakawa R, Sakurai Y, Hayashi T, Iwamoto M, Takamoto I, Kubota T, Suzuki R, Usami S, Jinnouchi H, Aihara M, Yamauchi T, Sakata T, Kadowaki T (2021) Association between tear and blood glucose concentrations: random intercept model adjusted with confounders in tear samples negative for occult blood. J Diabetes Investig 12:266–276. https://doi.org/10.1111/jdi.13344

254. Sen DK, Sarin GS (1980) Tear glucose levels in normal people and in diabetic patients. Br J Ophthalmol 64:693–695. https://doi.org/10.1136/bjo.64.9.693

255. Komkova MA, Eliseev AA, Poyarkov AA, Daboss EV, Evdokimov PV, Eliseev AA, Karyakin AA (2022) Simultaneous monitoring of sweat lactate content and sweat secretion rate by wearable remote biosensors. Biosens Bioelectron 202:113970. https://doi.org/10.1016/j.bios.2022.113970

256. Carpenter GH (2013) The secretion, components, and properties of saliva. Annu Rev Food Sci Technol 4:267–276. https://doi.org/10.1146/annurev-food-030212-182700

257. Kim EC, Doh SH, Chung SY, Yoon SY, Kim MS, Chung SK, Shin MC, Hwang HS (2017) Direct visualization of aqueous tear secretion from lacrimal gland. Acta Ophthalmol 95:314–322. https://doi.org/10.1111/aos.13335

258. Rentka A, Koroskenyi K, Harsfalvi J, Szekanecz Z, Szucs G, Szodoray P, Kemeny-Beke A (2017) Evaluation of commonly used tear sampling methods and their relevance in subsequent biochemical analysis. Ann Clin Biochem 54:521–529. https://doi.org/10.1177/0004563217695843

259. Fullard RJ, Carney LG (1984) Diurnal variation in human tear enzymes. Exp Eye Res 38:15–26. https://doi.org/10.1016/0014-4835(84)90134-9

260. Stuchell RN, Feldman JJ, Farris RL, Mandel ID (1984) The effect of collection technique on tear composition. Investig Ophthalmol Vis Sci 25:374–377. Retrieved on 24th November, 2021 from https://iovs.arvojournals.org/article.aspx?articleid=2159721

261. Vijay AK, Fadli Z, Lakkis C, Coles-Brennan C, Willcox MDP (2018) In Vitro Compatibility of Contact Lenses with Corneal Epithelial Cells. Eye Contact Lens 44:283–290. https://doi.org/10.1097/ICL.0000000000000408

262. Farandos NM, Yetisen AK, Monteiro MJ, Lowe CR, Yun SH (2015) Contact lens sensors in ocular diagnostics. Adv Healthc Mater 4:792–810. https://doi.org/10.1002/adhm.201400504

263. Alexeev VL, Das S, Finegold DN, Asher SA (2004) Photonic crystal glucose-sensing material for noninvasive monitoring of glucose in tear fluid. Clin Chem 50:2353–2360. https://doi.org/10.1373/clinchem.2004.039701

264. Ben-Moshe M, Alexeev VL, Asher SA (2006) Fast responsive crystalline colloidal array photonic crystal glucose sensors. Anal Chem 78:5149–5157. https://doi.org/10.1021/ac060643i

265. Ballerstadt R, Evans C, McNichols R, Gowda A (2006) Concanavalin A for in vivo glucose sensing: a biotoxicity review. Biosens Bioelectron 22:275–284. https://doi.org/10.1016/j.bios.2006.01.008

266. Gijs M, Ramakers I, Visser PJ, Verhey F, Waarenburg M, Schalkwijk C, Nuijts R, Webers C (2020) Detection of amyloid-beta and tau in tear fluid of patients with Alzheimer's disease. https://doi.org/10.21203/rs.3.rs-36499/v1

267. Park YM, Ahn J, Choi YS, Jeong JM, Lee SJ, Lee JJ, Choi BG, Lee KG (2020) Flexible nanopillar-based immunoelectrochemical biosensor for noninvasive detection of amyloid beta. Nano Converg 7:29. https://doi.org/10.1186/s40580-020-00239-2

268. Zhou L, Zhao SZ, Koh SK, Chen L, Vaz C, Tanavde V, Li XR, Beuerman RW (2012) In-depth analysis of the human tear proteome. J Proteomics 75:3877–3885. https://doi.org/10.1016/j.jprot.2012.04.053

269. Morad KN, Haitham A, Raneen J, Yoav YB, Manal A, Alaa G, Ivgi H, Salam K, Shifaa B, Lior HS, Lea GM, Izabella L, Ariel M, Samih B, Raz W, John F, Sylvia CK, Frederic P, David M, Barbara G, Gilles G, Gerald S, Farid N, Shira B, Raed S, Marwan H, Maayan G, Ohad R, Tal Z, Ilana D, Ofer N, Zaher B, Da-you S, Wei Z, Qingling H, Yueyin P, Li Tao HuL, Amir K, Eduard K, Tova R, Roberts S, Armands S, Guntis A, Inta LK, Ilze K, Ieva L, Ivars T, Douglas J, Stuart ZM, Jennifer F, John WW, Larry HW, Marc H, Marcis L, Nir P, Hossam H (2017) Diagnosis and classification of 17 diseases from 1404 subjects via pattern analysis of exhaled molecules. ACS Nano 11:112–125. https://doi.org/10.1021/acsnano.6b04930

270. Risby TH, Solga SF (2006) Current status of clinical breath analysis. Appl Phys B 85:421–426. https://doi.org/10.1007/S00340-006-2280-4

271. Liang R, Luo A, Zhang Z, Li Z, Han C, Wu W (2020) Research progress of graphene-based flexible humidity sensor. Sensors 20:5601. https://doi.org/10.3390/S20195601

272. Lewis JM, Savage RS, Beeching NJ, Beadsworth MBJ, Feasey N, Covington JA (2017) Identifying volatile metabolite signatures for the diagnosis of bacterial respiratory tract infection using electronic nose technology: a pilot study. PLoS ONE 12:0188879. https://doi.org/10.1371/journal.pone.0188879

273. Van Oort PM, De BS, Knobel WH, HH, Schultz MJ, and Bos LD, (2017) Exhaled breath metabolomics for the diagnosis of pneumonia in intubated and mechanically-ventilated intensive care unit (ICU)-patients. Int J Mol Sci 18:449. https://doi.org/10.3390/ijms18020449

274. Keulen KV, Jansen ME, Schrauwen RWM, Kolkman JJ, Siersema PD, Van KE, Jansen ME, Schrauwen RWM, Kolkman JJ, Siersema PD (2020) Volatile organic compounds in breath can serve as a non-invasive diagnostic biomarker for the detection of advanced adenomas and colorectal cancer. Aliment Pharmacol Ther 51:334–346. https://doi.org/10.1111/apt.15622

275. Pang Y, Jian J, Tu T, Yang Z, Ling J, Li Y, Wang X, Qiao Y, Tian H, Yang Y, Ren TL (2018) Wearable humidity sensor based on porous graphene network for respiration monitoring. Biosens Bioelectron 116:123–129. https://doi.org/10.1016/j.bios.2018.05.038

276. Yao Y, Chen X, Guo H, Wu Z (2011) Graphene oxide thin film coated quartz crystal microbalance for humidity detection. Appl Surf Sci 257:7778–7782. https://doi.org/10.1016/j.apsusc.2011.04.028

277. Minh TDC, Blake DR, Galassetti PR (2012) The clinical potential of exhaled breath analysis for diabetes mellitus. Diabetes Res Clin Pract 97:195. https://doi.org/10.1016/j.diabres.2012.02.006

278. Siegel AP, Daneshkhah A, Mather KJ, Agarwal M (2019) Volatile organic compounds in breath predict hypoglycemia well before plasma glucose levels fall. Diabetes 68:968. https://doi.org/10.2337/db19-968-p

279. Phillips M, Gleeson K, Hughes JM, Greenberg J, Cataneo RN, Baker L, McVay WP (1999) Volatile organic compounds in breath as markers of lung cancer: a cross-sectional study. Lancet 353:1930–1933. https://doi.org/10.1016/S0140-6736(98)07552-7

280. Xu H, Xiang JX, Lu YF, Zhang MK, Li JJ, Gao BB, Zhao YJ, Gu ZZ (2018) Multifunctional wearable sensing devices based on functionalized graphene films for simultaneous monitoring of physiological signals and volatile organic compound biomarkers. ACS Appl Mater Interfaces 10:11785–11793. https://doi.org/10.1021/acsami.8b00073

281. Majidi R, Nadafan M (2021) Application of nitrogenated holey graphene for detection of volatile organic biomarkers in exhaled breath of humans with chronic kidney disease: a density functional theory study. J Comput Electron 20:1930–1937. https://doi.org/10.1007/s10825-021-01737-0

282. Liu B, Huang Y, Kam KW, Cheung WF, Zhao N, Zheng B (2019) Functionalized graphene-based chemiresistive electronic nose for discrimination of disease-related volatile organic compounds. Biosens Bioelectron X 1:100016. https://doi.org/10.1016/j.biosx.2019.100016

283. Sanchez-VC SJP, Lozano J, Sayago I, Sanjurjo JL, Azabal A, Ruiz VS (2020) Graphene-doped tin oxide nanofibers and nanoribbons as gas sensors to detect biomarkers of different diseases through the breath. Sensors 20:7223. https://doi.org/10.3390/S20247223

284. Tung TT, Tran MT, Feller JF, Castro M, Van Ngo T, Hassan K, Nine MJ, Losic D (2020) Graphene and metal organic frameworks (MOFs) hybridization for tunable chemoresistive sensors for detection of volatile organic compounds (VOCs) biomarkers. Carbon 159:333–344. https://doi.org/10.1016/j.carbon.2019.12.010

285. Yin L, Kim KN, Lv J, Tehrani F, Lin M, Lin Z, Moon JM, Ma J, Yu J, Xu S, Wang J (2021) A self-sustainable wearable multimodular E-textile bioenergy microgrid system. Nat Commun 12:1–12. https://doi.org/10.1038/s41467-021-21701-7

286. Su Y, Yang T, Zhao X, Cai Z, Chen G, Yao M, Chen K, Bick M, Wang J, Li S, Xie G, Tai H, Du X, Jiang Y, Chen J (2020) A wireless energy transmission enabled wearable active acetone biosensor for non-invasive prediabetes diagnosis. Nano Energy 74:104941. https://doi.org/10.1016/j.nanoen.2020.104941

287. Soomro AM, Jabbar F, Ali M, Lee JW, Mun SW, Choi KH (2019) All-range flexible and biocompatible humidity sensor based on poly lactic glycolic acid (PLGA) and its application in human breathing for wearable health monitoring. J Mater Sci Mater Electron 30:9455–9465. https://doi.org/10.1007/s10854-019-01277-1

288. Selamneni V, Sahatiya P (2020) Bolometric effect enhanced ultrafast graphene based do-it-yourself wearable respiration sensor for personal healthcare monitoring. IEEE Sens J 20:3452–3459. https://doi.org/10.1109/jsen.2019.2961156

289. Yao Y, Chen X, Zhu J, Zeng B, Wu Z, Li X (2012) The effect of ambient humidity on the electrical properties of graphene oxide films. Nanoscale Res Lett 7:1–7. https://doi.org/10.1186/1556-276x-7-363

290. Borini S, White R, Wei D, Astley M, Haque S, Spigone E, Harris N, Kivioja J, Ryhänen T (2013) Ultrafast graphene oxide humidity sensors. ACS Nano 7:11166–11173. https://doi.org/10.1021/nn404889b

291. He J, Xiao P, Shi J, Liang Y, Lu W, Chen Y, Wang W, Théato P, Kuo SW, Chen T (2018) High performance humidity fluctuation sensor for wearable devices via a bioinspired atomic-precise tunable graphene-polymer heterogeneous sensing junction. Chem Mater 30:4343–4354. https://doi.org/10.1021/acs.chemmater.8b01587

292. Iyengar SA, Srikrishnarka P, Jana SK, Islam MR, Ahuja T, Mohanty JS, Pradeep T (2019) Surface-treated nanofibers as high current yielding breath humidity sensors for wearable electronics. ACS Appl Electron Mater 1:951–960. https://doi.org/10.1021/acsaelm.9b00123

293. Tang M, Zhang C, Zhang JY, Zhao QL, Hou ZL, Zhan KT (2020) Ultrafast response humidity sensor with high humidity durability based on a freestanding film of graphene oxide supramolecular. Phys status solidi 217:1900869. https://doi.org/10.1002/pssa.201900869

294. Wang Y, Zhang L, Zhang Z, Sun P, Chen H (2020) High sensitivity wearable and flexible humidity sensor based on graphene oxide/non-woven fabric for respiration monitoring. Langmuir 36:9443–9448. https://doi.org/10.1021/acs.langmuir.0c01315

Publisher's note Springer Nature remains neutral with regard to jurisdictional claims in published maps and institutional affiliations.